The role of *Zostera noltii* in wave attenuation

By Maike Paul

September 2011

GRADUATE SCHOOL OF THE

NATIONAL OCEANOGRAPHY CENTRE, SOUTHAMPTON

This PhD dissertation by Maike Paul has been produced under the supervision of the following persons

Supervisors

Prof Carl L Amos (School of Ocean and Earth Science)

Prof Robert J Nicholls (School of Civil Engineering and the Environment)

Chair of the Advisory Panel

Dr Justin Dix (School of Ocean and Earth Science)

UNIVERSITY OF SOUTHAMPTON

ABSTRACT

FACULTY OF NATURAL AND ENVIRONMENTAL SCIENCES
SCHOOL OF OCEAN AND EARTH SCIENCES

Doctor of Philosophy

THE ROLE OF *ZOSTERA NOLTII* IN WAVE ATTENUATION

by Maike Paul

Wave attenuation is a recognised function of seagrass ecosystems which is believed to depend on plant characteristics. In this case, *Zostera noltii* was studied to investigate how this particular species attenuates waves.

A profiling sonar was used to survey a *Zostera noltii* bed and describe its coverage and canopy height *in situ*. An algorithm was used to identify the seabed and to compute water depth, canopy height and coverage from the backscatter data. The algorithm was extended from previous methods and tested on two additional seagrass meadows of *Zostera marina* and *Posidonia oceanica* respectively to test the method's applicability. Each seagrass species showed a characteristic canopy height and spatial coverage distribution which allows a preliminary species identification, as each species has a typical canopy height and preferred depth range.

Data on wave attenuance were collected over the mapped *Zostera noltii* meadow to evaluate its effect on wave height. *Zostera noltii* shows a strong seasonality and the site was therefore monitored over an annual cycle to assess the effect of seasonal changes on wave attenuation. The site was exposed to wind waves and boat wakes which differ in wave period and steepness. This difference was used to investigate whether wave attenuation by seagrass changes with hydrodynamic conditions. A seasonal change in wave attenuation could be observed and results suggest that a minimum shoot density is necessary to initiate wave attenuation by seagrass. Moreover, a relationship between wave attenuance and vegetation Reynolds number was found which allows comparing the wave attenuating effect of *Zostera noltii* to other plant species.

To determine the effect of specific plant characteristics, tests were carried out in a laboratory flume. Seagrass mimics were used to investigate what effect shoot density, stiffness and leaf length have on wave attenuation. Previous studies found that wave attenuation increases with increased plant stiffness, leaf length and shoot density. This study confirmed the dependence on stiffness and extended the findings for leaf length and shoot density by showing that the leaf area index (density $*$ leaf length $*$ leaf width) is the determining factor for attenuation of a given wave in shallow water. The experiments were repeated with an underlying current to simulate field conditions where waves are superimposed on a tidal flow. The presence of a tidal current reduced the wave attenuating capacity of seagrass meadows suggesting that studies carried out under waves only overestimate wave attenuation compared to tidal environments.

Contents

List of Figures

List of Tables

Declaration Of Authorship

I, Maike Paul, declare that the thesis entitled: "THE ROLE OF *Zostera noltii* IN WAVE ATTENUATION" and the work presented in it are my own and has been generated by me as the result of my own original research.

I confirm that:

- This work was done wholly or mainly while in candidature for a research degree at this University;
- Where any part of this thesis has previously been submitted for a degree or any other qualification at this University or any other institution, this has been clearly stated;
- Where I have consulted the published work of others, this is always clearly attributed;
- Where I have quoted from the work of others, the source is always given. With the exception of such quotations, this thesis is entirely my own work;
- I have acknowledged all main sources of help;
- Where the thesis is based on work done by myself jointly with others, I have made clear exactly what was done by others and what I have contributed myself;
- Parts of this work have been published as:

Paul, M., Lefebvre, A., Manca, E., and Amos, C. L. (2011). An acoustic method for the remote measurement of seagrass metrics. Estuarine, Coastal and Shelf Science 93, pp. 68-79, doi: 10.1016/j.ecss.2011.04.006.

Paul, M., Amos, C. L. (2011). Spatial and seasonal variation in wave attenuation over *Zostera noltii.* Journal of Geophysical Research 116, C08019, doi: 10.1029/2010JC006797.

Paul, M., Bouma, T. J., and Amos, C. L. (2011). The effect of organism traits and tidal currents on wave attenuation by submerged vegetation. 5th International Short Conference on Applied Coastal Research, Aachen, June 2011.

Paul, M., Bouma, T. J., Amos, C. L. (accepted). Wave attenuation by submerged vegetation: combining the effect of organism traits and tidal current. Marine Ecology Progress Series, doi: 10.3354/meps09489.

Signed:

Date:

Acknowledgements

I just signed that this thesis is my work, which is correct. But the project that led to this thesis would not have been possible without the support from numerous people and institutions.

I would like to start by thanking a person who has not been involved in this project at all. Dr David Walker from Adelaide University introduced me to the problems of plant-wave interactions which sparked my interest in the subject and led to the project idea in the first place. I am also very grateful to Prof. Carl L. Amos who agreed to supervise the project. Throughout the project he has been a source of valuable guidance, feedback and advice, but equally gave me the space to make my own mistakes.

I received help with instruments and deployment techniques from Dr Charlie Thompson and John Davis. Barry Marsh provided support for video recordings in the lab and Kate Davis helped making figures look great. I had very fruitful discussions with Prof. Ian Townend who helped to improve my data analysis and was provided with MatLab code for zero-crossing and wave reflection by Dr U. Neumeier and Dr T. Baldock, respectively. My special thanks also go to Dr Tjeerd Bouma, who was kind enough to reply to my initial email and enthusiastic enough to allow me access to the flume facilities at NIOO and to help me interpreting the flume results. Thanks also to the rest of the NIOO staff who made my stay there very smooth, productive and enjoyable.

My field work would not have been possible without WightLink ltd. who allowed me to set up camp on their pier in Ryde and to use their facilities. James and Cheryl from Seahaven House made especially the field work in winter much more bearable by providing great breakfasts and an unlimited supply of hot water for tea and coffee. Simon Ball, Yining Chen, Sabine Hacker, Eleonora Manca, Chris Marsay, Moritz Müller, Iñaki de Santiago Gonzalez, Maria Wahle and Bronwyn Wake helped in the field on various occasions. I am also thankful for the help of Bob Wilkie and

his crew on R.V. Bill Conway. Their skill and experience made surveying in shallow and tricky conditions possible and allowed me to collect a great dataset.

For this project, I was in charge of my own funding and I am very grateful to the German Academic Exchange Service (DAAD) and IMarEST who both granted me a scholarship. As a result I did not need a part-time job and was able to focus fully on my PhD. The Solent Forum contributed to the surveys in Ryde and therefore allowed me to develop and test the seagrass mapping technique. A scholarship from the Peter Killworth Memorial Fund made my trip to the Netherlands possible and I am very grateful that I had the opportunity to work at NIOO.

I am very grateful for the support I received from my family. I'd like to thank Maren for remembering what it is like to do a PhD and therefore forgiving me when I was rubbish with birthday presents or generally being in touch. And I would like to thank my parents for their extraordinary support. Their help went well beyond the normal parental support of listening to moans, supportive words during doubts and the occasional magic appearance of money in a bank account. They tied 5400 cable ties and 11400 ribbons to a mesh to make sure the artificial seagrass would be finished in time for my lab work and my father volunteered (and admittedly enjoyed) to be my lab assistant and camping buddy in Yerseke.

Finally, my very special thanks go to Stephen Duffy, who supported all my work in every way he could, even though it meant spending long hours on Ryde pier. But moreover, I would like to thank him for the much needed reality checks and for making sure that I have a life outside my PhD.

Notation

a	m	wave amplitude
BI	-	backscatter intensity
$\overline{BI_b}$	-	averaged backscatter intensity for three bins 5 cm above the bed
$\overline{BI_w}$	-	averaged backscatter intensity of the water column
b	m	leaf width
C_D	-	drag coefficient
C_g	m s^{-1}	group velocity
C_μ	-	current parameter in Madsen's (1994) model
CS	m^2 Hz^{-1}	cross spectrum
$c,\ d,\ e$	-	best fit parameters
D	°	wave direction
E	J m^{-2}	wave energy density
E_s	N m^{-2}	modulus of elasticity
F	N m^{-2}	wave energy flux
f_e	-	energy dissipation factor
f_w	-	wave friction factor
g	m s^{-2}	gravital acceleration
H_{rms}	m	root-mean-square wave height
H_s	m	significant wave height
h	m	water depth

h_b	m	depth of seabed
K_s	-	shoaling coefficient
k	m^{-1}	wave number
k_N	-	equivalent Nikuradse roughness
L	m	wave length
LAI	$m^2\ m^{-2}$	leaf area index
M	-	number of discrete frequency components
m	-	slope of linear regression
N	-	number of leaves per m^2
p	-	constant to generate backscatter threshold
Re	-	wave Reynolds number
Re_v	-	vegetation Reynolds number
S_f	$m^2\ Hz^{-1}$	energy density spectrum
S_p	$m^2\ Hz^{-1}$	pressure spectrum
s	m	canopy height
spr	$^\circ$	wave spreading
T	s	wave period
u_b	$m\ s^{-1}$	near-bed horizontal orbital velocity
x	m	length of mimic meadow
y	m	distance from a reference point off shore of station 1.
z	m	vertical distance measured up from seabed
α	$^\circ$	angle of instrumented transect
β	$^\circ$	direction of wave propagation
γ	-	critical breaking parameter
$\Delta back$	-	difference in backscatter intensity
Δf_b	Hz	frequency bandwidth
ΔH	m	dissipated wave height per metre meadow

Δh	m	height above bed
Δr	m	projected distance between stations
Δx	m	measured distance between stations
δ	$^\circ$	excursion angle
ϵ_f	N m^{-3}	rate of frictional dissipation
θ_{BI}	-	backscatter threshold
ν	m^2 s^{-1}	kinematic viscosity
ρ	kg m^{-3}	density of water
φ	-	phase difference between bottom shear stress and wave orbital velocity
ω	s^{-1}	radian wave period

Subscripts

0	outer most station
2	second highest value
b	beginning of meadow
e	end of meadow
j	frequency component
m	maximum value
n	number of the shoreward station, or number of bin in the profile
p	pressure
r	representative parameter
u	East component of velocity
v	North component of velocity
w	wave only case
wc	combined wave and current case

1. Introduction

The world's coastlines are highly dynamic environments where waves and currents drive changes in bathymetry and coastline geometry. Areas that are exposed to high wave energy are generally unvegetated, but in medium to low energy coastal environments a variety of plant species and ecosystems can develop. Within these habitats, two groups can be distinguished: (1) terrestrial plants that are saltwater resistant and tolerate part or full submergence (e.g. mangroves, salt marsh) cover the intertidal, and (2) aquatic plants (e.g. seagrasses, kelp) grow in subtidal areas, although some species tolerate air exposure and extend into the intertidal. Coastal ecosystems are important providers of goods (e.g. fish, fertiliser, construction materials) and services (e.g. recreation, transport) (Burke et al., 2001) and coastal management therefore strives to protect, conserve and where possible expand natural coastal habitats (Koch et al., 2009). Yet it is necessary to provide effective coastal protection for people and infrastructure in coastal areas. To combine both demands, coastal management explores options that include the use of natural habitats for coastal protection purposes (de la Vega-Leinert and Nicholls, 2008).

1.1. Effect of vegetation on waves and currents

Submerged aquatic vegetation interacts with flow and changes the velocity profile throughout the water column (Figure 1.1). Velocities within the canopy are reduced compared to the free stream velocity as was shown during laboratory experiments

on *Zostera marina* (Gambi et al., 1990; Lefebvre et al., 2010); similar observations were made in a *Thalassia testudinum* meadow in St. Joseph Bay, Florida where the velocity within the canopy was less than above the canopy, but no velocity gradient with depth into the canopy could be observed (Koch and Gust, 1999). Above the canopy, a skimming layer with increased velocity may develop (Koch and Gust, 1999; Widdows et al., 2008). To investigate the onset of skimming flow, Thompson et al. (2004) deployed Sea Carousel (Amos et al., 1992) over *Zostera noltii* and *Cymodocea nodosa* which allowed them to control flow velocities in otherwise undisturbed seagrass beds. Their results show that roughness and therefore resistance reduces when the leaves start bending under increasing flow. This formation of a closed canopy leads to a skimming flow and reduced mixing between water bodies within and above the canopy (Thompson et al., 2004). Velocity profiles with low velocities within the vegetation and skimming flow above the canopy were also found in different species of salt marsh (Neumeier and Ciavola, 2004; Neumeier and Amos, 2006). A logarithmic velocity profile within the skimming layer may be used to calculate the roughness length of a salt marsh canopy (Neumeier and Amos, 2006) which is independent of water depth or flow velocity and only depends on canopy characteristics such as total biomass and shoot density (Leonard and Croft, 2006; Neumeier, 2007). Peterson et al. (2004) found a similar relationship between shoot density and flow velocity within the canopy for *Zostera marina* and *Halodule wrightii* in the field. Laboratory studies on *Zostera marina* did not confirm this relationship for relatively short meadows (Fonseca et al., 1982; Gambi et al., 1990; Lefebvre et al., 2010). However, within the infinite canopy of an annular flume, flow reduction was accentuated with increasing shoot density (Lefebvre et al., 2010) which indicates that differences in the experimental setup of laboratory studies may explain some of the discrepancies in results in the literature (Gambi et al., 1990).

In an attempt to describe the effect of vegetation on wave motion along a vertical profile, Verduin and Backhaus (2000) obtained wave energy spectra along a profile in an *Amphibolis antarctica* meadow: analogous to findings under unidirectional flow,

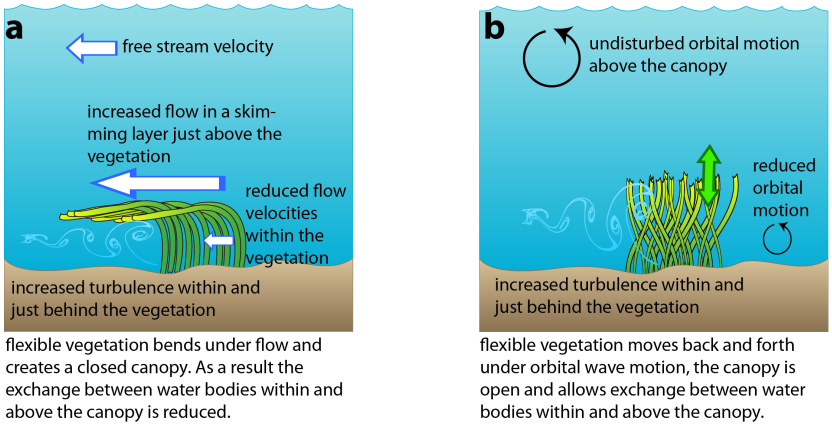

Figure 1.1.: Conceptual diagrams of state of the art knowledge about hydrodynamics in the presence of vegetation under a. unidirectional flow and b. waves.

they observed a damping effect within the canopy while maximum kinetic energy occurred just above the canopy. *Amphibolis antarctica* is a crown building species with approx. 15 cm long leafless stems and the majority of biomass is located in the upper half of the canopy where the leaves branch off the stems (Verduin et al., 2002). The kelp *Laminaria hyperborea* shows a comparable canopy structure and laboratory experiments yielded similar profiles of particle velocities under waves with a shoreward horizontal velocity directly above the canopy (Løvås and Tørum, 2001). No such profile could be observed within a canopy of the seagrass *Thalassia testudinum* (Koch and Gust, 1999). Within this meadow building species biomass is distributed evenly along the height of the canopy and Koch and Gust (1999) observed a steady decrease of orbital velocity with depth. This difference in velocity profiles between species with differing canopy shapes was confirmed by James and Barko (2000) who compared shear stress profiles between a crown building (*Myriophyllum sibiricum*) and a meadow forming (*Chara* sp.) macrophyte. Both species reduced wave-generated shear stress near the bed equally effectively, but *M. sibiricum* reduced shear stress higher up in the water column where the majority of its biomass is located (James and Barko, 2000).

Wave-induced motion varies on a much shorter time scale than uni-directional or tidal flow which gives velocity profiles less time to develop (Denny, 1988). Thus, the

effect of vegetation on wave motion is generally described by a reduction in total wave energy which has been observed for salt marsh (e.g. Möller et al., 1999; Bouma et al., 2010), kelp (e.g. Mork, 1996) and several seagrass species (e.g. Fonseca and Cahalan, 1992). Studies show that salt marsh is very effective at attenuating wave energy. Möller et al. (1999) found an average wave energy dissipation of 87% over 180 m and a more recent study by Cooper (2005) found dissipation rates between 72 and 91% over 110-250 m of mixed salt marsh. 92% and 100% of wave energy reduction were found over 20 and 30 m of *Spartina alterniflora* marsh respectively (Wayne, 1976; Knutson et al., 1982) and up to 86% were observed in a laboratory study over 3 m of *Spartina anglica* and *Puccinellia maritima* (Bouma et al., 2010). Bouma et al. (2010) confirmed observations that wave energy dissipation reduces with distance into the salt marsh (Möller, 2006; Augustin et al., 2009) and showed its dependence on vegetation density.

Results for kelp are a lot more variable and no significant wave dissipation was found for *Macrocystis pyrifera* with an average density of 10 per m^2 (Elwany et al., 1995). For *Laminaria hyperborea*, a reduction in wave energy of 70-85% over a distance of 258 m was observed (Mork, 1996) and Dubi and Tørum (1997) found a reduction of significant wave height of 50% over distances between 76 and 1390 m, depending on water depth. Observed wave reduction rates for seagrasses are of similar magnitude to kelp; Fonseca and Cahalan (1992) found a reduction in wave energy density of approx. 40% per metre of seagrass meadow in four different seagrass species and reductions of up to 80% have been observed in the field (Prager and Halley, 1999). Moreover, similarly to kelp, water depth has been observed to affect wave attenuation by seagrass meadows (Ward et al., 1984; Fonseca and Cahalan, 1992; Koch, 2001). Chen et al. (2007) suggest that wave dissipation by seagrass depends on the ratio of water depth to canopy height rather than on water depth alone, but targeted studies on the effect of submergence ratio are needed to verify this hypothesis. Newell and Koch (2004) compared wave attenuation over a *Ruppia maritima* bed in summer (leaf length $\sim$1 m) and autumn (leaf length $\sim$0.15 m) and found a reduction in

wave attenuation with increasing water depth as well as decreasing leaf length. Moreover, their results reveal that a minimum shoot density of 1000 shoots/m^2 is required for *Ruppia maritima* before wave attenuation is observed (Newell and Koch, 2004). The effect of shoot density on wave attenuation was also observed for *Thalassia testudinum* (Koch and Gust, 1999) and Nepf et al. (1997) confirmed the general relationship in the laboratory by using circular cylinders instead of natural vegetation. A more recent laboratory study (Bouma et al., 2005) quantified the effect of shoot density on wave attenuation using natural and artificial *Zostera noltii* shoots. Under the condition that natural and artificial shoots were comparable, results showed that an increase in shoot density by a factor of 30 can lead to a factor of 6.6 in wave reduction (Bouma et al., 2005). While the overall consensus of previous work is that wave attenuation increases with shoot density, the number of tested densities is generally too low (2-3) to qualify this relationship.

A field study on *Thalassia testudinum* showed that wave attenuation by seagrass not only depends on plant parameters, but also on wave frequency. Results suggest that the seagrass leaves move with a certain frequency and waves of the same frequency in a spectrum are not attenuated (Bradley and Houser, 2009). However, observed wave attenuation was predicted reasonably well by a model assuming rigid blades. A laboratory study with artificial *Posidonia oceanica* plants also found wave attenuation to be frequency dependent, but could not link this to plant motion as the latter was not measured (Manca, 2010). Natural seagrass meadows are exposed to wave spectra which are a combination of a wide range of wave conditions including ocean swell, wind generated waves and boat wakes. In order to predict dissipation of spectral wave energy, it is important to understand how seagrass interacts with waves of different frequencies (Augustin et al., 2009) and more field studies are required to verify the dependence of wave attenuation by seagrass on hydrodynamic forcing under natural conditions.

Previous studies showed that seagrasses attenuate wave energy, but also revealed

that results can only be considered applicable within species with very similar morphology (James and Barko, 2000), if at all. Between species with similar growth types (e.g. meadow forming plants) other plant characteristics limit comparison. Fonseca and Fisher (1986) showed that the shape and cross-section of seagrass leaves have an impact on friction under unidirectional flow. They observed that the friction factors for flat-bladed species (*Thalassia testudinum*, *Zostera marina* and *Halodule wrightii*) are similar, while the friction factor for a round-bladed (*Syringodium filiforme*) species differed significantly. In a similar study, Fonseca and Cahalan (1992) observed that leaf width and canopy height have an impact on wave attenuation by four species of seagrass, but did not quantify these observations. Within the approx. 60 species of seagrass identified around the world (Short et al., 2007) a great variety of growth types and shapes exists that leads to a unique morphology for each species. It is proposed that the relative effectiveness for each species may differ under unidirectional flow (Fonseca and Fisher, 1986) and the variety of results suggests that this will apply to wave attenuation. It is therefore necessary to investigate each seagrass species separately to quantify its effect on wave attenuation.

1.2. *Zostera noltii*

The species under investigation for this study is the dwarf eelgrass *Zostera noltii*. It is an intertidal seagrass that colonises a wide range of substrates from mud over silt to fine sandy bottoms (Auby and Labourg, 1996). It is a temperate European species that is highly abundant along the Atlantic coasts of Europe and around the British Isles (Figure 1.2); its distribution stretching from southern Norway in the north to Mauritania in the south. In the Mediterranean it is restricted to environments with changing salinities such as lagoons and estuaries, and it is the only seagrass still present in the Caspian and Aral Sea (Short et al., 2007).

It is highly abundant between mean high and low water neaps, but can be found in

Figure 1.2.: Geographical distribution of *Zostera noltii* in Europe (adapted from Borum et al., 2004).

depth down to 5 m in the Mediterranean (Curiel et al., 1996). *Zostera noltii* adapts to water depth by adjusting its growing behaviour. In shallow water it produces dense, but short (17-22 cm) meadows while it produces longer leaves (up to 45 cm) at deeper sites (Auby and Labourg, 1996; Curiel et al., 1996). *Zostera noltii* is an euryhaline species that builds large meadows in high salinities (15-30), but tolerates brackish conditions down to a salinity of 7 and was even observed to survive salinity decreases to less than 5 (Charpentier et al., 2005). *Zostera noltii* is characterised by ribbon-shaped, dark green leaves that have an average length of 22 cm and a width of 0.5-1.5 mm. Leaves shoot from a short open sheath in groups of 2-5 (Figure 1.3). The root systems consist of creeping rhizomes that are 0.5-2 cm thick and the internodes have 1-4 roots each (Phillips and Meñez, 1988).

Being a perennial species, *Zostera noltii* shows a strong seasonality with high growth rates in spring and summer and a dormant phase in winter (Curiel et al., 1996). In winter, shoot densities are minimal and shoot length reduces to 6-10 cm. In spring, shoot density increases rapidly and can remain at its maximum length till September (Auby and Labourg, 1996). Sexual reproduction takes place regularly, with the flowering period being adjusted regionally, indicating a relationship with temperature. However, seeding was not found to be the preferred recruiting method in any *Zostera noltii* meadow investigated so far (Auby and Labourg, 1996; Curiel et al., 1996; Alexandre et al., 2006). Instead, meadow growth is based on vegetative

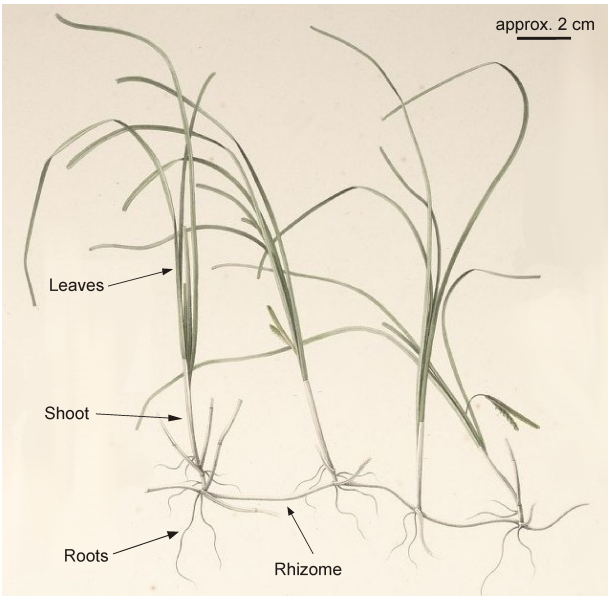

Figure 1.3.: Schematic diagram of *Zostera noltii* morphology (adapted from Hemprich and Ehrenberg, 1900).

reproduction. *Zostera noltii* is a very fast growing species that branches in almost each node (Brun et al., 2006). Ecologically, *Zostera noltii* plays an important role as a food source for migrating birds such as brent geese (*Branta bernicla*) and it is attributed a ground stabilising function (Den Hartog, 1970). Nevertheless, its silt-binding capacity is limited (Den Hartog, 1970) and vertical growth of rhizomes has been observed only once to date (Brun et al., 2005).

Zostera noltii is included in the IUCN Red List with the status Least Concern and the population trend 'decreasing' (IUCN, 2010), moreover it is classified as scarce in the list of Marine Natural Heritage Importance (Tyler-Walters, 2008). Seagrass beds are recognised internationally as important coastal ecosystems (Asmus and Asmus, 2000b,a) and *Zostera* beds are included in the OSPAR List of threatened and/or declining species and habitats for the regions I-IV and are considered as under threat in all locations (OSPAR, 2004). In the UK, it is included in the Habitat Action Plan under the UK Biodiversity Action Plan (Tyler-Walters, 2008).

It was chosen to investigate the effect of *Zostera noltii* on wave attenuation for various reasons:

1. *Zostera noltii* is one of two seagrass species around Britain and along European Atlantic coasts (Borum et al., 2004). The effect on wave attenuation of the other species, *Zostera marina*, was planned to be part of the research by a fellow PhD student. It was envisaged to compare results from both species in joint publications.

2. *Zostera noltii* shows a high seasonality in morphology (i.e. shoot density and leaf length). The influence of morphological parameters on wave attenuation has been observed in the laboratory (Fonseca and Cahalan, 1992; Bouma et al., 2005; Augustin et al., 2009; Prinos et al., 2010). Field studies on the effect of morphology are still lacking, mainly because data recording took generally place in summer and comparison of data from different study sites proves difficult as it may be affected by variation in bathymetry. The natural variation of shoot density and leaf length in *Zostera noltii* allows investigating the effect of those morphological parameters on wave attenuation in the same location and consequently over the same bathymetry.

3. Although *Zostera noltii* is highly abundant throughout Europe, only few studies addressed its interaction with hydrodynamics. In the past, research has focused on the larger *Zostera marina* and other non-European species. This study on *Zostera noltii* therefore complements previous research and expands the number of seagrass species which effect on wave attenuation has been quantified.

1.2.1. Previous work on *Zostera noltii*

So far, little work has been done on the influence of *Zostera noltii* on water movement. Thompson et al. (2004) investigated the influence of a *Zostera noltii* meadow on sediment erosion under unidirectional flow. Their experiments were conducted in the field using an *in situ* annular flume to generate defined flow velocities (Thompson et al., 2004). The results show that leaf bending leads to a closed canopy that

causes a skimming flow to develop when flow velocities exceed 0.5 m s^{-1}. Furthermore, the closed canopy reduces roughness and with it resistance which leads to reduced sediment erosion within the *Zostera noltii* meadow compared to a reference site over bare mud. The study was conducted during the dormant phase in February when shoot density and leaf length were at their minimum. However, the critical values are in agreement with other studies (Fonseca et al., 1982), but they are likely to vary throughout the year when the meadow starts growing back to its full extend. A similar study in the German Wadden Sea measured natural tidal flow over a mature *Zostera noltii* meadow. The experimental setup used to measure velocity profiles throughout a tidal cycle (Pasche and Deußfeld, 2003) did not allow for detection of a skimming layer as observed by Thompson et al. (2004). However, the results show that *Zostera noltii* can reduce flow velocities within the meadow by up to one third of the velocity above the canopy (Pasche and Deußfeld, 2003). The most recent study on the impact of *Zostera noltii* on flow was carried out in the laboratory to investigate the species' impact on waves in comparison to the salt marsh plant *Spartina anglica* (Bouma et al., 2005). During this study, various meadows of natural and artificial *Zostera noltii* shoots were exposed to regular waves and wave height reduction was recorded over a 2 m long transect of the meadow. Although the artificial shoots (5 mm wide) did not have the same dimensions as the natural *Zostera noltii* shoots ($\sim$1 mm wide) a good fit in bending angle and stiffness was obtained during flume experiments under unidirectional flow. Given this similarity, Bouma et al. (2005) showed that shoot density plays an important role in wave attenuation. They also observed a dependence of wave attenuation on the submergence ratio (defined as the ratio between water depth and vegetation height). While ratios of 1.2:1 would lead to wave attenuation of up to 22% at the highest shoot density (13,400 shoots/m^2), no wave attenuation could be observed at ratios of 2.4:1 (Bouma et al., 2005). To date, no field studies have been carried out to quantify wave attenuation by a natural *Zostera noltii* meadow.

1.3. Aims and Objectives

The aims of this thesis are:

1. To quantify the effect of a *Zostera noltii* meadow on wave attenuation. Previous field studies have addressed the effect of *Zostera noltii* on unidirectional flow (Pasche and Deußfeld, 2003; Thompson et al., 2004) and while wave attenuation by *Zostera noltii* was observed in the laboratory (Bouma et al., 2005), it has not yet been observed in the field. The first aim is therefore to measure wave attenuation across a natural *Zostera noltii* meadow, describe it with a friction factor and derive its drag coefficient. This field study will show whether laboratory results on *Zostera noltii* can be transferred into the field and consequently will improve the applicability of previous studies to the natural environment.

2. To measure changes in the impact of *Zostera noltii* on wave attenuation. Work on other species suggest that shoot density (Bouma et al., 2005; Chen et al., 2007; Augustin et al., 2009) and submergence ratio (Ward et al., 1984; Fonseca and Cahalan, 1992; Koch et al., 2006a) affect wave attenuation by vegetation. *Zostera noltii* shows high fluctuations in density throughout the year (Curiel et al., 1996) and grows in the intertidal zone where water depth changes over the tidal cycle. It is therefore expected that a change in wave attenuation by *Zostera noltii* should occur on short (hourly) and medium (monthly) time scales. Consequently, the second aim of this thesis is to determine changes in wave attenuation over a tidal and annual cycle.

3. This study finally aims to identify the main driving mechanisms influencing wave attenuation over *Zostera noltii*. It is hypothesised that plant specific (morphological) and location specific (wave and tidal conditions) parameters are the main influencing factors for wave attenuation by *Zostera noltii*, and thus this study will focus on these influences.

Morphological parameters under investigation are leaf length, shoot density and stiffness. As *Zostera noltii* is known to show high seasonality in above ground biomass (Curiel et al., 1996), it is proposed to determine how changes in biomass (i.e. leaf length and shoot density) affect wave attenuance throughout the year. Although shoot stiffness will not change within the species, this parameter is included in the study. Stiffness determines how much a plant moves under the influence of waves and currents. Depending on its stiffness, a plant will bend under a unidirectional current and the stiffer the plant the lower the bending angle at a given velocity (Fonseca and Koehl, 2006). Under waves, the plants will move back and forth with the orbital motion; plant stiffness will determine whether the shoots move in a cantilever or whip like motion. The movement will change from the former to the latter with increasing wave height and the rate of this transition varies with stiffness (Manca, 2010). Shoot stiffness is a species-specific parameter and by assessing its impact on wave attenuation, it can indicate how different seagrass species and vegetation types affect wave attenuation. Results of *Zostera noltii* may be placed in the wider context of submerged aquatic vegetation by including stiffness in this study.

To link wave attenuation to the measured morphological parameters of this study, it is necessary to monitor seagrass distribution and morphology across the area where waves are measured. While it is possible to record some morphological parameters such as leaf length and shoot density on foot or during dive visits at a particular site, it is labour intensive and thus impractical to carry out such a survey over a large area of several hectares (Warren and Peterson, 2007). Moreover, the plant coverage and canopy height are difficult to assess in sublittoral settings (Grillas et al., 2000). In areas with high turbidity, visibility during dive surveys may be too low to determine coverage of a larger area. Furthermore, site visits carried out on foot during low water in the littoral zone could not measure canopy height as the seagrass is usually lying flat. A secondary objective of this project is therefore to develop a widely applicable technique to map seagrass that also provides information on seagrass coverage and canopy height. Those two parameters define the seagrass'

physical roughness and an attempt is made to relate it to hydrodynamic roughness.

To evaluate the effect of hydrodynamic forcing, wave height and period are measured and the effect of an underlying steady current is assessed. Seagrass meadows can be exposed to a combination of natural sea state and boat wakes. Natural sea state is a combination of various wave heights and periods which change over time and space (Kamphuis, 2000). Artificial waves generated by boat wakes show a different steepness compared to natural waves (based on their ratio of wave height to period, Fonseca and Cahalan, 1992). One objective of this study is to investigate how different wave types (natural versus boat generated) are attenuated by *Z. noltii*. Differences between wave attenuation of natural waves and boat wakes by seagrass may need to be taken into account when assessing wave impacts in coastal areas. Finally, the effect of an underlying current is considered. Previous studies that addressed wave attenuation by vegetation were carried out in laboratory flumes where waves were generated in otherwise still water (Fonseca and Cahalan, 1992; Bouma et al., 2005, 2010) or at field sites with very low tidal influence (Ward et al., 1984; Nepf et al., 1997; Koch and Gust, 1999). While these studies helped to improve the general understanding of processes involved in wave attenuation by vegetation, their results may not be applicable to tidal environments where waves are accompanied by an underlying current. As *Zostera noltii* is an intertidal species, it can be exposed to high currents in addition to waves (de los Santos et al., 2010). It is thus important to determine the influence of currents on wave decay in order to quantify wave attenuation by *Zostera noltii* correctly.

1.4. Thesis outline

Chapter 2 presents the seagrass mapping technique that was developed to monitor seagrass coverage and canopy height. The method is based on a technique developed by Lefebvre et al. (2009) which was adapted to use in a wider range of environmental conditions. It was tested on three types of seagrass; *Zostera noltii* being one of them. The chapter is adapted from a manuscript published in Estuarine, Coastal and Shelf Science (Paul et al., 2011b).

Chapter 3 describes a field study on the evolution of natural waves and boat wakes across a *Zostera noltii* meadow along a transect perpendicular to the shore. The study was carried out in Ryde, Isle of Wight, over a duration of 13 months to capture changes in wave attenuation caused by seasonal variation of seagrass. The chapter is based on a paper published in the Journal of Geophysical Research - Oceans (Paul and Amos, 2011).

The work presented in Chapter 4 investigates in detail how leaf length, shoot density and stiffness affect wave attenuation by vegetation. Experiments were carried out under controlled conditions in a laboratory flume. Additionally, the effect of an underlying unidirectional current was investigated during these experiments. Seagrass mimics were used to disentangle the effect of morphological parameters. The mimic dimensions for this laboratory study are based on *Zostera noltii* which provides the link of these experiments to the previous chapters. The chapter is an adaptation from a manuscript submitted to Marine Ecology Progress Series (Paul et al., accepted) and a paper presented at the 5$^{\text{th}}$ International Short Conference on Applied Coastal Research (SCACR) in Aachen (Germany) in June 2011 (Paul et al., 2011a).

Finally, Chapter 5 summarises the main findings of this study. After a discussion in the wider context of wave attenuation by submerged vegetation a recommendation for future work is given.

2. An acoustic method for the remote measurement of seagrass metrics

2.1. Abstract

Seagrass meadows are ecosystems of great ecological and economical value and their monitoring is an important task within coastal environmental management. In this chapter, an acoustic mapping technique is presented using a profiling sonar. The method has been applied to three different sites with meadows of *Zostera marina*, *Zostera noltii* and *Posidonia oceanica* respectively, with the aim to test the method's applicability.

From the backscatter data the seabed could be identified as the strongest scatterer along an acoustic beam. The presented algorithm was used to compute water depth, seagrass canopy height and seagrass coverage and to produce maps of the survey areas. Canopy height was estimated as the distance between the bed and the point where backscatter values decrease to water column values. The algorithm was extended from previous methods to account for a variety of meadow types. Seagrass coverage was defined as the percentage of beams in a sweep where the backscatter 5-10 cm above the bed was higher than a threshold value. This threshold value is dynamic and depends on the average backscatter value throughout the water column.

The method is therefore applicable in a range of turbidity conditions. Comparison with results from other survey techniques (i.e. dive surveys, underwater videos) yielded a high correlation which indicates that the method is suited to measure seagrass coverage and height.

Analysis of the data showed that each seagrass species has a characteristic canopy height and spatial coverage distribution. These differences were used to undertake a preliminary species identification, as each species has a typical canopy height and preferred depth range. Furthermore, the results show that these differences can be used to track boundaries between species remotely. Finally, the application of the meadow distribution pattern to the health of a meadow is discussed.

2.2. Introduction

Seagrass meadows are highly productive ecosystems of ecological and economical importance. They provide shelter for juvenile fish and other animals (Connolly, 1994) and habitat for epiphytic algae and fauna that serve as prey for larger invertebrates and fish (Pihl et al., 2006). Additionally, the meadows provide food for herbivores that graze on the leaves (Heck and Valentine, 2006). Seagrass meadows are also recognised as stabilisers of the coast, binding sediments with their root systems (Den Hartog, 1970) and attenuating waves and currents (Gambi et al., 1990; Fonseca and Cahalan, 1992; Lefebvre et al., 2010). Preservation and restoration of seagrass beds are therefore essential goals of coastal environmental management programs and require regular mapping of the seagrass meadows (Dennison et al., 1993).

Various techniques have been used in the past to map and monitor seagrass, including physical sampling, optical and acoustical methods. Physical sampling by divers provides accurate localised data, but is time and labour intensive, especially if a large area is to be surveyed regularly. Optical methods, based on satellite or

aerial imagery, can be applied reliably in intertidal areas when images are taken during low tide. In the sublittoral zone those methods are limited by cloud coverage, sea surface roughness and water clarity (Vis et al., 2003). An alternative option is the use of a towed underwater video camera which can give a detailed record of abundance and species composition (Norris et al., 1997; McDonald et al., 2006). But here, data quality is limited by water clarity and interpretation of the video is time-consuming and subjective (Crawford et al., 2001; Short et al., 2007).

Within the acoustic domain, side-scan and multi-beam sonars, as well as unidimensional single beam instruments such as echosounders and current profiling sonars, have been used to map seagrass (e.g. Duarte, 1987; Warren and Peterson, 2007). The principle behind the use of an acoustic technique is that a strong acoustic backscatter arises from changes in the medium the sound travels through. These changes take place at the water-bottom and the water-plant interfaces, but sources of scatter also include bubbles, suspended sediment, organisms (i.e. fish) and even salinity and temperature gradients (Lavery et al., 2003; Warren et al., 2003). Seagrasses contain a system of gas-filled lacunae that provides gas exchange between organs and buoyancy to the leaves (Phillips and Meñez, 1988). Moreover, the lacunae increase the contrast in acoustic impedance between seagrass leaves and the surrounding water and hence are one factor for increased backscatter intensity at the water-plant interface. In shallow water environments, vegetation and the seabed generally contribute most to backscatter intensity and can be discriminated from other sources (Warren and Peterson, 2007).

Side-scan sonars provide maps of seagrass distribution and qualitative changes in coverage, but they do not give a measure of canopy height or bathymetric depth (Pasqualini et al., 1998). Moreover, data from towed systems such as side-scan sonars are difficult to position accurately and data quality decreases in shallow water where the instrument movement is affected by roughness on the water surface (Kenny et al., 2003). It is possible to acquire data on canopy height from multi-

beam sonars, but instrument cost might be disproportionate to acquired data as the efficiency of survey area decreases with water depth (Komatsu et al., 2003).

Echosounders and Acoustic Doppler Current Profilers (ADCPs) have been used to estimate the presence of a canopy and height of submerged aquatic vegetation (SAV) (e.g. Warren and Peterson, 2007; Sabol et al., 2009). Both systems sample in one dimension and only provide data along a narrow track directly underneath the instrument. A study in the Caloosahatchee estuary used a high frequency narrow beam digital echosounder to measure canopy geometry of three different seagrass species but was not able to discriminate between them (Sabol et al., 2002). The system was able to detect vegetation down to canopy heights of 7 cm and low biomass (60 g m^{-2} wet weight), but used a commercial system for data processing (Sabol et al., 2009).

ADCPs are designed to measure velocity profiles throughout the water column. However, ADCP data appears to be suitable to identify SAV populations and quantify canopy height. Warren and Peterson (2007) showed that the maximum backscatter value can be identified as the seabed and the point with the largest change in backscatter intensity gives a good proxy for the top of a *Zostera marina* canopy. However, many ADCPs lack the vertical resolution to measure canopy height with accuracy at centimetre scale.

An important part of the structural description of a seagrass meadow is an estimation of the seagrass coverage, expressed as a percentage of area covered by plants with respect to the area not covered (Buia et al., 2004). In the past, estimation of coverage required divers or remotely operated vehicles to either assess coverage visually (Grillas et al., 2000) or by counting presence and absence of the SAV in a grid. The latter can be done directly *in situ* or can be derived from photographs taken vertically from a fixed distance above the bed (Buia et al., 2004). Single beam echosounders lack the ability to quantify spatial coverage or density of SAV to either side of the survey track, since they cover a line rather than an area during

surveying. ADCPs may be able to provide some spatial coverage based on the slope of the backscatter intensity above the bottom (Warren and Peterson, 2007), but this method has not yet been validated in detail.

Lefebvre et al. (2009) used a Sediment Imaging Sonar (SIS) to record a high-resolution acoustic image of the seabed and the water column. This single beam sonar has a rotating head and therefore acquires data two dimensionally, i.e. directly below the instrument and to either side of the ship's track. The instrument can be mounted on the ship's hull and can therefore be positioned more accurately than towed systems. Hull mounting also allows the use in shallow water where data quality from towed systems would be poor due to water surface movement. In water deep enough for towed systems, multi-beam sonars can provide a higher resolution dataset on canopy height and coverage than the SIS. However, the SIS is a cost effective alternative as instrument costs are lower and surveys can be carried out at higher boat speeds due to hull mounting. The SIS is able to sample at high vertical resolution (centimetre scale) which allows a higher accuracy in estimating canopy height than ADCP based surveys and the instrument settings allow adjusting the sweep angle and therefore the horizontal area covered per sweep.

Lefebvre et al. (2009) surveyed within an angle of 46.8° centred downward which yielded a length of bed surveyed per sweep approximating water depth (bed length = water depth ±16%). From these data they were able to compute water depth and canopy height directly below the instrument head as well as seagrass coverage for a *Zostera marina* meadow for the entire sweep. It gave both the height of the canopy and quantitative information of spatial coverage. A disadvantage of the method is that calculations of canopy height are based on threshold values that were found empirically for a particular study site (Lefebvre et al., 2009). These values may vary for different seagrass species, different locations or even different seasons when turbidity, salinity and/or temperature vary from the ones in the described study.

To date, the SIS has been deployed over *Zostera marina* beds only. In order to

test whether the SIS is able to map and quantify different species of seagrass it was deployed over two additional meadows of *Zostera noltii* and *Posidonia oceanica* respectively. Additionally, the computation method was revised herein to reduce the influence of site specific empirical parameters. Moreover, the algorithm was extended to better distinguish between unvegetated beds and seagrass canopies with an inhomogeneous backscatter profile and hence to detect other seagrass species. The main aim of this study was to compare data collected with the SIS over the three different seagrass species and explore whether the instrument, in combination with the improved method of analysis, could be used to detect different seagrass species and even distinguish between them. The ability to discriminate between species would give the advantage of using the method to monitor seagrass extent and species boundaries within mixed meadows. A second objective of this study was to produce quantitative maps of seagrass coverage, a parameter that can be used to identify a meadow's health. By quantifying this parameter the presented method could provide a means of comparing coverage of seagrass meadows between sites as well as over time.

2.3. Material and Methods

2.3.1. Calshot, U.K. – *Zostera marina* site

Zostera marina is the dominant seagrass species in the northern Atlantic, but is also widely distributed in the northern Pacific (Short et al., 2007). Its ribbon-shaped, dark green leaves generally grow 20-50 cm in length (although lengths up to 3 m have been observed) and vary in width between 2 and 10 mm (Fonseca and Cahalan, 1992). Shoots grow from rhizomes which spread to form extensive meadows in sheltered, sublittoral (3 to 13 m below mean sealevel) waters with a growth maximum around the spring low water mark (Den Hartog, 1970; Tubbs and Tubbs, 1983; Den Hartog, 1994).

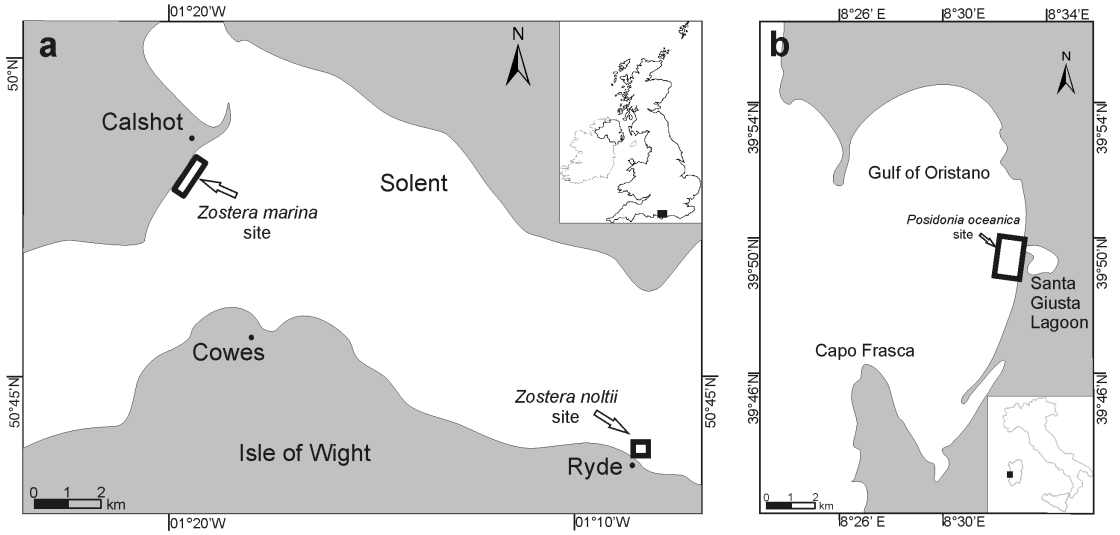

Figure 2.1.: Locations of survey sites for a. Calshot (*Zostera marina*) and Ryde (*Zostera noltii*), and b. Oristano (*Posidonia oceanica*).

The *Zostera marina* meadow mapped during this study is situated off Calshot beach, in the West Solent on the English south coast (Figure 2.1a). The beach is an extension of Calshot spit which has been morphologically stable for the last 125 years (Lobeck, 1995) and consists of gravel with sandy patches. The site is sheltered by the Isle of Wight and consequently waves are generally small, however suspended particulate matter (SPM) concentrations of 30 mg/L lead to low visibility (Collins and Ansell, 2000). The tidal range is 2 m during neap tides and reaches 4 m over spring tides. Only the latter exposes the lower intertidal zone, situated between 2.7 m and 1.7 m below mean sealevel (MSL). In this area *Zostera marina* can be observed during extreme low tides and the meadow's extension below the low water line was mapped in 2007 (Lefebvre et al., 2009).

A boat-based survey of the site was carried out around spring high tide on 12$^{\text{th}}$ September 2007 during calm conditions. In addition to the SIS, a towed underwater video camera (Divecam-550C from Bowtech Products Ltd., Aberdeen, UK) was deployed. It was mounted downward on a sledge and towed approx. 20 m behind the vessel to obtain coverage measurements of the survey area (Lefebvre et al., 2009). A total area of 44.6 ha was covered within four survey lines parallel to the shore,

each approximately 1.5 km long and spaced 50-100 m apart. The site was visited from the shore and by divers prior to the survey to obtain information about leaf length and shoot density. On 24th and 31st July 2007, SCUBA divers surveyed 20 locations within the area, using a 30 x 30 cm quadrat to measure shoot density. Leaf lengths from the base to leaf tip were measured with a tape measure to the nearest centimetre and the 10 longest leaves were measured at each location. The same quadrats were used at 17 locations that were visited on foot during low tide on 2nd and 3rd August 2007. A more detailed description of these surveys can be found in Lefebvre et al. (2009).

2.3.2. Ryde, U.K. – *Zostera noltii* site

Zostera noltii is a temperate European species that is highly abundant along the Atlantic coasts of Europe and around the British Isles; its distribution stretching from southern Norway in the north to Mauritania in the south (Den Hartog, 1970). It is an intertidal seagrass that is highly abundant between mean high and low water neaps, but can be found in depths down to 5 m in the Mediterranean (Van Lent et al., 1991; Auby and Labourg, 1996; Curiel et al., 1996). Its dark green leaves are ribbon-shaped with a width of 0.5-1.5 mm and a length of approximately 20 cm (Phillips and Meñez, 1988). *Zostera noltii* shows strong seasonality with high growth rates in spring and summer and a dormant phase in winter (Curiel et al., 1996).

The surveyed *Zostera noltii* meadow is located on the north coast of the Isle of Wight, across the Solent from Calshot (Figure 2.1a). It covers approximately 40 ha of Ryde Sand, an intertidal sand flat extending from a recreational beach. The sand flat is composed of fine sand (Tonks, 2008) and is uniform in appearance with a mean slope of 1:550 from the backing seawall towards the low water line. Like the Calshot site, Ryde Sand is sheltered from swell of the English Channel by the Isle of Wight, and incoming waves are small. The tidal range varies from 2 m for neap tides to 4 m for spring tides. During low tides, *Zostera noltii* can be observed between

0.7 and 2.7 m below MSL, and is succeeded by *Zostera marina* at the lower boundary.

A boat survey was carried out on 8th June 2009 during a spring high tide. In total, 10 lines were recorded during a 2.5 h survey, six of them running parallel to the shore and four perpendicular. Lines were spaced 30-80 m apart and a total area of 24 ha was covered. Conditions were calm during most of the survey, but towards the end, chop caused considerable rolling of the boat during the survey of the lines perpendicular to the shore. The site was re-visited on foot during low tide on 24th June 2009 to measure leaf lengths and to identify seagrass species and coverage at designated locations within the survey area. Leaf lengths were measured from leaf base to tip with a ruler to the nearest 0.5 cm at four locations within a 30 x 30 cm quadrat and at each location 10 randomly chosen replicates were taken. Photographs were taken at eight designated locations with a digital camera positioned vertically 1.2 m above the ground and each photograph covered approx. 0.5 m^2 of seabed. Percent coverage was estimated by overlaying the photos with a regular grid in CorelDRAW©. All positions during this survey were recorded with a handheld GPS (Garmin, accuracy ±5 m).

2.3.3. Oristano, Italy – *Posidonia oceanica* site

Posidonia oceanica is a large perennial seagrass species endemic to the Mediterranean Sea. The plant has ribbon-like leaves, 1 cm wide and up to 0.75 m long (Buia et al., 2004), and is characterised by stiff vertical and horizontal rhizomes. The oldest leaves senesce and detach from the rhizome during the first autumn storms (Mateo et al., 2003). Average leaf length can vary seasonally, whilst in a healthy meadow, stem density generally varies little over time (Gacia and Duarte, 2001). *Posidonia oceanica* meadows have been observed in shallow areas where they form discrete patches and occur in reticulate to continuous beds in deeper waters until coverage becomes patchy again at the lower boundary of the meadow (Borg et al., 2005) which can be found in a depth up to 50 m in clear water conditions

(Buia et al., 2004). *Posidonia* colonises several types of substrata from sandy beds (De Falco et al., 2000; Lasagna et al., 2006) to rocky shores (Cancemi et al., 2000). It can also grow on old matte reefs that are an ensemble of root systems, rhizomes of the old plants and sediment (Ballesta et al., 2000).

The *Posidonia oceanica* meadow surveyed for this study is located in the microtidal Gulf of Oristano (west coast of Sardinia, Italy) near the small fishing harbour at the inlet of the Santa Giusta Lagoon (Figure 2.1b). The area is located in the central part of an asymmetrical 20 km long sandy beach, interrupted only by the mouths of several coastal lagoons and the Tirso River. The site is exposed to swell from the southwest and to the prevailing north-westerly winds and it is characterised by a shallow *Posidonia oceanica* meadow. The study area extends to a maximum depth of about 8 m and the intertidal area was not surveyed.

A survey was conducted in the Gulf of Oristano on 13th and 14th May 2007. A total of 17 lines were surveyed with a line spacing of about 100 m. On 14th May, visual observation of the seabed from the vessel allowed direct comparison with SIS real time data due to high water clarity (SPM 8 mg/L). Moreover, *Posidonia* shoot density and leaf lengths were measured by divers. The stem density was recorded at 14 stations using a 50 x 50 cm standard sampling quadrat following the sampling method of Duarte and Kirkman (2001). Leaf length was measured to the nearest 0.5 cm from the leaf base to the leaf tip of 5 randomly chosen leaves at each station using a ruler. The stations were randomly picked along a cross-shore transect.

2.3.4. Survey methodology

The SIS surveys were carried out using the R.V. Bill Conway in Calshot and Ryde and a small dory in Oristano. During all three surveys, the same SIS was deployed on a downrigger on the starboard side of the boat (Figure 2.2a) and positions were recorded with the onboard differential GPS (Trimble, submetre resolution) on R.V. Bill Conway and a Garmin GPS (resolution $\pm$1 m) during the survey in the Gulf

Table 2.1.: Instrument settings and survey specific parameters for all three survey sites.

	Calshot	Ryde	Oristano
transmit pulse [μs]	40	40	62
vertical resolution [cm]	1.5	1.5	4.7
sweep angle range from downward vertical [°]	-23.4 to 23.4	-22.5 to 22.5	-35 to 55
sweep rate [s]	10.4	10.0	20.0
depth of transducer head below surface [m]	0.94	0.72	0.80
water temperature [°C]	18.3	16.2	19.3
salinity [-]	34.8	32.4	37.6
absorption coefficient [dB km^{-1}]	0.391	0.397	0.395
velocity of sound [m s^{-1}]	1516	1506	1522
boat speed [m s^{-1}]	1	1	2

of Oristano. The SIS (Marine Electronics Ltd.) is a high frequency (1.1 MHz), profiling single beam sonar that records an acoustic image of the water column and underlying seabed for each sweep (Figure 2.2a). The instrument recorded continuously and each sweep was recorded in 10-20 s, depending on total sweep angle (Table 2.1). The sweep rate, in conjunction with the boat speed, led to a zigzag track of data recording (Figure 2.2b) during which 10-40 m of boat track were covered. The lateral extent of each sweep depended on water depth and sweep angle and varied between 1.5 and 11 m. The Sediment Imager converter 1.0 (Marine Electronics Ltd.) was used to convert the images data into an ASCII file containing beam angle, distance from transducer head and backscatter. Backscatter data are returned uncalibrated as linear relative integer values (0-255) and the instrument does not incorporate a time-variable gain circuit. Comparing uncalibrated backscatter data can cause inaccuracies, because seawater absorbs sound differently when temperature and salinity change (Roe et al., 1996). For this study the inaccuracies are considered small, because all temperature and salinity profiles showed well-mixed water columns and absorption coefficients (Ainslie and McColm, 1998) did not differ significantly between sites (Table 2.1).

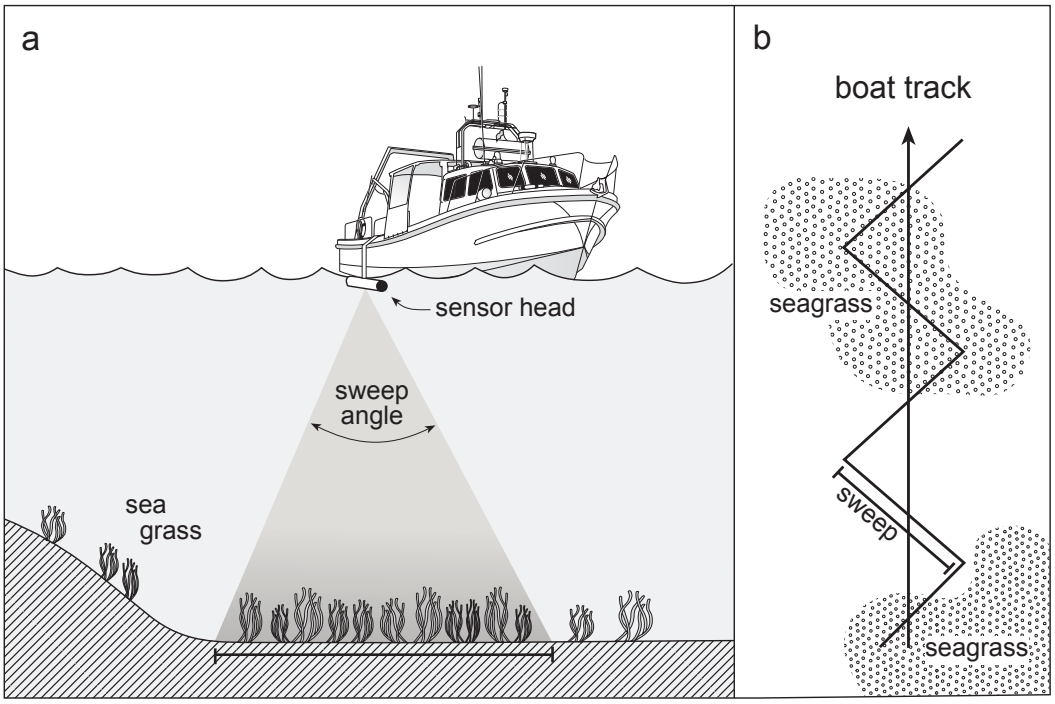

Figure 2.2.: Schematic setup of the SIS during survey. a. The shaded area highlights the part of water column and seabed recorded during a sweep; b. The position of sweeps with respect to the boat track (not to scale). Each sweep is composed of 53 to 103 beams along which 21 to 67 data points (bins) were recorded per metre of water depth.

Table 2.1 summarises the SIS settings used during surveys and a detailed description of the instrument can be found in Lefebvre et al. (2009). Within a sweep, beams were 0.9° apart and horizontal resolution along a sweep therefore depended on water depth and beam angle from the vertical; it was independent from the sweep angle. At a water depth of 4 m, for example, horizontal resolution directly below the sensor head was 6.3 cm and at the edge of the sweep horizontal resolution was 7-9 cm, depending on total sweep angle (Table 2.1). Vertical resolution depended on the transmit pulse duration and varied between 1.5 and 4.7 cm for the respective surveys (Table 2.1). To acquire accurate depth values from the acoustically obtained image the correct value for velocity of sound was entered into the software prior to starting the survey. The required value was computed *in situ* from temperature and salinity measurements at each site respectively (Table 2.1).

2.3.5. SIS data processing

Data for each sweep were processed individually following the approach of Lefebvre et al. (2009). The data close to the transducer head were considered as noise due to reflections from the water surface and the transducer head. Therefore the first 0.5 m below the transducer head were excluded from the analysis. Within the remaining profile, the depth of the maximum backscatter along each beam was defined as the depth of the seabed. Thereafter, the height of the canopy and coverage were calculated as follows.

Canopy height

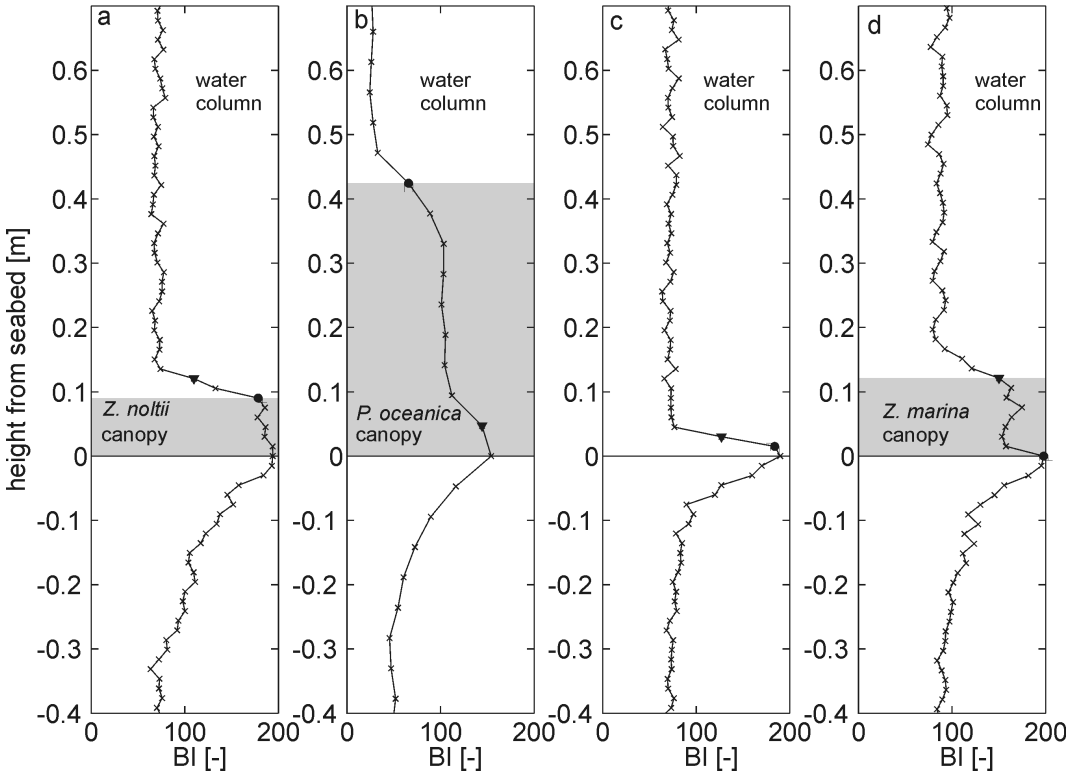

Figure 2.3.: Backscatter intensity (BI) profiles for different vegetation types. The seabed was identified at the maximum backscatter value and set to zero. The dots represent the depth at which the difference of backscatter intensity ($\Delta back_m$) to the bin above is highest and the triangles represent the second highest value ($\Delta back_2$). Values below zero are from the substratum and the grey area indicates the seagrass canopy. a. *Zostera noltii*; b. *Posidonia oceanica*; c. unvegetated bed; d. *Zostera marina*.

To eliminate distortion due to beam angle, canopy height for each sweep was calculated from a vertical profile of backscatter intensity perpendicular to the seabed. Such a profile was achieved by averaging over the five centre beams of each sweep which reduced variability and resulted in an average beam angle of 0° (Lefebvre et al., 2009). To obtain information about canopy height and therefore identify the presence or absence of seagrass, a method similar to the one employed by Warren and Peterson (2007) to assess SAV coverage from ADCP data was adopted. The method differs from the one used by Lefebvre et al. (2009) which was purely empirical. Warren and Peterson's (2007) method was adapted by introducing the use of the second highest difference in backscatter intensity to distinguish between unvegetated profiles and vegetated profiles that show high backscatter values mainly in the upper part of the canopy. The algorithm consequently improves accuracy compared to previous methods.

To estimate canopy height the difference in backscatter intensity ($\Delta back$) between bins along the averaged beam was calculated as:

$$\Delta back_n = BI_n - BI_{n-1} \tag{2.1}$$

where BI is the backscatter intensity at the n^{th} bin and the bin with n = 1 is closest to the transducer head. This definition yields positive values when a bin has a higher backscatter intensity than the bin above. Backscatter profiles within the *Zostera noltii* meadow showed a region of high values just above the bed with a rapid drop in backscatter to water column values (Figure 2.3a). Profiles within the *Posidonia oceanica* meadow also had almost constant values throughout the canopy and showed maximum backscatter intensity ($\Delta back_m$) at the top of the canopy, but values within the meadow were lower than the maximum backscatter intensity at the bed (Figure 2.3b). In unvegetated areas, $\Delta back_m$ was found at or close to the bed (Figure 2.3c). Therefore, the top of the seagrass canopy was identified as the maximum backscatter difference and the canopy height s was computed as:

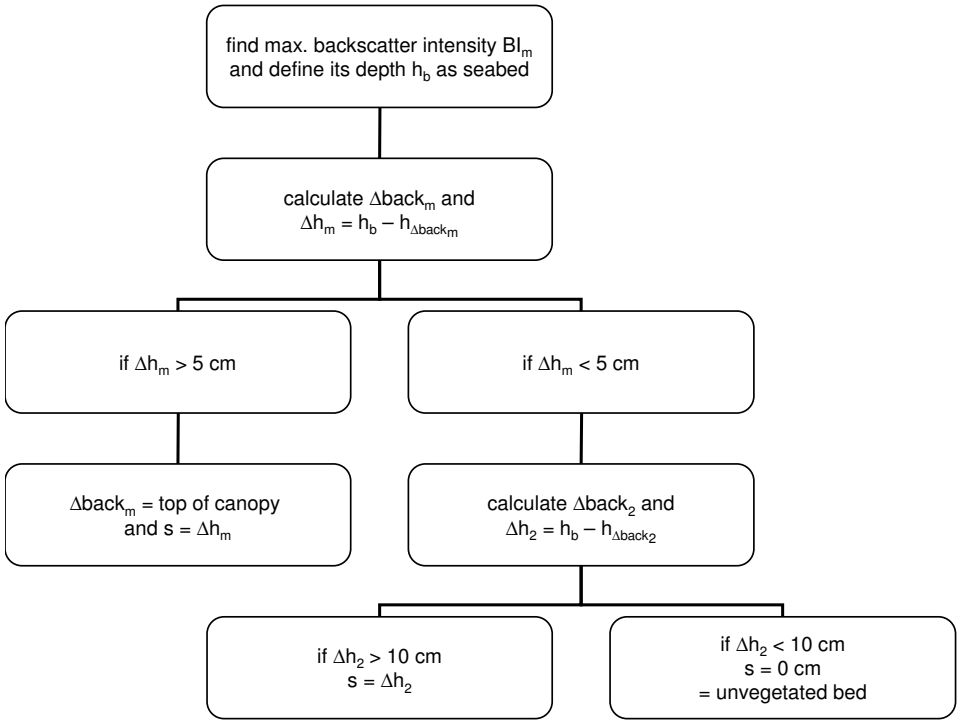

Figure 2.4.: Schematic of method for determining canopy height.

$$s = h_b - h_{\Delta back_m} \tag{2.2}$$

where h_b is the depth of the seabed and $h_{\Delta back_m}$ is the depth of $\Delta back_m$. Within the *Zostera marina* meadow, however, many of the backscatter profiles showed a different behaviour, with the upper edge of the canopy clearly distinguishable in the profile but $\Delta back_m$ located at or near the bed (Figure 2.3d).

In order to correctly evaluate canopy height in those profiles, the second highest difference in backscatter intensity between adjacent bins ($\Delta back_2$) was calculated if $\Delta back_m$ was at or within 5 cm of the seabed. Two scenarios were then identified (Figure 2.4): either $\Delta back_2$ was less than 10 cm above the seabed or it was $\geq$10 cm above the seabed. In the first case the location was identified as unvegetated while in the second case the position of $\Delta back_2$ was defined as the top of the canopy and

$$s = h_b - h_{\Delta back_2} \tag{2.3}$$

with $h_{\Delta back_2}$ being the depth of $\Delta back_2$, was used instead of eq. 2.2. The threshold of 10 cm was found empirically and the approach gave good agreement (72%) of canopy height values with observed canopy heights in the backscatter profiles with the shape shown in Figure 2.3d. Consequently, it was applied to the data from all three sites. To reduce computation time and the effect of noise in the water column, the difference in backscatter intensity was calculated for a defined region above the bed only. It was set to 0.8 m for all three surveys, but could be adjusted to match an expected maximum canopy height for future surveys.

Coverage

Seagrass coverage was calculated as the percentage of beams in a sweep that contained seagrass. Using an approach similar to Lefebvre et al. (2009), backscatter values of three bins were averaged ($\overline{BI_b}$) in an area just above the bed. Bins closer than 5 cm to the bed can still show increased backscatter values due to scattering from the bed and were not considered reliable when identifying the presence or absence of vegetation. The three averaged bins therefore started with the first bin that was at least 5 cm above the bed (Figure 2.5). This region was chosen because high backscatter values close to the bed indicated seagrass coverage irrespective of species and the method could therefore be applied to all three survey sites. The averaged value for each beam was compared to a threshold value of the form

$$\theta_{BI} = \overline{BI_w} + p \tag{2.4}$$

with $\overline{BI_w}$ being the background backscatter value and p being a constant. $\overline{BI_w}$ was defined for each sweep as the mean backscatter intensity of the water column between 0.5 m below the instrument head and 0.8 m above the bed, and was calculated along the profile averaged over the five centre beams (Figure 2.5). The constant p was added to generate the threshold value for identification of seagrass presence. The value $p = 50$ was found empirically for all three sites and was consistent with the

constant value of 120 used by Lefebvre et al. (2009) in Calshot. Finally, a beam was defined as containing seagrass if

$$\overline{BI_b} > \theta_{BI} \tag{2.5}$$

As the threshold value was defined relative to background backscatter values throughout the water column (eq. 2.4) the method was independent of changing backscatter values due to turbidity.

It would be possible to geo-reference each beam in a sweep and hence obtain high resolution coverage data. However, as the length of seabed covered per sweep is small compared to the lengths of survey lines in this study, it would not be possible to present the whole dataset in a sufficient resolution. It was therefore decided to express seagrass coverage as the percentage of beams in a sweep with a backscatter intensity value that satisfies eq. 2.5, i.e. beams that contain seagrass, and hence give one coverage value per sweep. This provides a spatial average for a sweep length of, in this case, 1.5 to 11 m, depending on water depth and sweep angle.

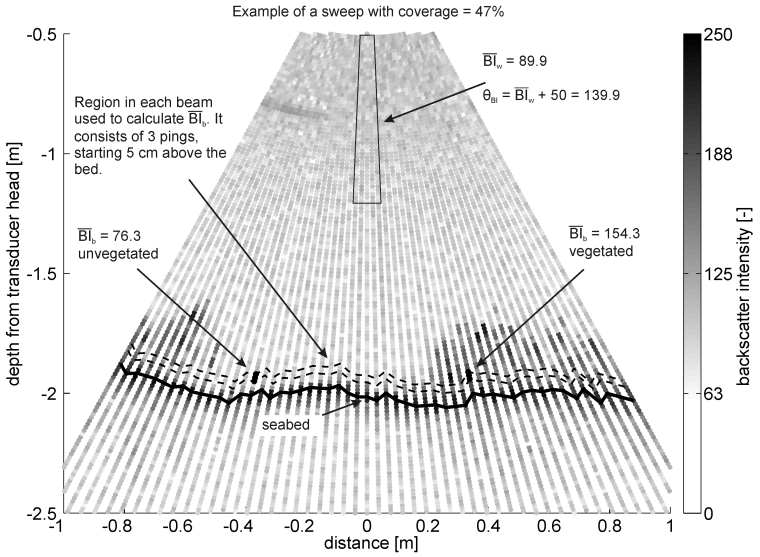

Figure 2.5.: Calculation of coverage for a sweep. $\overline{BI_w}$ is calculated using the five centre beams from 0.5 m below the sensor head to 0.8 m above the bed. A beam was identified as containing seagrass if $\overline{BI_b} > \overline{BI_w} + 50$.

Spatial alignment

Navigation data were used to plot the spatial distribution of the survey lines and linear interpolation was used to generate a regular spacing along the track plot. Subsequently, results from the SIS data were assigned to their sampling locations on the track plot using the file time stamp. Additionally, the depth of the seabed was corrected for the depth of the transducer head below the surface and the tidal height during the survey (after Lefebvre et al., 2009) to yield bathymetric data relative to mean sealevel along the survey lines. Maps were generated in arcMAP® and bathymetric data were interpolated using the Natural Neighbour interpolation with a raster cell size of 5 m in Calshot and Ryde and 10 m in Oristano. All depths in this chapter are given below mean sealevel (MSL) to provide a comparison between the different study sites.

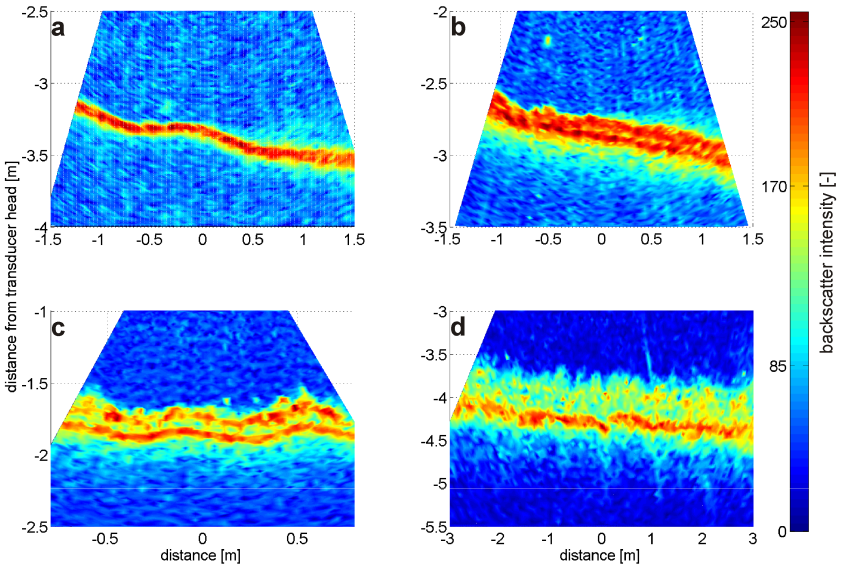

Figure 2.6.: Examples of SIS sweeps over a. unvegetated seabed; b. *Zostera noltii*; c. *Zostera marina* and d. *Posidonia oceanica*. The strongest backscatter is on the seabed while a strong backscatter above the seabed shows the presence of seagrass. Distance along the x-axis is given as distance from the centre beam of the sweep and the length of seabed covered by the sweep depends on water depth. The image of an undulating seabed is caused by ship movement.

2.4. Results

A total of 3,684 sweeps were recorded during the surveys. Within all sweeps the strongest backscatter intensity represented the seabed irrespective of seagrass presence (Figure 2.6). Manual inspection of all vertical profiles confirmed that the algorithm correctly identified the seabed in all cases, resulting in bathymetric information along the survey lines.

2.4.1. Calshot

For more than 99% of the 1,786 profiles processed for the Calshot site canopy height values were within the expected height range (20-50 cm) of *Zostera marina*. For 10 profiles, the values were above the expected height range and visual inspection identified the profiles as outliers, where $\Delta back_m$ was located at the bed and $\Delta back_2$ was higher up in the water column due to noise or the presence of another scatterer, e.g. fish or algae. Figure 2.7a shows the distribution of canopy heights. The cleaned distribution (canopy height $<$ 50 cm) has a mean value ($\pm$standard deviation) of 15$\pm$7 cm and a skew of 1.1.

The present method showed high canopies ($>$0.2 m) in the centre of the survey area in a depth of 2.5 to 2.0 m (Figure 2.9a), which agrees well with the high canopy values ($>$0.15 m) found for the same area by the previous study (Lefebvre et al., 2009). This high canopy continued to the northern end of the survey area where *Zostera marina* had been observed during on-foot surveys at low tide. Additionally, values of 0.15-0.2 m were found along the western edge of the survey area where seagrass presence was clearly seen on aerial photographs (CCO, 2009). Seagrass coverage showed the same spatial distribution as the canopy height with maximum values ($>$60%) in the centre of the survey area and scarce seagrass abundance ($<$25%) in shallow areas ($<$1.5 m) and along the central part of the survey line closest to shore (Figure 2.9b).

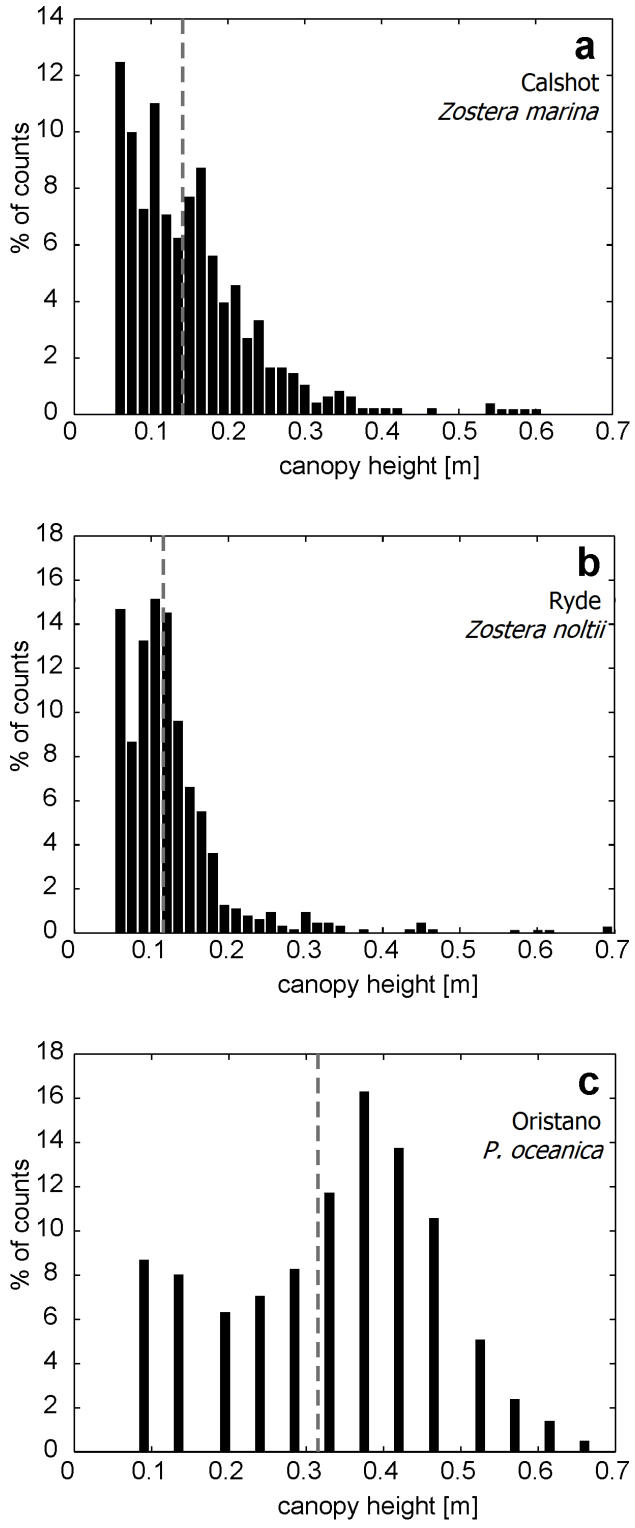

Figure 2.7.: Histograms of canopy height for a. Calshot (n = 1786); b. Ryde (n = 890) and c. Oristano (n = 1008). Bin size is 1.5 cm in all cases and the different appearance of c. is caused by the difference in the dataset's vertical resolution (Table 2.1). The dashed line indicates the mean value.

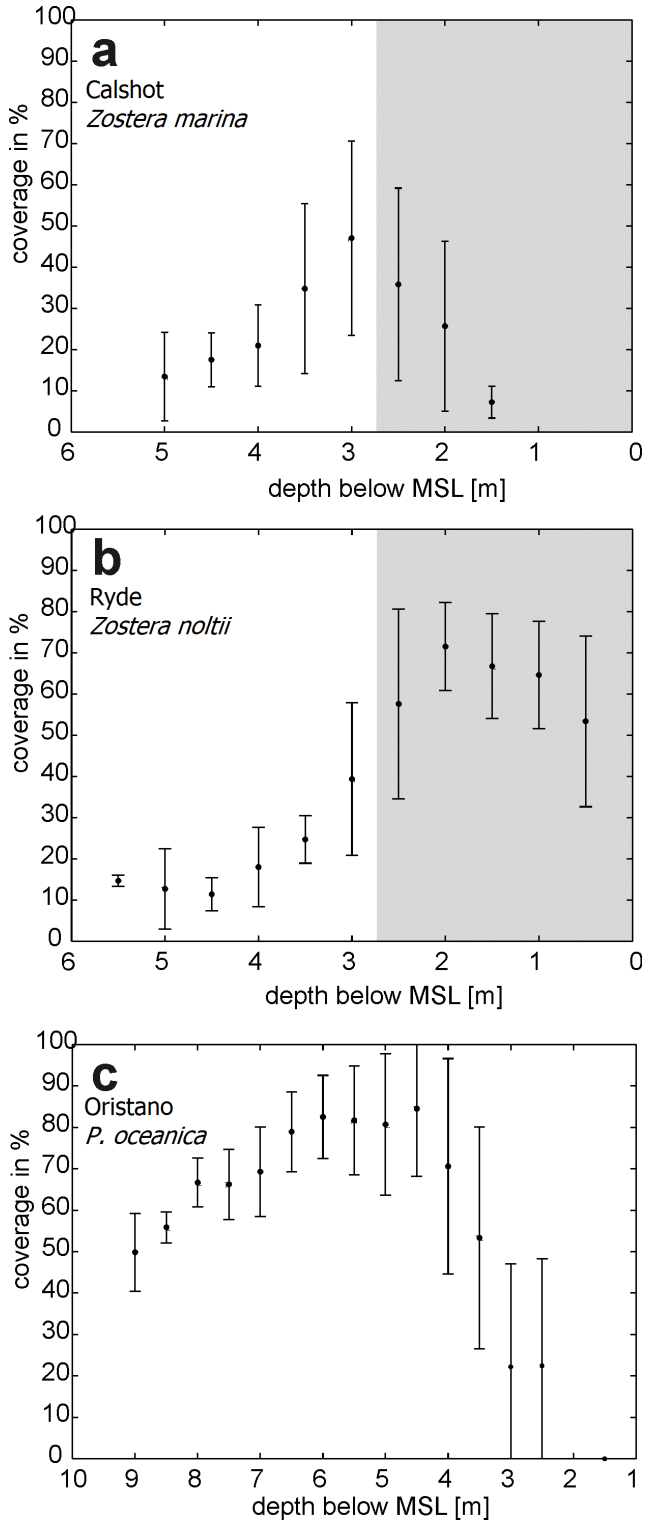

Figure 2.8.: Seagrass coverage in % per sweep in relation to water depth for a. Calshot (n = 1776); b. Ryde (n = 884) and c. Oristano (n = 1008). Data are pooled in 0.5 m bins. The grey areas indicate the intertidal zone above lowest astronomical tide; note that the intertidal was not covered in Oristano.

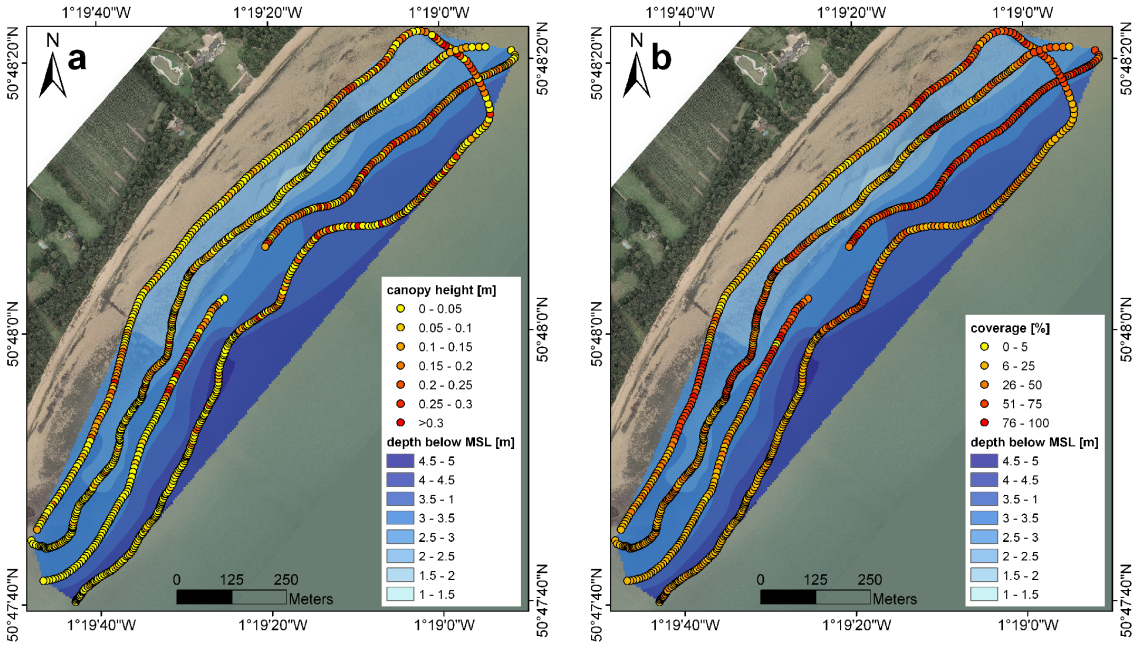

Figure 2.9.: Spatial distribution of a. canopy height and b. coverage for Calshot. Bathymetry was interpolated (Nearest Neighbour in arcMAP®) from seabed depth with a cell size of 5 m. Aerial photo (2005, ortho-rectified) courtesy of the Channel Coastal Observatory (CCO, 2009).

With decreasing depth, coverage increased until it reached a peak of 47±23% just below the lowest astronomical tide at 3 m. Coverage dropped to values of less than 10% in depths of 1.5 m with further decreasing depth (Figure 2.8a). This agrees well with the species depth distribution (sublittoral, with a preference for the upper sublittoral). Coverage was generally low (<50%) which corresponds with the results from the video survey where the majority of the area was classed as small (decimetre) patches (Lefebvre et al., 2009).

2.4.2. Ryde

At Ryde, 6 profiles resulted in canopy heights of more than 0.5 m which could be identified as outliers by visual inspection of the profiles with $\Delta back_m$ at the bed and $\Delta back_2$ located higher up in the water column due to noise or other sources of scattering. They were removed from the dataset, while the remaining 884 profiles yielded canopy heights within the expected range of up to 0.5 m for *Zostera* sp.

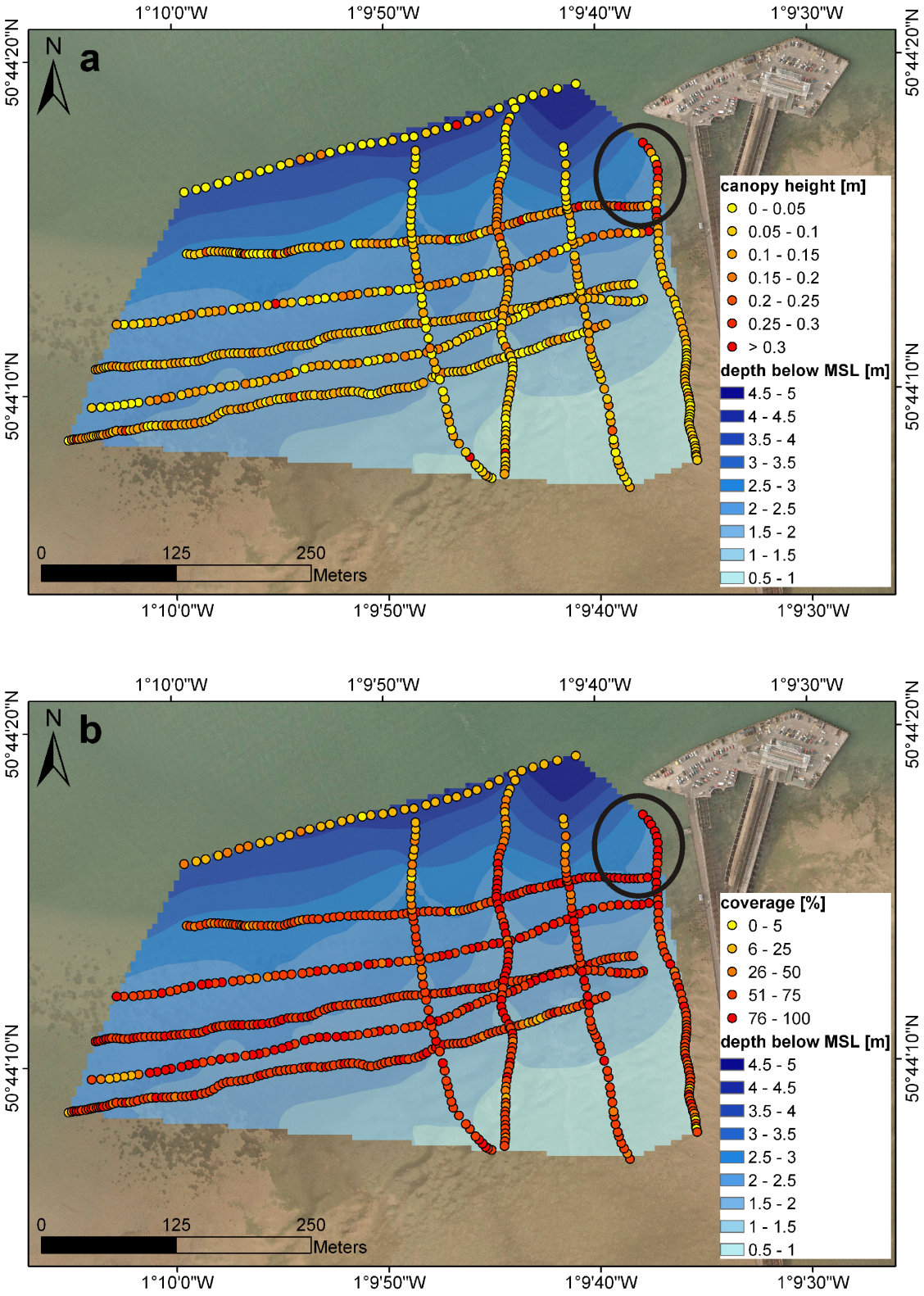

Figure 2.10.: Spatial distribution of a. canopy height and b. coverage for Ryde. Bathymetry was interpolated (Nearest Neighbour in arcMAP®) from seabed depth with a cell size of 5 m. The undulations in the depth contours are an artefact from the survey line spacing. The circle marks the area where *Zostera marina* was identified. Aerial photo (2005, ortho-rectified) courtesy of the Channel Coastal Observatory (CCO, 2009).

The mean canopy height for the cleaned distribution (canopy height $<$ 50 cm) in Ryde was 12±6 cm and the population had a pronounced positive skew of 2.3 (Figure 2.7b). The spatial distribution of canopy height in Ryde showed a fairly homogeneous canopy in the central region of the survey area (Figure 2.10a), mainly in depths between 1 and 2 m, and the on-foot survey confirmed the presence of *Zostera noltii* throughout this region. Canopy height values in the northeast corner of the survey area were unexpectedly high for *Zostera noltii*. Both, the central region and the northeast corner were characterised by >75% coverage (Figure 2.10b). Coverage reduced slightly towards the shore and dropped to low values at the northward edge of the survey area. Here the bathymetry dropped towards the Solent's navigation channel and grab samples confirmed the absence of seagrass.

In Ryde, the seagrass coverage showed low values in deep water and rose quickly to a maximum (72±11%) at a depth of 2 m and then slowly decreased with decreasing depth (Figure 2.8b). The high canopy in the northeast corner and the presence of seagrass in the sublittoral zone down to 5.5 m suggested the presence of a different seagrass species, as *Zostera noltii* has not been reported in such depths in the Solent (Samiaji, 2001). This was further confirmed by the change in backscatter profiles from the centre to the northeast corner of the survey area. In the central region profiles showed high backscatter values just above the bed that dropped abruptly to water column values similar to profiles characteristic of *Z. noltii* canopies. The profiles in the northeast corner, on the other hand, showed a slow decrease in backscatter within the first 10 cm above the bed, then increased again to a second maximum between 10 and 20 cm above the bed before slowly dropping to water column values which resemble profiles recorded in *Zostera marina* canopies. The presence of *Z. marina* in the northeast corner was confirmed during the on-foot survey and explains the seagrass coverage down to 5.5 m in Figure 2.8b.

2.4.3. Oristano

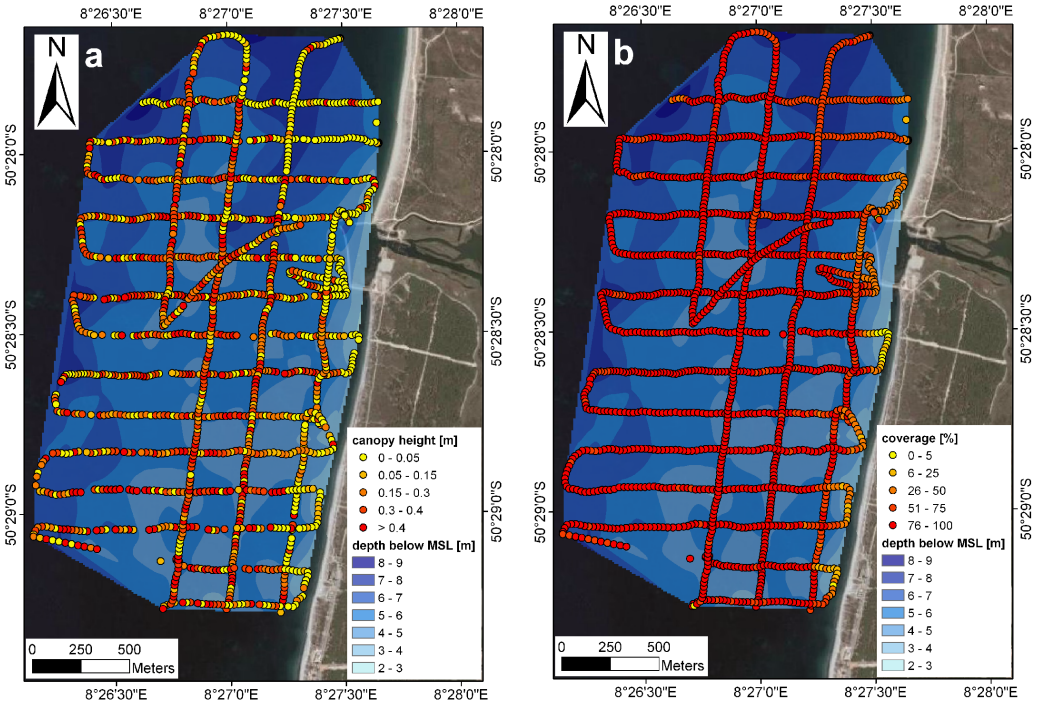

Figure 2.11.: Spatial distribution of a. canopy height and b. coverage for Oristano. Bathymetry was interpolated (Nearest Neighbour in arcMAP®) from seabed depth with a cell size of 10 m. Aerial photo from Google Earth™ (2007).

All 1,008 profiles in the Oristano dataset gave canopy heights that lie within the expected height values for *Posidonia oceanica* of up to 0.75 m (Figure 2.7c). With a mean value of 31±12 cm and a mode of 33 cm the canopy height distribution showed a lower skewness (-0.4) than the distributions for the two *Zostera* species, indicating the structural difference of the two genera.

Canopy height distribution showed the absence of seagrass close to the shoreline (Figure 2.11a) which was confirmed during on-foot visits to the shore. Furthermore, it showed the highest canopies (>0.4 m) in a depth range of 4 to 5 m, while shallower (2.5 to 4 m) and deeper areas (7 to 5 m) were covered by lower canopies which corresponded to observations made during dive surveys. The area close to the shore was identified as unvegetated or sparsely covered (coverage <25%) and the channel that reaches into the survey area from the northeast was characterised by lower

coverage (50-75%) than the rest of the area (>75%, Figure 2.11b). Both observations have been confirmed by divers. The northeastern part of the survey area is adjacent to a lagoon inlet which could explain the reduction in coverage, because the lower limit of *Posidonia oceanica* has been observed at approx. 9 m in turbid waters and near fresh water inlets (Gobert et al., 2006).

The bathymetric distribution of coverage in Oristano (Figure 2.8c) showed a maximum (85±16%) at 4.5 m and stayed above 80% down to depths of 6 m before it slowly reduced with increasing depth. In shallower waters, coverage dropped to zero at 2 m.

2.4.4. Method validation

Leaf length was recorded during the on-foot and dive surveys. Seagrass generally bends with currents and hence canopy height is often smaller than leaf length, e.g. in Calshot maximum leaf lengths of 40 to 80 cm were recorded while divers observed canopy heights between 15 and 30 cm (Lefebvre et al., 2009). Nevertheless, canopy heights computed from the SIS were compared to leaf length measurements. The SIS sweep closest to the sampling location was chosen for comparison and the average distance between those points was 5.7±4.6 m. As expected, the canopy heights calculated from SIS data in Calshot were smaller than recorded leaf lengths (Figure 2.12a). However, they agree well with canopy heights measured *in situ* (15-30 cm). For Ryde and Oristano, a comparison between estimated canopy height and measured leaf lengths showed a good correlation ($R^2 = 0.73$, $p < 0.001$, $n = 16$, Figure 2.12a). The slope differed from unity ($m = 0.77$), which could be explained by the difference between canopy height and leaf length. The mean canopy height in Ryde (12±6 cm) was slightly smaller than the mean leaf length (14±3 cm) which can be explained by leaf bending under tidal currents. For *Posidonia oceanica*, the canopy height (31±12 cm) matched the observed leaf length (32±4 cm) well.

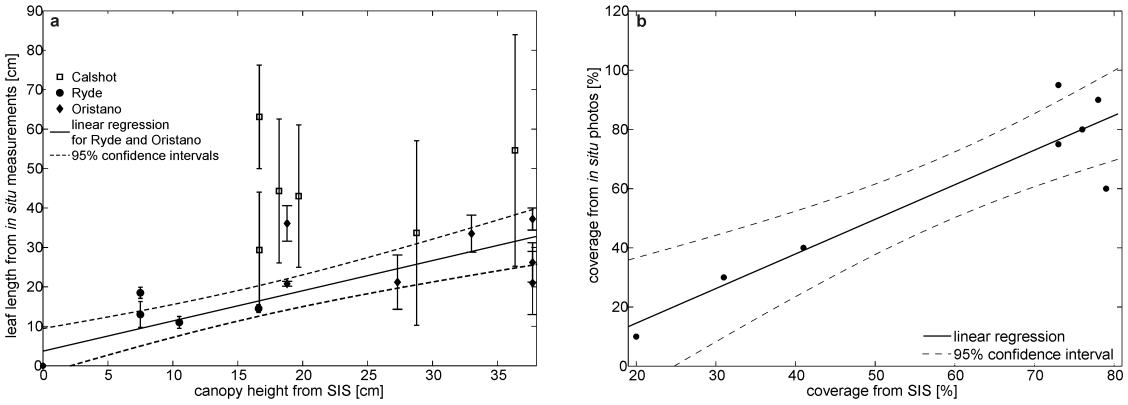

Figure 2.12.: Comparison of a. canopy height (SIS = $0.77 * in situ + 3.70$, $R^2 = 0.73$) and b. coverage (SIS = $0.73 * in\ situ + 15.27$, $R^2 = 0.85$) for values measured *in situ* versus values estimated with the SIS. Note that for the canopy height, data from Calshot was excluded from linear regression and *in situ* coverage data was only obtained in Ryde.

Coverage in Calshot was compared to video data by Lefebvre et al. (2009) and a satisfactory agreement ($R^2 = 0.61$) was found. For the Ryde data, coverage was compared to estimates derived from *in situ* photography at eight locations which led to very good agreement (m = 0.73, $R^2 = 0.85$, p = 0.001, Figure 2.12b). The coverage estimates of *Posidonia oceanica* in Oristano yielded a good agreement with analysis of aerial photography carried out by De Falco et al. (2006). Overall, the good agreements with various other methods of canopy height and coverage determination indicate that the SIS and the presented algorithm provide a robust method for estimating seagrass canopy height and coverage.

2.5. Discussion

The results show that the presented method yields good results in a wide range of water depths (0.8-8 m), turbidities (SPM = 8-30 mg/L) and sea states (calm to choppy) and is therefore robust against the effects of varying environmental conditions. However, so far the SIS has only been deployed during summer and early autumn, when above ground biomass was high and it is not yet known how the method performs in winter when above ground biomass is low.

This study also shows that it can be applied to seagrass species of different morphologies. All seagrass species have a lacunal system that give buoyancy to the leaves (Phillips and Meñez, 1988) and increase scattering at the water-plant interface. The lacunal system in *Zostera* sp. is more pronounced than in *Posidonia* sp. (Kuo and Den Hartog, 2006) which may explain the higher backscatter values relative to the bed within the *Z. noltii* and *Z. marina* canopies compared to *P. oceanica* (Figure 2.3). It could also explain the difference in profile shapes between species in this study. The seagrass in Calshot and Ryde bent under a tidal current, which led to an uneven vertical distribution of biomass throughout the canopy: leaves stay upright close to the bed and bending only takes place further up along the leaf; the location of this bending point depending on species and current velocity. From there upwards, the leaves will align themselves almost horizontally and their biomass will accumulate in a layer at the top of the canopy (Fonseca et al., 1982). This layer will also contain most of the leaves' lacunae and therefore may cause higher backscatter intensity than the lower part of the canopy. In *Z. noltii*, the bending point is located close to the bed and the different parts of the canopy could not be clearly differentiated within the profile (Figure 2.3a and 2.6b). For *Z. marina*, however, the bending point was higher up because the seagrass leaves are generally longer and stiffer than for *Z. noltii* and the SIS resolution was sufficient to detect the two parts of the canopy (Figure 2.3d and 2.6c). *P. oceanica*, on the other hand, did not bend, as tidal currents were negligible in Oristano. The profiles therefore show an even distribution of backscatter intensity throughout the canopy (Figure 2.3b and 2.6d).

Lefebvre et al. (2009) suggested that different seagrass species might create different backscatter intensities, leading to the maximum backscatter values being located within the seagrass canopy instead of at the bed. Such behaviour was found in a few profiles during a previous study with *Zostera marina* (Warren and Peterson, 2007) and would lead to misinterpretation of bathymetric depth and all other parameters. Using an averaged profile over the five centre beams reduced possible backscatter maxima within the canopy. In a gentle sloping terrain, the bed will be at the

same height along the distance covered by the five centre beams (0.3-0.8 m) and will therefore create a strong backscatter in the averaged profile. The height of high backscatter in the canopy, however, is likely to vary from beam to beam and consequently will be averaged out. Thus, at all three sites during this study the seabed was always the strongest scatterer, which was confirmed by manual inspection of all vertical profiles. This result suggests that bed detection is not significantly affected by the presence of SAV, thus reliable calculation of bathymetric depth even within the seagrass meadows is possible.

Canopy heights were in good agreement with observations based on other methods (Figure 2.12a and Figure 4a in Lefebvre et al., 2009). The introduction of $\Delta back_2$ in the algorithm made it applicable to varying profile types (Figure 2.3) and hence is an improvement to the method described by Warren and Peterson (2007). Their method would have identified profiles similar to the one shown in Figure 2.3d as unvegetated and could therefore not have been used to assess *Zostera marina* presence and canopy height in the Solent correctly. The regression line in Figure 2.12a over-predicts low canopy heights ($<$16 cm) and slightly under-predicts values $>$16 cm. This discrepancy may be caused by the use of leaf length from the *in situ* measurements as a proxy for canopy height. Inaccuracies may also partly be caused by the vertical resolution of the data which lead to inaccuracies of 10-14% for all three sites. Another source of inaccuracy may come from the averaging of the five central beams to calculate canopy height causing the two outermost beams to be 3.6° apart. The length of seabed between those two beams varied with water depth and ranged from 0.3 to 0.8 m. Any changes of canopy height along this distance affected the result's precision and may explain some of the discrepancies found between direct and SIS measurements.

Accuracy of canopy height estimations also depend on present hydrodynamic forcing. Currents reduce canopy height by bending leaves and canopy height will decrease with increasing flow velocity until a maximum bending angle is reached (Vogel, 1994;

Boller and Carrington, 2006). Current velocity and direction at a given location change over the tidal cycle which may lead to changing canopy heights in SAV exposed to tidal currents. Another possible reason for canopy height variation is wave motion which moves flexible vegetation back and forth (Chapter 4). As a result, canopy height may change on very short timescales. The canopy heights derived from backscatter values can therefore only be seen as estimates as they give a momentary value and cannot be considered constant over any given amount of time.

Discrepancies in canopy heights from Calshot may also have been caused by the sampling schedule. The *in situ* observations were made in summer (July-August) while the SIS survey was carried out approximately six weeks later in mid September. It is possible that the different sampling dates resulted in observations of different growth states of the *Zostera marina* meadow. In summer, the meadow will have reached its peak in the growth cycle with maximum leaf lengths and shoot densities, while in September the autumn decline might have set in (Den Hartog, 1970), resulting in generally lower values. However, it is not clear whether this difference in sampling dates affected the quality of validation results. No data are available on growth cycles of *Zostera marina* and Chapter 3 showed that leaf lengths do not change significantly throughout the year for *Zostera noltii* in the Solent which suggests that a six week gap in the sampling schedule may not affect data quality significantly.

Spatial resolution during this study was generally low. The spatial resolution along the boat track depends on boat speed and sweep angle; it was 10-40 m in this study. Based on the used settings (Table 2.1), the surveys covered approx. 10 ha per hour. Such surveying speed allows seagrass mapping even in intertidal areas (e.g. in Ryde), where sufficient water depth is only maintained for a short time (i.e. 1-2 h) during each tidal cycle. However, the low spatial resolution may increase inaccuracies in the detection of meadow edges and patch sizes.

Survey resolution could also affect derivation of coverage and canopy height maps.

Table 2.2.: Statistical values for canopy height distributions at all three sites.

	Calshot	Ryde	Oristano
mean [cm]	15	12	31
standard deviation [cm]	7	6	12
mode [cm]	6	11	33
skewness [-]	1.1	2.3	-0.4
number of data points	481	634	1107

Natural coverage and canopy height are randomly distributed and it is therefore difficult to interpolate such data correctly, even at high resolutions. Thus, the low resolutions in this study did not allow interpolation of the data. Without interpolation, however, an overview map strongly depends on the specific sampled locations and maps of the same location may vary depending on the position of survey lines. It is therefore recommended for future use of the method to carefully assess the required resolution of the resulting map and to adjust the spacing of survey lines accordingly.

The canopy height distributions for the three sites show different peak and skewness values (Table 2.2). A one-way ANOVA showed that all three datasets were significantly different at the 0.01 level. This outcome suggests that canopy height can give an initial indication of which seagrass species might be present at the surveyed site. Moreover, changes in canopy height on the medium scale could indicate a change of seagrass species. This was the case in Ryde where canopy heights in the northeast corner were considerably higher than throughout the rest of the survey area and an *in situ* survey confirmed *Zostera marina* in that region while the remaining area was occupied by homogeneous *Zostera noltii*. This case gives a first indication that it might be possible to map boundaries between species in addition to the overall extend of SAV. Such a feature would be very useful in regions where species succeed one another with increasing depth (i.e. *Zostera noltii* and *Zostera marina* in temperate waters), but also in regions where pioneer and climax species co-exist in the same habitat (i.e. *Cymodocea nodosa* and *Posidonia oceanica* in the

Mediterranean). More detailed surveys of species boundaries are required to explore the method's capability of identifying different species within one survey.

Seabed length per sweep in this study varied from 1.5 to 11 m which altered the reference value for coverage throughout each survey. It would be possible to standardise the reference value by restricting computation of coverage to a defined length of seabed on either side of the centre beam. However, such a restriction would discard data obtained outside this defined length which may not be desirable, given that it is a strength of this method to collect data over a swath and not just along a narrow path along the ship's track. The computation of coverage was based upon a threshold value; beams that exceeded this value were defined as containing seagrass. The threshold is based on the mean background value throughout the water column and the method therefore can be equally applied in clear and turbid waters. In relatively clear conditions such as Oristano (SPM = 8 mg/L), backscatter throughout the water column was small ($\overline{BI_w} \approx 40$) while in more turbid conditions such as the Solent a higher SPM value of approx. 30 mg/L (Collins and Ansell, 2000) led to higher backscatter throughout the water column with $\overline{BI_w} \approx 80$ (Figure 2.3). With such differences in mean backscatter of the water column, a constant threshold value could not be applied. The threshold of mean water backscatter plus 50 (eq. 2.4) was found empirically and seems to match the conditions at all three study sites, suggesting that it is a suitable value for a range of conditions and seagrass species. Future use of the SIS and the presented method will show how widely applicable this empirical threshold is.

Coverage measurements were compared to three other methods of coverage determination and the good correlation indicates that the SIS provides robust estimation of seagrass cover. The presented method summarises coverage of a whole sweep in a single value which is plotted along the boat track. While those values give a robust indication of coverage, the method lacks spatial resolution which could be provided by side-scan or multi-beam sonars.

Table 2.3.: Appearances of a seagrass meadow and possible implications (Duarte et al., 2006).

appearance of the meadow	possible reasons for appearance
continuous	healthy and well established located in the species' preferred growth depth
reticulate	colonisation of a new area located outside the species' preferred growth depth
discrete patches	colonisation of a new area fragmentation of an existing meadow located at the boundaries of the species' possible growth depth range

Coverage distribution at all three sites showed the highest coverage in the preferred depth range of the respective species. Most SAV have a preferred growth depth (Den Hartog, 1970) which could be used as an indicator of seagrass species. Coverage values, however, will vary for sites of the same species depending on health and growth state of the meadow. A healthy, well established seagrass bed will return high coverage values indicating a continuous meadow without major gaps. Seagrass patches, on the other hand, indicate either colonisation of a new area or fragmentation of an existing meadow (Duarte et al., 2006). Seagrass coverage is therefore an important parameter for identifying a seagrass meadow's health (Table 2.3). Monitoring changes in seagrass coverage requires a method that is not influenced by observer bias. Direct surveys carried out by divers are subjective and bias can only be reduced by using the same person for the survey every time. This can prove problematic if a site needs to be surveyed over several decades. The presented method provides an unbiased quantification of coverage and therefore allows comparison of survey results carried out by different people, provided the same settings are used during each survey. In addition to the instrument settings environmental conditions such as flow velocities need to be considered when comparing results from different surveys. As mentioned previously, tidal currents can cause seagrass to bend and therefore affect canopy height. If canopy height from different surveys should be

compared, it is recommended to survey during similar stages of the tidal cycle in order to have a similar flow effect on canopy height.

Overall, the developed method provides a fast and cost effective alternative to existing methods that can also be applied in shallow water depths. Comparison with other sampling methods suggests that the method is able to estimate canopy height and coverage correctly, but a more systematic approach is required to calibrate these results. It is therefore suggested to carry out combined SIS and dive surveys to sample coverage and canopy height simultaneously with both methods for comparison.

2.6. Conclusions

The presented method for seagrass mapping is able to provide quantitative data on spatial distribution, coverage and canopy height of seagrass meadows. By providing all three parameters during one survey, the method is an improvement compared to other methods currently used for seagrass mapping, i.e. dive or camera surveys, side-scan sonars. The method was improved compared to previous algorithms by reducing the influence of turbidity in the water column which is survey specific. Contant threshold values were replaced by dynamic threshold parameters that are defined relative to background backscatter values. Another improvement over previous methods is the introduction of the parameter $\Delta back_2$. By evaluating the position of $\Delta back_2$, the algorithm is able to identify inhomogeneous seagrass canopies even if the location of $\Delta back_m$ would suggest an unvegetated profile.

The method also quantifies seagrass coverage which can be used to describe a meadow's health and monitor its change with consecutive surveys in a non-biased way. Moreover, as shown in Ryde, the combined information on canopy height and depth of maximum coverage can be used as an indicator of species. Identification of species allows tracing of species boundaries within a mixed meadow and therefore can

improve resolution of habitat maps. However, ground-truthing by divers or on foot will still be necessary to confirm observations made during the boat based survey, but these can be carried out as targeted visits to special points of interest which would reduce the amount of required diving and the associated costs significantly.

3. Spatial and seasonal variation in wave attenuation over *Zostera noltii*

3.1. Abstract

Wave attenuation is a recognised function of seagrass ecosystems which is believed to depend on plant characteristics. This chapter presents field data on wave attenuance collected over a 13 month period in a *Zostera noltii* meadow. The meadow showed a strong seasonality with high shoot densities in summer (approx. 4,600 shoots/m^2) and low densities in winter (approx. 600 shoots/m^2). Wave heights and flow velocities were measured along a transect at regular intervals during which the site was exposed to wind waves and boat wakes that differ in wave period and steepness. This difference was used to investigate whether wave attenuation by seagrass changes with hydrodynamic conditions. A seasonal change in wave attenuation was observed from the data. Results suggest that a minimum shoot density is necessary to initiate wave attenuation by seagrass. Additionally, a dependence of wave attenuation on hydrodynamics was found. Results suggest that the threshold shoot density varies with wave period and a change in energy dissipation towards the shore was observed once this threshold was exceeded. An attempt was made to quantify the bed roughness of the meadow; the applicability of this roughness value

in swaying vegetation is discussed. Finally, the drag coefficient for the meadow was computed: A relationship between wave attenuance and vegetation Reynolds number was found which allows comparing the wave attenuating effect of *Zostera noltii* to other plant species.

3.2. Introduction

Wave attenuation has been recognised as an important ecosystem function of seagrass meadows (Madsen et al., 2001) that contributes to the economic value of such ecosystems (Koch et al., 2009). Attempts have been made to quantify the economic value of ecosystems and at present, the valuation process is based on the assumption that ecosystem functions vary linearly with plant characteristics (Barbier et al., 2008). However, laboratory experiments showed that plant traits such as shoot density and canopy height lead to a non-linear response in wave height reduction (Fonseca and Cahalan, 1992; Bouma et al., 2010) and linearity may therefore be an inappropriate approximation (Koch et al., 2009).

While non-linear relationships have been observed in laboratory studies (Méndez et al., 1999; Bouma et al., 2010), only few field studies are available to quantify the non-linear response of wave attenuation to changing vegetation characteristics. Some vegetation characteristics may require a minimum value before their effect on wave attenuation can be observed; Newell and Koch (2004) for example found that a minimum shoot density was required for *Ruppia maritima.* Other characteristics, e.g. population growth, may lead to an asymptotic relationship (Koch et al., 2009). To date, most studies were carried out on short time scales and during summer months, when above ground biomass was high. Such results cannot be applied to the whole year if a species shows a high seasonality (Widdows et al., 2008). For example, Verduin et al. (2002) sampled for five to ten minutes in an *Amphibolis antarctica* meadow and repeated data collection in spring and autumn; Bradley

and Houser (2009) studied a *Thalassia testudinum* bed and collected data for a duration of seven hours in early autumn while Prager and Halley (1999) acquired data for two days in late autumn in a *Thalassia* meadow. For the seagrass *Ruppia maritima* ten day deployments were carried out in August (Ward et al., 1984), and June and October (Newell and Koch, 2004). While the combined interpretation of those studies would provide a better understanding of the affect of changes in *Ruppia maritima* on wave attenuation, none of them includes the winter state with low above ground biomass.

In addition to the temporal scale, the spatial distribution needs to be considered when assessing the non-linear relationship between wave attenuation and vegetation. Previous studies on submerged vegetation found an exponential wave decay with distance into the vegetation (Kobayashi et al., 1993; Möller et al., 1999; Bouma et al., 2010) and that this exponential relationship changed with canopy height and density (Newell and Koch, 2004; Bouma et al., 2010). While individual studies have addressed the change of wave decay with distance from the meadow edge on short time scales (Bradley and Houser, 2009), no data are yet available to confirm its dependence on seagrass characteristics under field conditions.

In the field, seagrass meadows are exposed to a wide range of wave conditions. Depending on the site, they experience long period ocean swell, locally-generated short period wind waves or boat wakes. Boat wakes can lead to erosion along otherwise stable coastlines, because they have a higher height/length ratio than natural waves (Fonseca and Cahalan, 1992) which may also lead to a different interaction with seagrass. An understanding of this interaction would be desirable for planning new boat activity in coastal regions as it would allow estimations of wake impact on the coast (Fonseca and Cahalan, 1992). However, boat wake attenuation over seagrass has not been investigated in detail (Ciavola, 2005).

Several formulae exist to describe wave attenuation and the associated energy dissipation caused by bed features (e.g. Nielsen, 1992; Madsen, 1994). These formulae

were initially developed for monochromatic wave conditions (Jonsson, 1966); Madsen (1994) extended them to spectral waves to make them applicable to more natural conditions. All models use a hydraulic length scale k_N to describe bed roughness. For flat beds, k_N equals the Nikuradse sand grain roughness, and an equivalent bed roughness is used when bed forms are present (Kamphuis, 1975). This approach is valid for a wide variety of bed features; Mathisen and Madsen (1996a,b, 1999) applied it to evenly spaced triangular bars in a wave flume and it has been successfully used to estimate the bed roughness of a coral reef flat (Lowe et al., 2005). However, the models are based on the assumption that k_N is constant and independent of hydrodynamic conditions. Depending on the species, seagrass can be flexible and it is known to sway in an oscillating fashion under waves, changing its shape throughout a wave cycle. It is not yet known how this movement affects the plant's roughness (Bradley and Houser, 2009; Manca, 2010) and it is therefore uncertain, whether a constant k_N can be applied to vegetated areas.

An alternative method to describe wave energy dissipation caused by vegetation is based on the drag individual plants pose on the flow (Dalrymple et al., 1984). The model developed by Dalrymple et al. (1984) estimates the drag per unit plant area which makes it independent of plant parameters such as height and density. It would therefore allow comparison of the wave attenuating effect of different plant species. A weakness of the model is, however, that is assumes the vegetation to be rigid. Méndez et al. (1999) examined the effect plant motion has on vegetation drag. They applied their theory to data from a laboratory study on artificial kelp (Asano et al., 1988) and found that a model which assumes vegetation rigidity underestimates the drag coefficient. The same was found when the model was applied to field data from a *Thalassia testudinum* bed (Bradley and Houser, 2009). However, Bradley and Houser (2009) also showed that the simplified model by Dalrymple et al. (1984) is a reasonable first approximation.

The studies described above indicate that there is a systematic relationship between

seagrass attributes and wave attenuation across species. However, the magnitude of wave attenuation differs between species, as a difference in plant morphology will affect the plant's wave attenuating capacity. The same was found for the effect of vegetation on unidirectional flow where quantitative results cannot be transferred from one species to another (Fonseca and Fisher, 1986). Consequently, wave attenuating parameters need to be quantified for each seagrass species separately.

This chapter describes the results of a series of field experiments carried out across a *Zostera noltii* meadow over a period of 13 months in order to assess the change in wave attenuation throughout a year. From this data, bed roughness and vegetation drag were estimated and the applicability of the relevant formulae was evaluated.

3.3. Study site

Measurements of wave height and period as well as flow velocities were carried out within a *Zostera noltii* meadow on Ryde Sand, an intertidal extension of a recreational beach on the north coast of the Isle of Wight, UK (Figure 3.1). *Zostera noltii* is a temperate, intertidal seagrass species with a preferred growth depth between high and low water neaps, however, it can be found in depths to 5 m in the Mediterranean (Van Lent et al., 1991; Auby and Labourg, 1996; Curiel et al., 1996). Its ribbon-shaped leaves are 0.5-1.5 mm wide and 6-22 cm long (Phillips and Meñez, 1988; Tyler-Walters, 2008) and above ground biomass shows a strong seasonality of high values in summer and low values in winter (Curiel et al., 1996). Shoots grow from a rhizome system which builds a dense mesh by branching in almost every node (Brun et al., 2006). The root/rhizome system is located approx 3-5 cm below the sediment surface (Duarte et al., 1998) and its biomass remains constant throughout the year (Pergent-Martini et al., 2005).

Ryde Sand has a triangular shape, it is approx. 2.5 km long and the central part reaches approx. 2 km into the Solent. It is composed of fine sand (Tonks, 2008) and

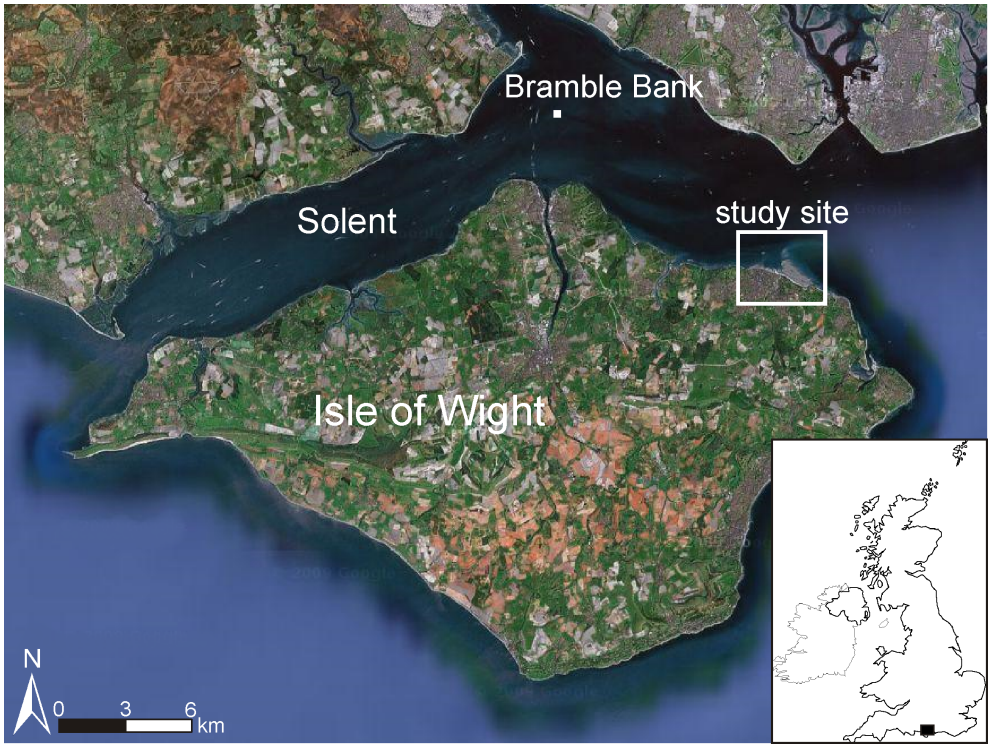

Figure 3.1.: Ryde Sand on the north coast of the Isle of Wight. The box highlights the whole sand flat.

slopes gently (1:550) towards the adjacent navigation channel. The western half of the sand flat is covered by approx. 40 ha of reticulate to continuous *Zostera noltii* meadow which extends from +2.5 to 0 m Chart Datum (CD). At the lower boundary a succession by *Zostera marina* can be observed, but its extent is unknown. The *Zostera noltii* meadow is dissected by a hovercraft route and a pier that serves as ferry terminal. The pier is built on stilts that have a diameter of 25 cm. Stilts are arranged in rows of six parallel to the shore and the spacing between rows is 5.5 m. Refraction and reflection from these structures could not be observed *in situ* and their effects were not evident in bed forms during low tide. Hence, the pier is considered to have only a minor effect on local waves. This study was carried out west of the pier where little recreational use in the form of small vessels takes place.

The sand flat is sheltered from swell from the English Channel by the Isle of Wight and the study site is exposed to two main sources of waves: (1) wind waves generated by NW winds with 2-4 s periods and (2) boat wakes caused by the ferries arriving

and departing from the pier head with 10 s periods (pers. observation). Prevailing wind direction in the Solent is south to north-west, but due to the location on the north coast of the Isle of Wight, Ryde is sheltered from southerly and south-westerly wind and the local prevailing wind direction that generated waves is north-west (MetOffice, 2010). The tidal range is 4 m during spring tides and 2 m during neap tides with the tidal flow peaking at high and low water indicating a progressive wave.

3.4. Material and Methods

3.4.1. Data collection

The site was visited monthly during spring low tide over a 13 month period from October 2008 to October 2009. During each visit shoot density was measured at four stations randomly chosen within a defined 50 x 50 m region using a 0.3 x 0.3 m quadrat (Figure 3.2). Additionally, the length of 10 randomly chosen leaves was measured at each station to obtain a record of leaf length variation over the growth cycle. During the October 2008 visit, only one station was sampled due to adverse weather conditions. Five times during the data collection period wave and flow data were collected over two consecutive tidal cycles with deployment and recovery

Figure 3.2.: Measuring shoot density in a 0.3 x 0.3 m quadrat during the site visit in July '09.

taking place during low tide. The deployments took place on 15-16 October '08, 25-26 February '09, 26-27 May '09, 7-8 July '09 and 7-8 October '09. During each deployment instruments were arranged along a cross-shore transect (Figure 3.3) approx. 30 m west of the pier. This proximity to the pier was chosen for two practical reasons: (1) It protected the instruments from possible recreational traffic and (2) it extended the transect as far as possible as some instruments had to be connected to the logging station on the pier through 130 m cables. The transect was aligned with the incoming boat wakes at 170° to capture these waves as accurately as possible. This set the transect oblique to prevailing winds, but the majority of wind waves were still captured along the transect and within a wave angle of ±20° of it due to natural variation in the wind field. Stations were between 30 and 95 m apart and an optical level was used to record their elevations with respect to Chart Datum.

For all but the May deployment three Electromagnetic Current Meters with an integrated Seapoint Sensor (EMCM, Valeport Model 808, Figure 3.4) were used to sample sea surface elevation and two dimensional horizontal flow velocities at stations 1, 3 and 5. They were mounted on quadropods with the pressure sensor positioned 0.35 m and the current meter 0.13 m above the seabed. They were set to sample at 4 Hz in bursts of 8.5 minutes every 13 minutes. From February 2009 onwards, four pressure transducers (PDCR 1830, Druck Ltd., Figure 3.4) were added to the transect at stations 2, 4, 6 and 7. Their sensors were placed directly on the seabed and were connected to a power supply and logging station on the adjacent pier through cables. They sampled continuously at 8 Hz, however, data acquisition was restricted to water depths <2.7 m due to the operating range of the PDCR's. In May, 3D velocity data were obtained using an Acoustic Doppler Velocimeter (ADV, Nortek Vectrino) at station 6, sampling continuously at 25 Hz. Barometric data were obtained from an offshore station on Bramble Bank (www.bramblemet.co.uk), 12 km northwest of Ryde (Figure 3.1).

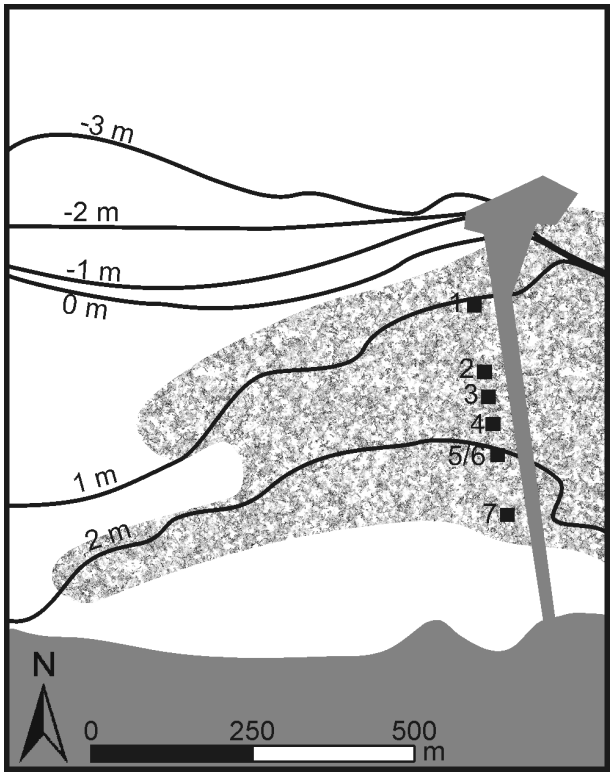

Figure 3.3.: Instrument locations and sand flat bathymetry. Bathymetry is relative to Chart Datum; 0 m marking the boundary between the intertidal and subtidal zones. The shaded area indicates known distribution of seagrass. Note that stations 5 and 6 are at the same location, but refer to different types of instruments.

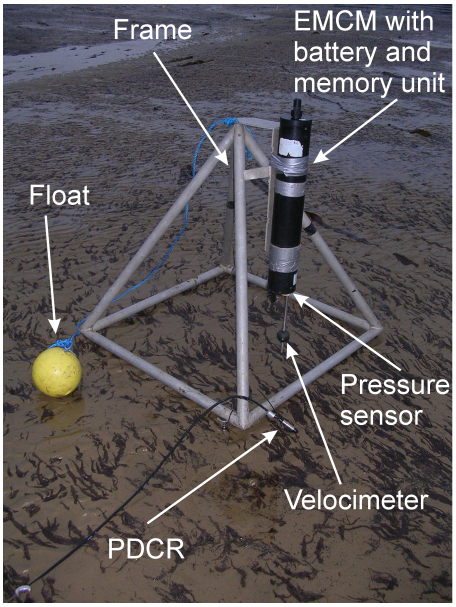

Figure 3.4.: Electromagnetic Current Meter (EMCM) mounted on a quadropod and pressure transducer (PDCR) during deployment at station 5/6 in February '09.

3.4.2. Data analysis

Wave conditions

Data from all instruments were split into synchronous five minute intervals with a minimum of 1200 samples per interval. Velocities from the EMCM's were converted into North and East components using the instrument internal compasses. Pressure data from all stations were used to estimate the wave energy spectrum applying Welch's periodogram method. Each interval was split into four segments with 50% overlap and a Hanning window was applied to each segment to reduce spectral leakage. Linear wave theory was applied, since recent studies under similar conditions showed that it is a valid approximation for wind waves (Lowe et al., 2007; Bradley and Houser, 2009; Mullarney and Henderson, 2010) as well as boat wakes (Koch, 2002; Ciavola, 2005; Garel et al., 2008). The segments were then averaged to obtain a smoothed pressure spectrum S_p with a bandwidth of $\Delta f_b = 1/128$ Hz which was converted to an energy density spectrum S_f:

$$S_{f,j} = \left[\frac{\cosh k_j h}{\rho g \cosh k_j (h - z)}\right]^2 S_{p,j} \tag{3.1}$$

where the index j denotes the frequency component, h is mean water depth, z is the vertical distance of the pressure sensor above the seabed, ρ is water density, g is gravity and k is wavenumber according to the dispersion relation

$$\omega^2 = gk \tanh kh \qquad \text{where} \qquad \omega = \frac{2\pi}{T} \tag{3.2}$$

and T is the wave period.

Velocity and pressure spectra at stations 1, 3 and 5 were used to obtain wave direction and directional spread. Following the method of Gordon and Lohrmann (2001), a 4-quadrant arc tangent was applied to the real parts of the pressure-velocity cross-spectra for the east (CS_{pu}) and north (CS_{pv}) velocity components to obtain wave

direction $D = \arctan 2(CS_{pu}, CS_{pv})$. Wave spreading ($spr$) was computed according to

$$spr = \sqrt{\frac{1-R}{2}} \qquad \text{where} \qquad R = \sqrt{\frac{(CS_{uu} - CS_{vv})^2 + 4CS_{uv}^2}{(CS_{uu} + CS_{vv})^2}} \tag{3.3}$$

where CS_{uu} and CS_{vv} are velocity component power spectra and CS_{uv} is the cross spectrum of the u and v velocity components (Krogstad et al., 1998). For the May deployment, the same method was applied using the ADV's velocity data together with the pressure data from station 6.

The total energy in the wave spectrum was determined to obtain the zero order moment and hence significant wave height H_s for each five minute interval:

$$H_s = 4\sqrt{\sum_{j=1}^{M} S_{f,j} \Delta f_b} \tag{3.4}$$

where M is the total number of frequency components.

All instruments were deployed along the same transect. For processing, however, they were split into two groups according to instrument type to avoid inaccuracies caused by differences in instrument operation. The respective groups consist of stations 2, 4, 6 and 7 for the PDCR's and stations 1, 3 and 5 for the EMCM's. Results from both groups were subsequently combined for analysis unless stated otherwise.

Wave dissipation

Waves interact with the seabed when travelling towards the shore. The main impacts on waves that can cause a change in shape or contained energy are breaking, reflection, shoaling and bottom friction (Madsen, 1976). The sand flat was sloping very gently (∼1:550) and hence slope related impacts such as breaking, reflection and shoaling are expected to have a low impact on approaching waves. Breaking

of random waves is controlled by water depth; previous studies have shown that linearity is a valid approximation (Thornton and Guza, 1982; Soulsby, 1997):

$$H_{rms} = \gamma h \tag{3.5}$$

where H_{rms} is the root-mean-square wave height and γ is a critical breaking parameter. Recent studies have found $\gamma = 0.2 - 0.6$ for planar and gentle sloping (<1:100) beaches (Raubenheimer et al., 1996; Lentz and Raubenheimer, 1999; Raubenheimer et al., 2001). Breaking was observed visually during deployments only when h was too low for the instruments to record accurately. To exclude any effect through partial breaking at higher water depths, data with $\gamma > 0.2$ were removed from the present dataset.

Reflection occurs over sloping bathymetries; the steeper the slope, the more wave energy will be reflected (Battjes, 1974; Magne et al., 2005). Reflection in this study could be neglected, because the sand flat slope was ∼1:550 and comparison with results for linear ramps showed that reflection at such shallow slopes are negligible (Magne et al., 2005). Possible reflection from the meadow itself was minimised by positioning all stations of the instrumented transect within the meadow. Moreover, it has been shown that wave energy reflection by vegetation is negligibly small (Méndez et al., 1999; Méndez and Losada, 2004). Shoaling, on the other hand, was taken into account and its impact was removed from each frequency component of the wave spectrum at stations 2-7 based on the spectrum of the previous station (Dean and Dalrymple, 1991):

$$H_n = H_{n-1} K_s \qquad \text{where} \qquad K_s = \sqrt{\frac{C_{g,n-1}}{C_{g,n}}} \tag{3.6}$$

where K_s is the shoaling coefficient and n indicates the number of the shoreward station. Once breaking, reflection and shoaling have been considered, a change in wave height between stations along the instrumented transect could be used to

estimate bottom friction following the approach of Lowe et al. (2005). Bottom friction will act on waves in shallow water and will reduce the wave energy flux towards the shore. Wave energy flux is defined as:

$$F = EC_g \tag{3.7}$$

where E is the wave energy density and C_g is the group velocity and can be obtained for each frequency component j following linear wave theory:

$$E_j = \frac{1}{2}\rho g a_j^2 \tag{3.8}$$

$$C_{g,j} = \frac{1}{2}\left(1 + \frac{2k_j h}{\sinh 2k_j h}\right)\frac{\omega_j}{k_j} \tag{3.9}$$

where $a_j = \sqrt{2S_{f,j}}$ is the wave amplitude.

Assuming that waves of all frequency components within a spectrum propagate in the same direction the one-dimensional wave energy equation (Lowe et al., 2005) can be applied to estimate the rate of energy dissipation caused by friction ϵ_f per unit area:

$$\frac{\Delta F}{\Delta r} = -\epsilon_f \tag{3.10}$$

$$\Delta r = \Delta x \cos(\alpha - \beta) \tag{3.11}$$

where Δr is the projected distance between stations at which energy flux is known. Lowe et al. (2005) derived Δr from the measured distance Δx between stations and the wave angle to account for the angle between the direct line connecting the stations α and the direction of wave propagation β.

An original model for ϵ_f was developed for monochromatic waves (Jonsson, 1966).

Based on this model, Madsen (1994) developed a weighted-average approach which places more weight on the frequency components that contain most wave energy. This approach yields representative parameters to extend the monochromatic models to spectral wave conditions. Following this approach, the representative maximum near-bed horizontal orbital velocity $u_{b,r}$ is defined as:

$$u_{b,r} = \sqrt{\sum_{j=1}^{M} u_{b,j}^2} \tag{3.12}$$

where $u_{b,j} = a_j \omega_j / \sinh k_j h$ is the velocity corresponding to the j^{th} frequency component. Furthermore, Madsen (1994) presented a model that derived ϵ_f for a given frequency, j, from the maximum near bed horizontal orbital velocity, $u_{b,j}$, using the energy dissipation factor $f_{e,j}$:

$$\epsilon_{f,j} = \frac{1}{4} \rho f_{e,j} u_{b,r} u_{b,j}^2 \tag{3.13}$$

Following his weighted approach a representative energy dissipation factor $f_{e,r}$ can be estimated (Lowe et al., 2005):

$$f_{e,r} = \frac{\sum_{j=1}^{M} f_{e,j} u_{b,j}^2}{\sum_{j=1}^{M} u_{b,j}^2} \tag{3.14}$$

The energy dissipation factor gives an estimate of how the whole seagrass meadow affects energy dissipation of the entire wave field and is likely to change throughout the growth cycle or spatially within a meadow. An alternative method for computing ϵ_f was derived by Dalrymple et al. (1984) who used the drag coefficient C_D to describe the drag individual seagrass leaves induce on the flow:

$$\epsilon_f = \frac{2}{3\pi} \rho C_D b N \left(\frac{kg}{2\omega} \right)^3 \frac{\sinh^3 ks + 3 \sinh ks}{3k \cosh^3 kh} H^3 \tag{3.15}$$

where b is the leaf width normal to the flow, N is the number of leaves per m^2 and s is the canopy height. This equation accounts for seasonal and spatial changes

of the meadow through the plant parameters b, N and s, and therefore implies that C_D is species specific. The expression assumes rigid vegetation and that the drag coefficient accounts for the horizontal movement of the vegetation (Dalrymple et al., 1984; Méndez and Losada, 2004). While this assumption is a simplification of reality, where seagrass sways with the orbital water motion under waves, Bradley and Houser (2009) showed that it is a reasonable first approximation if the plant motion is not known.

3.5. Results

3.5.1. Seagrass variation

Seagrass growth was strongly seasonal over the 13 month period. Shoot densities (Figure 3.5a) showed a distinct variation over the growth cycle with maximum shoot densities in summer and minimum values in winter. The average density was 1,980±488 shoots/m^2 (±standard deviation) with a minimum of 625±225 shoots/m^2 in February and a maximum of 4,636±858 shoots/m^2 in August. Leaf lengths (Figure 3.5b) showed low values in February and March, but almost constant values of 12-16 cm throughout the rest of the year with an annual average of 13±3 cm. Mean values exceeded 16 cm only in October 2008. This value is based on a smaller sample population which may have led to an over-estimation of the leaf length. The lack in variation of leaf length throughout the year is unexpected, as length differences between summer and winter have been observed in other *Zostera noltii* meadows (Auby and Labourg, 1996; Curiel et al., 1996). This discrepancy could be due to the sampling method applied in this study. Measured leaves were chosen arbitrarily and consequently leaves of all lengths were measured. It is possible that a seasonal variation would have been visible if only the longest leaves of a shoot would have been recorded.

The observed values for shoot density and leaf length are low compared to values

observed in the Mediterranean (up to 22,000 shoots/m^2 and 45 cm leaf length; Curiel et al., 1996; Sfriso and Ghetti, 1998). But they agree well with observations made in similar climatic conditions (i.e. the Wadden Sea) where maximum shoot densities of 2,000-4,900 shoots/m^2 and leaf lengths of 6-20 cm have been observed (Pasche and Deußfeld, 2003; Schanz and Asmus, 2003). This indicates that the *Zostera noltii* meadow in Ryde is well developed and healthy and appears to be representative of meadows at similar latitudes.

3.5.2. Wave and tidal conditions

The tidal flow showed a progressive wave for all deployments with maximum values ($\sim$0.3 m s^{-1}) during high and low water and generally lower flow velocities closer to shore (Appendix A). The main flow was in an East-West direction and hence nearly perpendicular to the instrumented transect (Figure 3.6). While its influence on present waves is consequently negligible (Madsen, 1994), the current is likely to affect the seagrass. Seagrass will bend in the presence of a current (Fonseca and Koehl, 2006; Backhaus and Verduin, 2008) and therefore change its canopy height and orientation relative to wave advance with changing flow velocities and direction. As a tidal current was present during all deployments, it was not included in the scope of this study.

During all deployments, wind waves were generated by north-westerly winds which caused part of the waves to travel along the instrumented transect (Figure 3.7). Intervals with waves travelling in an East-West direction ($\pm$45°) were excluded from analysis to ensure that waves which encountered possible interference from the adjacent pier were not considered. Spectral analysis (eq. 3.1) was used to compute wave spectra for all intervals (Appendix A) and analyses of wave spectra showed that 90% of the energy was contained in the frequency range 0-1 Hz for the majority of the spectra (>90%). Consequently, only frequencies up to 1 Hz were considered for analysis. The spectra (Figure 3.7) show that wind waves for all deployments

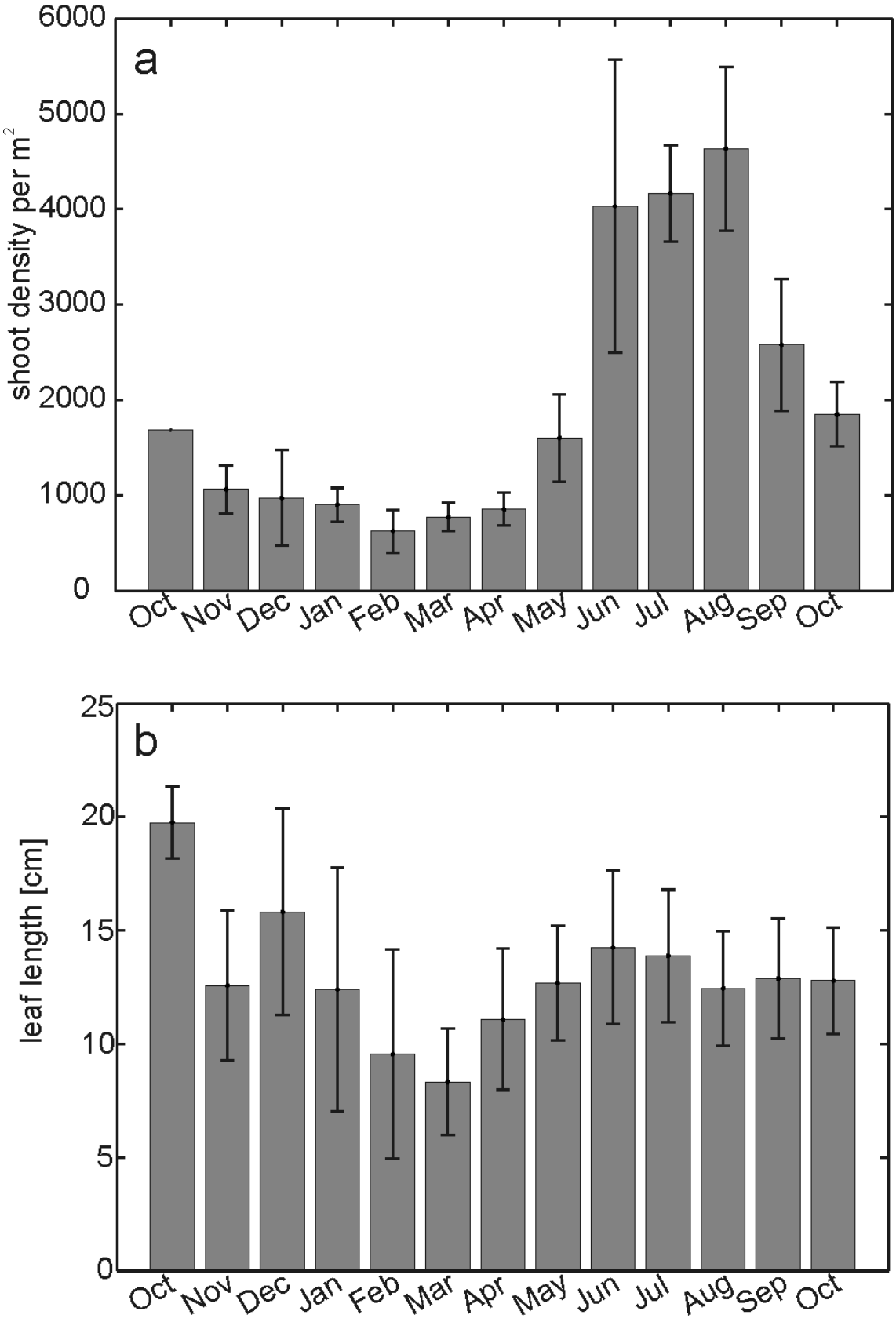

Figure 3.5.: Growth of *Zostera noltii* in Ryde over the 13 month period of monitoring. a. shoot density per m^2 and b. leaf length. Variability is expressed by the standard error.

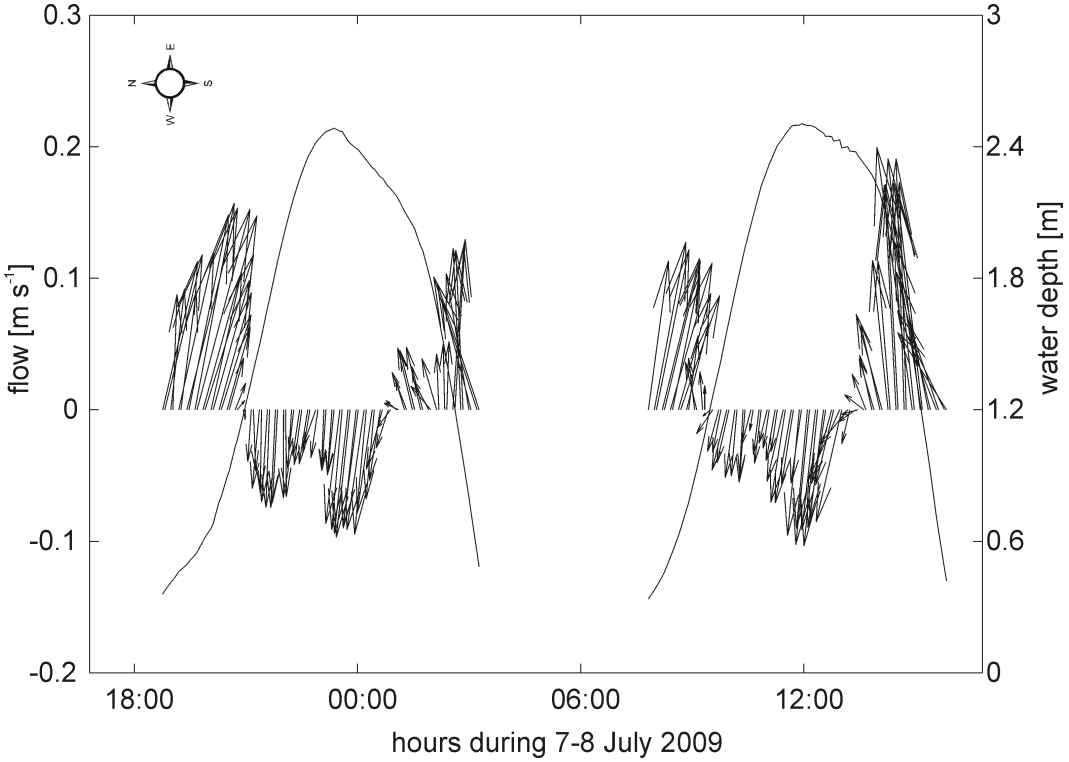

Figure 3.6.: Representative example of tidal flow conditions at station 5 in July '09. The solid line represents the tidal elevation.

occurred in a similar frequency range. Energy dissipation took place across all frequency bands and was most pronounced in July. In October '08 an increase in energy density along the transect was observed which could not sufficiently be explained with known sources of reflection and refraction. The October '08 data was therefore excluded from further analysis. Significant wave height (eq. 3.4) was calculated from these spectra and maximum wave heights varied from 13 cm in October '09 to 18 cm in July (Table 3.1).

Boat wakes were identified from the data's timestamp, as the timetable for ferries leaving and arriving on the pier was known. Boat wakes were also clearly visible in timeseries during calm conditions as they differed significantly from wind waves (Figure 3.8). Accurately identified boat wake timeseries were used to determine the boat wake's frequency (0.1 Hz) and consequently to separate boat wakes from wind waves in all spectra by splitting them into two frequency ranges: $f = 0 - 0.2$ Hz for boat wakes and $f = 0.2 - 1$ Hz for wind waves.

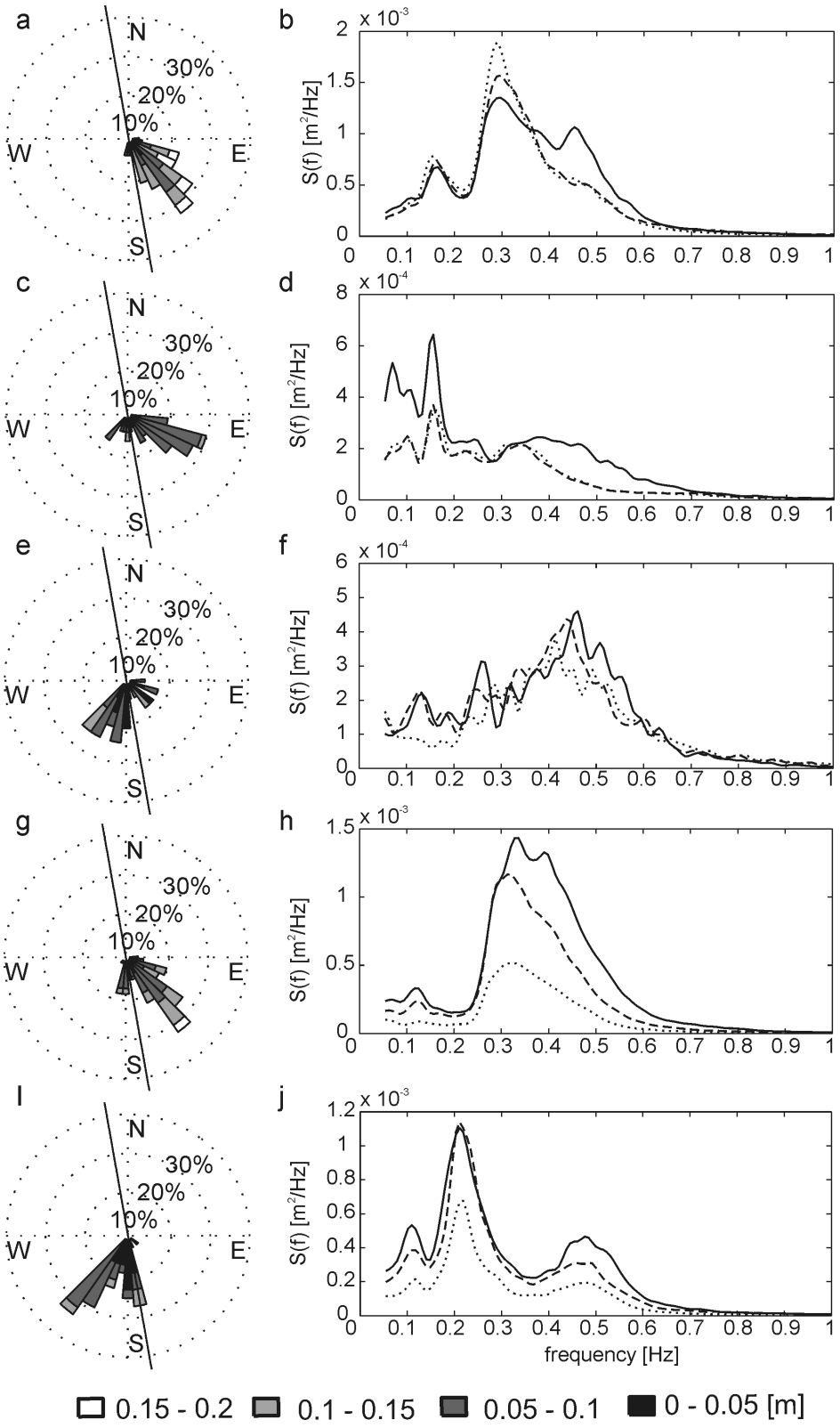

Figure 3.7.: Wave roses and mean spectra for deployments October '08 (a & b), February (c & d), May (e & f), July (g & h) and October '09 (i & j) after removing waves from easterly directions. The wave roses show the directions waves travel towards and the solid line represents the transect angle. In the spectra, the solid line represents the outer most station, the dashed line station 3 or 4 (depending on availability) and the dotted line the inner most station.

Table 3.1.: Observed significant wave height H_s, period T and wave length L for deployments.

dates of deployment	mean H_s [m]	max H_s [m]	mean T [s]	mean L [m]
25-26 February '09	0.05	0.15	4.96	19.19
26-27 May '09	0.07	0.16	3.23	11.55
7-8 July '09	0.07	0.18	3.11	10.82
7-8 October '09	0.06	0.13	3.96	15.24

3.5.3. Wave attenuation

As wave energy is directly related to wave height (eq. 3.8), change in wave height between two stations can be used to compare energy dissipation between deployments once shoaling has been removed. Shoaling coefficients ranged from 1 to 1.05, leading to a maximum increase in wave height of 5% between consecutive stations. Time series of H_s for each deployment (Figure 3.9) show that wave heights reduce along the transect in small water depths ($h \lesssim 1$ m), while a change in wave height at higher water depths can only be observed in July and October '09. To explore the difference in wave height reduction between deployments, wave height evolution along the transect for water depths <1.5 m was examined (Figure 3.10). PDCR stations only were used to exclude inaccuracies caused by comparison of different instrument types. Nevertheless, an increase in wave height between station 4 (normalised distance 1.1 m) and 6 (normalised distance 1.6 m) can be observed for all deployments. It is not known what caused this increase in wave height, especially as possible refraction from the adjacent pier was excluded during data processing, but one possible cause is the experimental setup at station 6. Station 5 and 6 were at the same location and were used to compared instrument performance. As a result, the PDCR at station 6 was deployed next a metal frame that mounted the EMCM at station 5 (and the ADV in May). As a result, the PDCR at station 6 may have been influenced by the proximity of the frame and the other instrument.

Reduction in wave height was greatest in July, when seagrass density was high

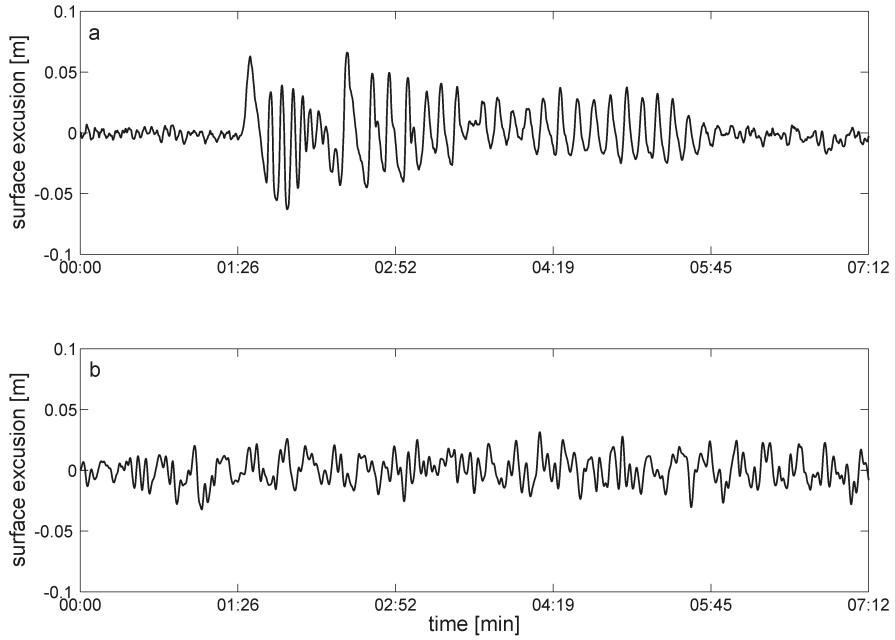

Figure 3.8.: Time series of representative a. boat wake generated by a ferry leaving from the pier head and b. wind wave conditions.

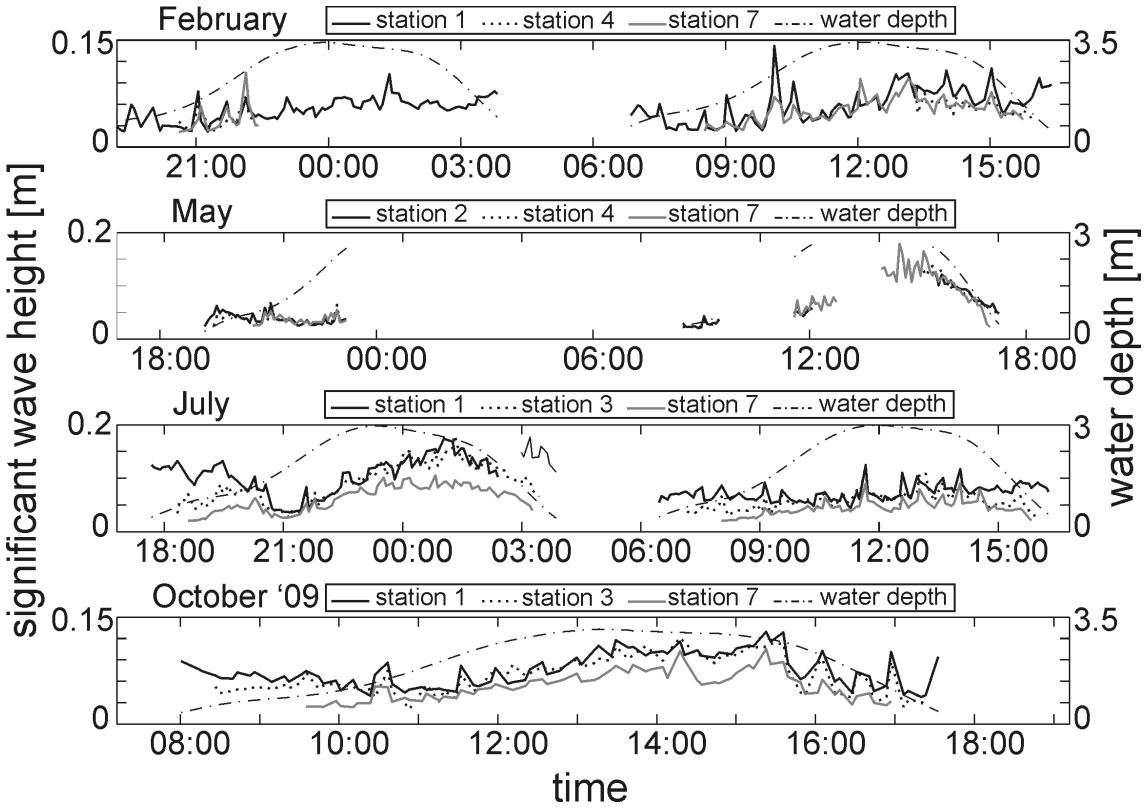

Figure 3.9.: Time series of significant wave height for each deployment. Some stations have been omitted for clarity.

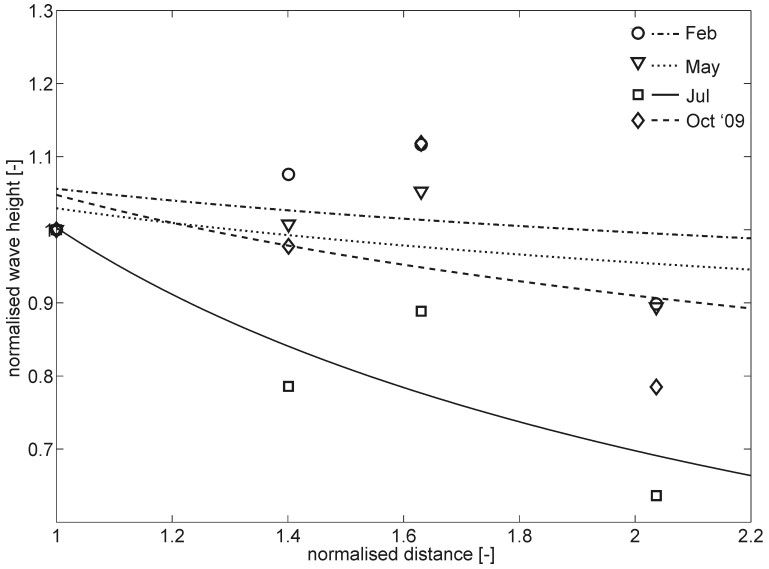

Figure 3.10.: Mean normalised significant wave height in water depths <1.5 m for all deployments and corresponding regression lines, see Table 3.2 for regression parameters.

(4,164±506 shoots/m^2). With a reduction of up to 20% between consecutive stations, the observed wave height reduction was four times higher than the effect of shoaling (<5%), indicating that the seagrass has an effect on wave height reduction. For all other deployments wave height reduction was less than 10% and therefore similar to the effect of shoaling. Moreover, the data alternate around a value of approx. 1 and hence the data show no significant wave attenuation. Values at stations 4 and 6 of the February, May and October '09 deployments show an increase of wave height of up to 15% compared to values at station 2. While this percentage appears high, absolute values show that the increase is <0.5 cm in all cases and can therefore be neglected based on instrument accuracy.

Table 3.2.: Statistical values for the relationship of H_s with water depth of the form $H_s/H_{s0} = c(y/y_0)^d$, where the index 0 denotes values at the outer most station and y is the station's distance from a reference point off shore of station 1.

	c	d	R^2	H_{s0} [cm]
February '09	1.06	-0.08	0.07	4.5
May '09	1.03	-0.11	0.23	5.1
July '09	1.01	-0.52	0.74	5.9
October '09	1.05	-0.20	0.19	3.4

Table 3.3.: Mean values of $f_{e,r}$ for wind waves ($f = 0.2 - 1$ Hz) and boat wakes ($f = 0 - 0.2$ Hz) for all deployments. Uncertainties are expressed as the standard deviation of the scatter.

	wind waves	boat wakes
February '09	0.07±0.09	0.08±0.1
May '09	0.06±0.04	0.05±0.03
July '09	0.08±0.07	0.17±0.19
October '09	0.08±0.05	0.09±0.04

Based on the observed reduction in wave height the energy dissipation factor $f_{e,r}$ was computed from the wave spectra using equations 3.10 to 3.14. To satisfy the condition of eq. 3.10, only intervals with a wave spread of $<10°$ were used. Although Δr in eq. 3.10 accounts for the angle between the transect and wave direction, it was decided to restrict data to intervals where the angle was $<20°$. At a larger angle, waves cannot be considered to be travelling along the transect and therefore would not give information about wave attenuation between stations.

The site was exposed to wind waves and boat wakes which could be distinguished by the difference in wave period (Figure 3.8). This was used to separate the two wave types in the wave spectra and to investigate whether waves of different frequencies are attenuated differently. For wind waves, $f_{e,r}$ was constant throughout the year (ANOVA, F = 0.14, p = 0.97) and similar to values for boat wakes. The summer mean ($f_{e,r} = 0.17 \pm 0.19$) of boat wake values is an order of magnitude higher than for the other deployments (Table 3.3).

Figure 3.11 shows $f_{e,r}$ for each shoreward station. For wind waves (Figure 3.11a-d), values do not differ along the transect, but are distributed around the mean value. For boat wakes a similar behaviour can be observed during autumn, winter and spring, resulting in similar mean values to wind waves (Figure 3.11e,f and h). In summer, however, a decrease of $f_{e,r}$ towards the shore was observed (Figure 3.11g).

While a difference in $f_{e,r}$ can be observed with varying seagrass coverage and vitality, it is also dependent on the maximum near-bed horizontal orbital velocity (equations

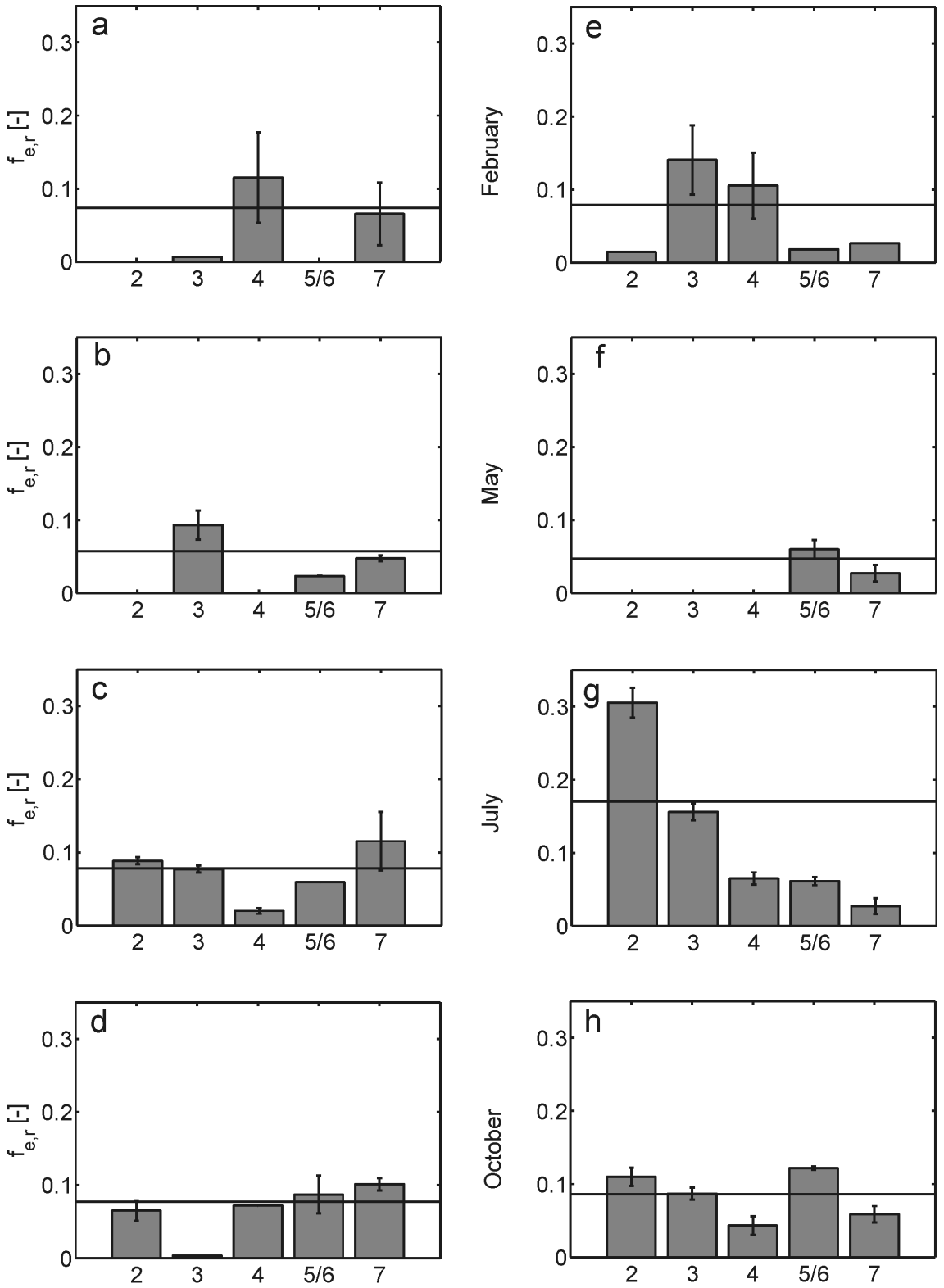

Figure 3.11.: Comparison of $f_{e,r}$ between stations for each deployment for wind waves (a-d) and boat wakes (e-h). The solid line indicates the respective mean value and variability is represented by the standard error.

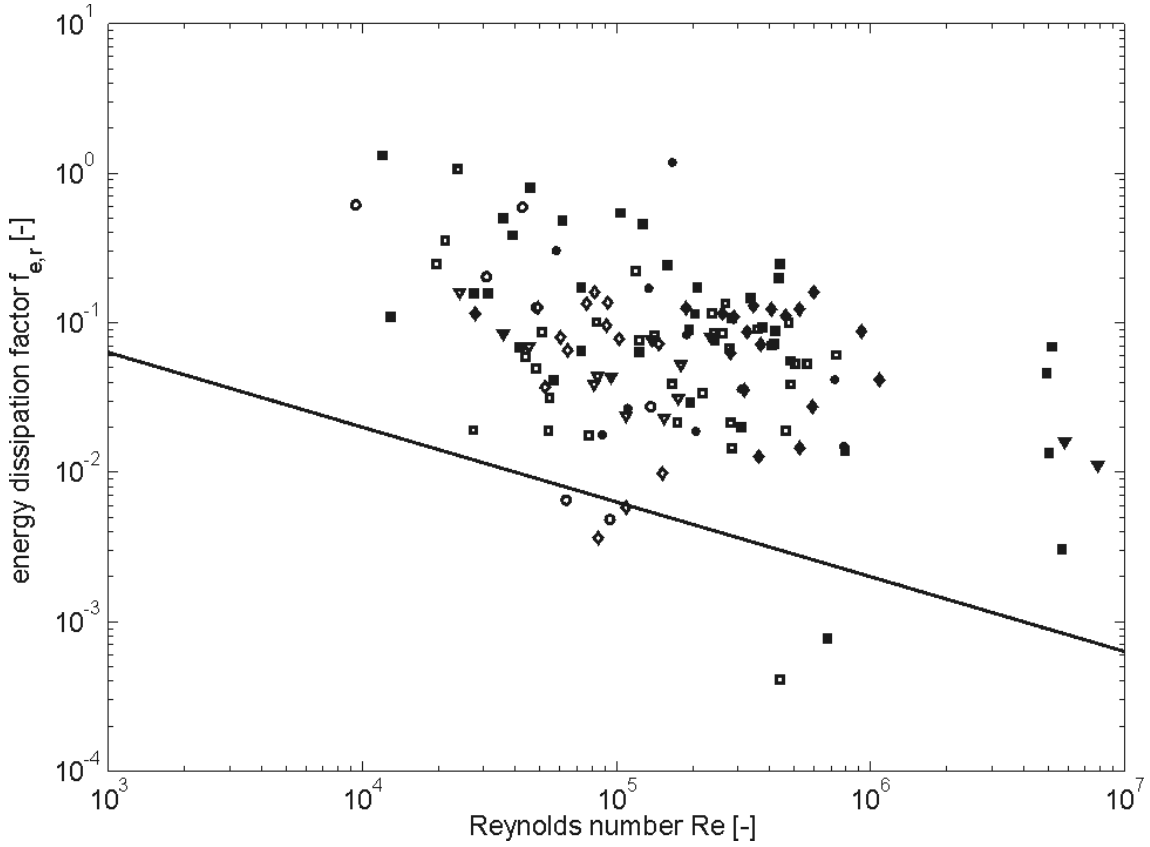

Figure 3.12.: Relationship of energy dissipation factor $f_{e,r}$ and wave Reynolds number Re for all deployments. filled symbols = boat wakes; open symbols = wind waves; ◯ = February; ▽ = May; □ = July; ◊ = October'09. The solid line represents the relationship to Re under conditions of laminar flow $f_{e,r} = 2/\sqrt{Re}$.

3.13 and 3.14) and the relationship to wave Reynolds number ($Re = u_{b,r}^2/(w\nu)$, ω = wave angular frequency and ν = kinematic viscosity) has been suggested by Iwagaki and Kakinuma (1967). Figure 3.12 shows the relationship between $f_{e,r}$ and Re for all deployments separated into boat wakes and wind waves.

The majority of values are above the theoretical relationship for laminar conditions and hence are fully turbulent. It has been observed for rough turbulent conditions that the wave friction factor f_w is independent of Reynolds number and solely depends on the relative roughness $u_b/\omega k_N$ where k_N is the equivalent Nikuradse roughness (Kamphuis, 1975). Wave friction factor and energy dissipation factor are linked through the phase lag φ between bottom shear stress and wave orbital velocity

$$f_{e,r} = f_w \cos\varphi \tag{3.16}$$

$$\varphi = 33 - 6\log\frac{u_b}{\omega k_N} \tag{3.17}$$

It can therefore be assumed that a similar relationship with relative roughness exists for $f_{e,r}$ (Madsen, 1994). Several formulae have been proposed to describe the relationship between friction factor and relative roughness: The one by Nielsen (1992) is the most widely used:

$$f_w = \exp\left[5.5\left(\frac{u_b}{\omega k_N}\right)^{-0.2} - 6.3\right] \tag{3.18}$$

Using this relationship between energy dissipation factor and relative roughness, an attempt was made to estimate k_N. The equivalent Nikuradse roughness was initially defined to evaluate bed forms as roughness elements and describe bed roughness through a single parameter (Nielsen, 1992). However, the application of this parameter to flexible vegetation is unproven.

Madsen (1994) proposed an alternative to eq. 3.18 in his spectral model which includes a parameter C_μ to account for the effect of an underlying current. While a variable current existed during the present experiments (Figure 3.6), it was chosen to neglect its effect on f_w for several reasons. While a current is likely to cause bending of the flexible vegetation leaves, it is not known in detail how the current affects seagrass. Additionally, experiments over fixed beds showed that k_N is bed specific and not affected by changing hydrodynamic conditions (Mathisen and Madsen, 1999). Equation 3.18 should therefore yield a good first approximation, especially as values of C_μ are generally close to unity (Madsen, 1994).

Eq. 3.16, in conjunction with eq. 3.17 and 3.18, did not show a significant trend (Table 3.4). By contrast, the values appeared to alternate around a common mean and any change throughout the year seemed to fall within the natural variability.

Table 3.4.: Average energy dissipation factors $f_{e,r}$ and bed roughnesses k_N for all deployments. Variability is expressed as the standard deviation of the scatter.

	$f_{e,r}$	k_N
February '09	0.07±0.1	0.14±0.07
May '09	0.02±0.02	0.17±0.04
July '09	0.06±0.05	0.14±0.06
October '09	0.05±0.03	0.21±0.15

The mean value for this study was $k_N = 0.17$ m which is similar to roughnesses found for rough and rippled beds. Mathisen and Madsen (1996a,b, 1999) estimated bed roughnesses of 0.14-0.28 m over evenly-spaced, triangular bars during laboratory experiments and a field study found $k_N = 0.16$ m for a coral reef (Lowe et al., 2005). Iwagaki and Kakinuma (1967) carried out measurements over rippled sand of grain sizes similar to those grain sizes found in Ryde; thus from their data $k_N = 0.13$ m was derived.

Because the energy dissipation factor is dependent on the seasonality of seagrass characteristics, it is not appropriate to compare the wave attenuation effect between different species. A parameter more suitable for such a comparison is the drag coefficient C_D (equation 3.15). A comparison of the time averaged drag coefficient shows that C_D behaves similar across frequencies for all deployments (Figure 3.13). For frequencies <0.4 Hz the values alternate around a constant value of 1.67±0.07 before they increase with increasing frequency. The latter is in agreement with observations by Bradley and Houser (2009) who found an increase of C_D with increasing frequency for f > 0.4 Hz in a *Thalassia testudinum* bed. They also observed a reduction in C_D at f = 0.38 Hz and suggested that this can be attributed to the relative motion of the seagrass which is not uniform across frequencies. While in this study a slight increase at 0.2 Hz and a decrease at 0.45 Hz could be observed in July, this variation was not significantly different from the other deployments (ANOVA, F = 1.19, p = 0.31, n = 70). The dependence of C_D on seagrass motion as suggested by Bradley and Houser (2009) could therefore not be found during the

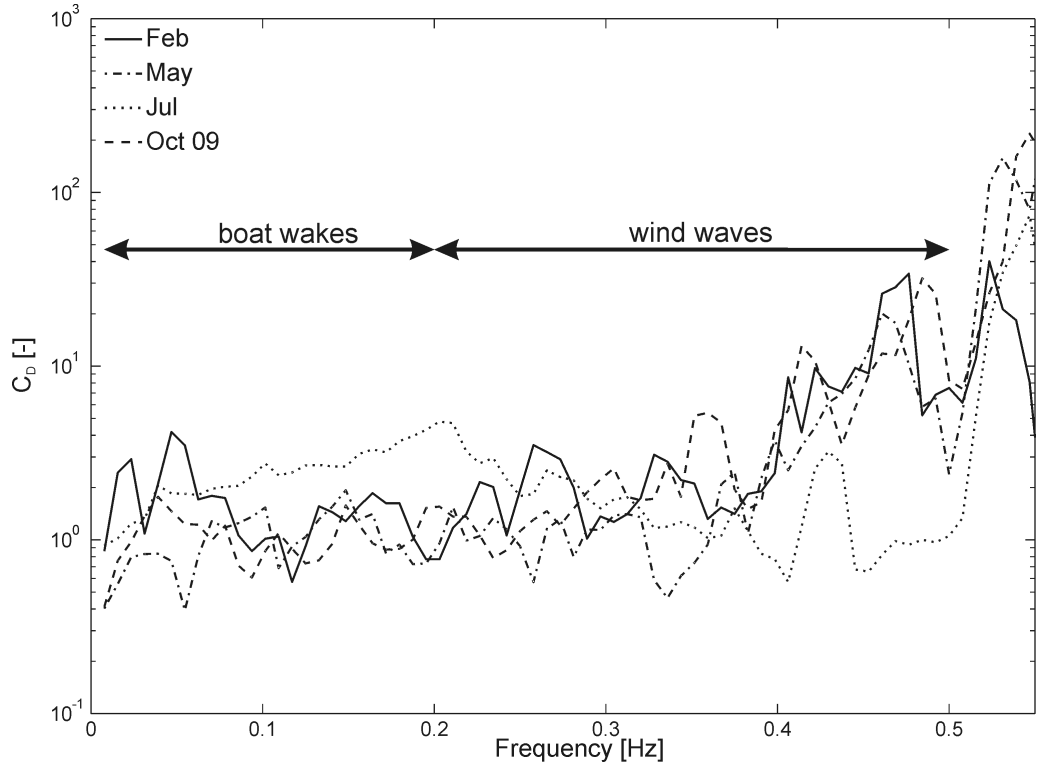

Figure 3.13.: Time and spatial averaged drag coefficient by wave frequency.

present study. This could be due to the presence of an underlying current for parts of the tidal cycle, which would affect the swaying motion of the seagrass. No data are available on the relative motion of *Z. noltii* in Ryde and the above hypothesis could therefore not be addressed within this study. However, the results show that there is no significant difference in C_D for boat wakes and wind waves and values from both wave types can be evaluated together.

In previous studies a relationship of the representative drag coefficient with the vegetation Reynolds number ($Re_v = bu_b/\nu$) has been found (Kobayashi et al., 1993; Méndez et al., 1999; Bradley and Houser, 2009). The vegetation Reynolds number is considered more suitable in this case than the wave Reynolds number, because, like C_D, it includes a vegetation parameter rather than wave parameters only. A relationship of C_D with Re_v can be observed with an increase at low Reynolds numbers and approaching a constant value for $Re_v \gtrsim 600$ (Figure 3.14). Previous studies proposed a relationship of the from $C_D = a + (b/Re_v)^c$ (Kobayashi et al., 1993; Méndez et al., 1999; Bradley and Houser, 2009) which yielded for the present

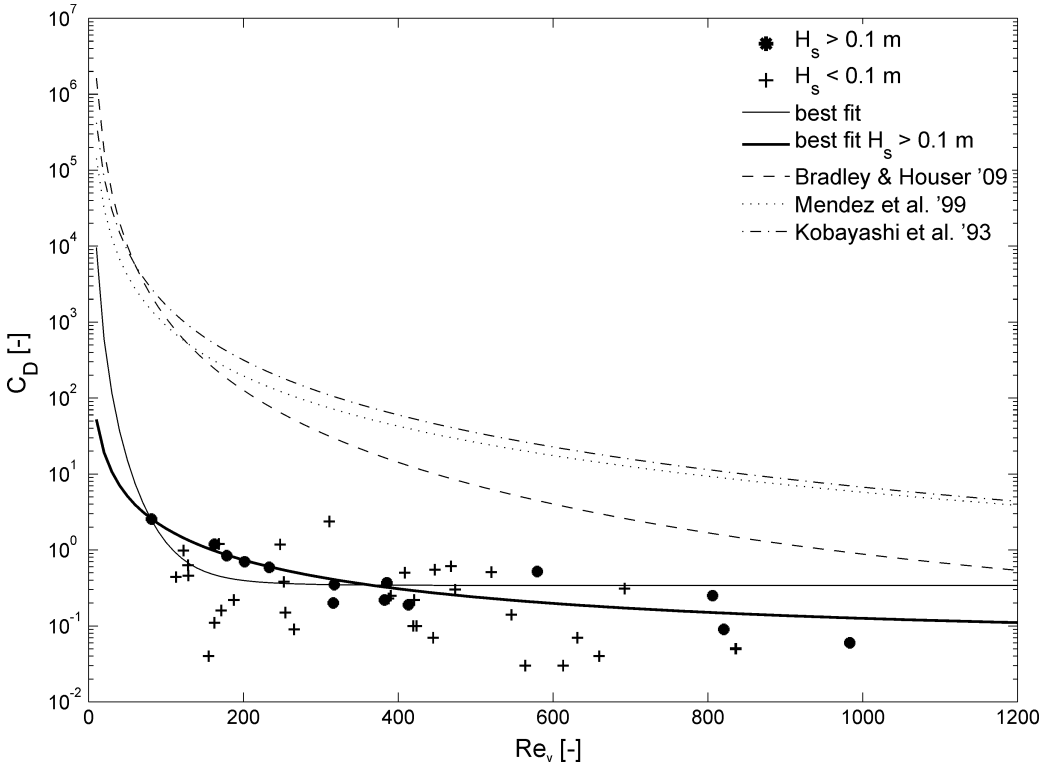

Figure 3.14.: Relationship between C_D and vegetation Reynolds number Re_v, the best fit for all data and $H_s > 0.1\,m$. Also shown are the best fit lines for Bradley and Houser (2009)($C_D = 0.1+(925/Re_v)^{3.16}$), Méndez et al. (1999)($C_D = 0.08 + (2200/Re_v)^{2.2}$) and Kobayashi et al. (1993)($C_D = 0.08 + (2200/Re_v)^{2.4}$).

data ($R^2 = 0.37$, n = 46):

$$C_D = 0.34 + \left(\frac{97.9}{Re_v}\right)^{4.02} \tag{3.19}$$

The scatter is caused by the varying hydrodynamic conditions throughout the study; especially wave height affects C_D as it appears in eq. 3.15 with a power of 3. If only data with $H_s \geq 0.1$ m is considered, a good fit ($R^2 = 0.96$, n = 14) of the form:

$$C_D = 0.06 + \left(\frac{153}{Re_v}\right)^{1.45} \tag{3.20}$$

can be achieved (Figure 3.14) and values for $H_s < 0.1$ m scatter around this fit.

3.6. Discussion

It is widely accepted that seagrass attenuates waves (Ward et al., 1984; Fonseca, 1996; Newell and Koch, 2004; Koch et al., 2006a, 2009) and although laboratory studies have shown that wave height reduction responds non-linearly to vegetation traits such as density and canopy height as well as distance into the meadow (Fonseca and Cahalan, 1992; Kobayashi et al., 1993; Méndez et al., 1999; Bouma et al., 2010) field studies to support these observations are still scarce (Newell and Koch, 2004; Bouma et al., 2005; Bradley and Houser, 2009). The present study investigated wave attenuation over a *Zostera noltii* meadow at four different stages during the growth cycle and found a dependence of energy dissipation on seagrass traits as well as hydrodynamics.

Due to the variable nature of the study environment, it was necessary to make several assumptions during data analysis. For example, wave refraction from the adjacent pier was not considered in detail. Effects of refraction were not observed in the wave field or bed ripples *in situ* which led to the conclusion that its effect is small. However, it is possible that refracted waves have an impact on the incoming waves along the instrumented transect. Waves measured during this study were generally small ($\sim$0.1 m) which means that even refracted waves of 1 cm could have a decisive influence. To eliminate refraction effects as much as possible, waves from the direction of the pier were excluded from analysis, but refraction was not taken into account in more detail. It is therefore possible, that some effect of refraction is still present in the dataset.

Another influencing parameter not taken into account in this study is the presence of a tidal current. Tidal currents were present during all deployments and changed significantly over the tidal cycle (Figure 3.6). While their influence on incident waves was considered negligible (Madsen, 1994), they may have affected the group velocity C_g which was used to calculate the wave energy flux F. This possible effect, however, was neglected as no wave groups were detected within the dataset and

the value for C_g is merely theoretical in this case. Moreover, the current's effect on C_g is considered small compared to the effect an underlying current has on the seagrass. Flexible vegetation will streamline under a current (Fonseca and Koehl, 2006; Backhaus and Verduin, 2008) and therefore change its roughness. As the movement of seagrass in Ryde was not known, the effect of an underlying current was not included in this study but is addressed in more detail in Chapter 4.

Nevertheless, the data show that the representative energy dissipation factor $f_{e,r}$ decreased towards the shore for boat wakes in July while it remained constant across the sandflat for all other deployments and hydrodynamic conditions. This difference in behaviour could be due to the seagrass presence. While seagrass is present during all other deployments, shoot density in July is at least twice that of other deployments. Newell and Koch (2004) found that a minimum shoot density was required for *Ruppia maritima* to have a measurable effect on wave attenuation. This might also be true for *Zostera noltii*: the data suggest that the threshold lies between approx. 2,000 and 4,000 shoots/m^2. Above this threshold, the seagrass changes the wave attenuating function of the bed, causing higher friction at the outer stations and therefore attenuating the waves more effectively. Similar behaviour has been found in salt marsh (Möller et al., 1999; Bouma et al., 2005) and although it is not necessarily beneficial for the plants that cause wave attenuation, it will create more suitable conditions for other plants within the meadow and can therefore be considered as a division of labour within the ecosystem (Bouma et al., 2005). While seagrass is morphologically very different from salt marsh vegetation, and its flexible leaves bend a lot more under flows, an exponential decay of wave attenuation has been observed in *Thalassia testudinum* (Bradley and Houser, 2009) and is therefore likely at high densities for *Z. noltii* as well.

The effect of density and wave frequency did not reflect in the values for bed roughness k_N despite its relationship to $f_{e,r}$ described in eq. 3.16, in conjunction with eq. 3.17 and 3.18. Values derived for all deployments did not differ significantly (Table

3.4) and fell within the range of roughnesses estimated for rough and rippled beds (Iwagaki and Kakinuma, 1967; Mathisen and Madsen, 1996a,b, 1999; Lowe et al., 2005). It is therefore possible that the effect of sand ripples present at the study site dominate k_N and compared to this, the effect of *Z. noltii*'s above ground biomass was too small to be detected under field conditions. That the values do not correlate with seagrass growth may also be due to the range of water depths covered in this study. Figure 3.9 shows wave height reduction did not take place in water deeper than $\gtrsim$1 m. The majority of data that fit the quality criteria wave spread $<10^{\circ}$ and $\alpha - \beta < 20^{\circ}$ (in eq. 3.11) to calculate $f_{e,r}$ and k_N, however, came from depths $>$1.5 m. It could be possible that the effect of *Zostera noltii* on wave attenuation in such water depths is very small and differences between deployments could therefore not be detected in the mean values for $f_{e,r}$ and k_N (Table 3.4). Another possible reason why the estimated values do not correlate with seagrass growth could lie within the method itself. Madsen's (1994) relationship between friction factor and bed roughness is based on the assumption that k_N is independent of ambient hydrodynamic conditions. This assumption has been validated for fixed beds in laboratory studies (Mathisen and Madsen, 1999), but may not be valid for flexible vegetation. Vegetation moves with the orbital motions under waves; it changes its shape constantly and hence its roughness is not likely to remain constant. Consequently, vegetated areas may not satisfy the assumption that their roughness is independent of hydrodynamic forcing and models based on k_N may not be applied reliably over vegetated beds. If this is the case, Madsen's (1994) method may not be suitable to determine the bed roughness and therefore wave friction associated with a vegetated bed.

An alternative parameter to describe energy dissipation is the drag coefficient C_D which is independent of the seasonality of seagrass density and leaf length, but shows a relationship with hydrodynamics in the form of the vegetation Reynolds number Re_v (Figure 3.14). Figure 3.14 also shows the curves derived by Kobayashi et al. (1993), Méndez et al. (1999) and Bradley and Houser (2009) respectively.

Kobayashi et al. (1993) developed a model for wave damping of monochromatic waves under the assumption that vegetation can be represented by fixed cylindrical elements. They applied their model to data obtained by Asano et al. (1988) who carried out laboratory experiments on artificial kelp. Méndez et al. (1999) extended the model to random waves and also used the data from Asano et al. (1988) to validate their model. The resulting relationship gives slightly lower values than the one by Kobayashi et al. (1993). Bradley and Houser (2009) applied equation 3.15 to field data obtained in a *T. testudinum* meadow and derived the relationship shown in Figure 3.14.

From the empirical fits, a difference between species can be seen and it is possible to deduce a dependence of C_D on vegetation stiffness. Under the assumption that polypropylene represents the kelp's plant stiffness well during Asano et al.'s (1988) laboratory experiments, they will have been stiffer than *T. testudinum* or *Z. noltii*. This would lead to a higher drag coefficient for a given value of Re_v. The difference between *T. testudinum* and *Z. noltii* can be explained in a similar fashion, because *T. testudinum* leaves are less flexible than *Z. noltii* leaves (Kuo and Den Hartog, 2006).

Overall, the observed effect of *Zostera noltii* on wave attenuation in Ryde was small. Within the wave heights measured during this study an effect on $f_{e,r}$ could only be observed at the highest densities in July and no annual variation was observed in the time averaged bed roughness k_N. Bed roughness values may therefore have been dominated by present bed forms and k_N may therefore not be a suitable parameter to include the effect of *Zostera noltii* in numerical models. The drag coefficient, however, may be a suitable parameter to describe the effect of vegetation on wave attenuation. Although the model used in this chapter (equation 3.15) neglects plant movement by assuming rigid vegetation, it has been successfully used in the past together with a relationship between Re_v and C_D of the form:

$$C_D = c + \left[\frac{d}{Re_v}\right]^e \tag{3.21}$$

with c, d and e being best fit parameters. Although the relationship presented in this study (equation 3.20) is based on a limited range of Reynolds numbers, it is a promising start to include *Z. noltii* in wave attenuation models.

3.7. Conclusions

The results show that *Zostera noltii* has an effect on wave attenuation which varies seasonally with shoot density. However, a minimum density was required before attenuation could be observed. The existence of such a threshold suggests a non-linear relationship between the two parameters. Moreover, the density threshold varies with hydrodynamics; the higher the wave period is, the lower is the required density to initiate wave attenuation.

Once the threshold density is exceeded, a change in energy dissipation with distance from the shore can be observed, but the present dataset is not sufficient to establish whether this change in linear or non-linear. A clear non-linear relationship has been found, however, for the drag coefficient C_D. It describes the drag per unit plant area and is therefore independent of seasonal parameters such as height and density. Consequently, it can be applied all year round, but it changes with hydrodynamic conditions. While a strong relationship with Reynolds number was found for waves with a wave height $\geq$0.1 m, scatter increased when waves with a lower wave height were considered.

Overall, the data show that wave attenuation over vegetation does not only depend on plant characteristics, but also on the hydrodynamics that act on the plants. As hydrodynamic forcing is likely to be higher (i.e. storms) in winter when shoot densities are low, *Z. noltii* may play a limited role in shore protection by wave attenuation. Nevertheless, the combined interaction of plant characteristics and

hydrodynamics adds to the complexity of estimating the economic value of seagrass meadows and describing the effect plant attributes have on wave attenuation is only the beginning.

4. Wave attenuation by vegetation: the effect of organism traits and tidal current

4.1. Abstract

Accurate wave height prediction along the shore plays an important role in coastal protection and management. To account for the effect of submerged vegetation in wave attenuation models, it is important to understand how the interaction between vegetation characteristics and hydrodynamic forcing affects wave attenuation. To determine the effect of vegetation characteristics, seagrass mimics were used that varied in (1) blade stiffness, (2) shoot density and (3) leaf length; to investigate the effect of hydrodynamic forcing wave attenuation in the absence and presence of a tidal current was studied. Results show that wave attenuation is positively correlated with blade stiffness. For a given wave in shallow water, attenuation is dependent on a combination of shoot density and leaf length which can be described by the leaf area index. The presence of a tidal current strongly reduced the wave attenuating capacity of seagrass meadows and this reduction was most pronounced at high shoot densities. Thus, most studies that have been carried out under waves only will

structurally overestimate wave attenuation for tidal environments, emphasising that tidal currents need to be taken into account in future studies on wave attenuation by vegetation.

4.2. Introduction

The interaction of seagrass with hydrodynamics is widely recognised to affect ecological processes such as nutrient transport and pollen dispersal (Verduin et al., 2002), sediment dynamics (Fonseca, 1996) and coastal erosion (Stein et al., 1989). One component of this effect is wave attenuation which has been addressed for a variety of seagrass species (Fonseca and Cahalan, 1992; Koch and Gust, 1999; Verduin and Backhaus, 2000; Méndez and Losada, 2004) and studies have shown that submerged seagrass vegetation can have a significant impact on wave attenuation. To correctly account for the effect of seagrass on wave attenuation in coastal protection and management, it is necessary to understand which vegetation traits and hydrodynamic parameters drive wave attenuation by vegetation (Teeter et al., 2001; Patil and Singh, 2009).

In a laboratory study, Fonseca and Cahalan (1992) found a reduction in wave energy density of approx. 40% per metre of seagrass meadow for four different seagrass species and reductions of up to 80% have been observed in the field (Prager and Halley, 1999). A comparative study between seagrass and salt marsh species (Bouma et al., 2005) indicated that plant stiffness affects wave attenuation, though this effect was not found when comparing rigid structures with mimics that moved in a cantilever motion (Augustin et al., 2009). The effect of stiffness on wave attenuation has been described for large macroalgae (Koehl, 1996; Denny and Gaylord, 2002). However, when comparing wave attenuation over stiff *Spartina anglica* and flexible *Puccinellia maritima* marsh vegetation, Bouma et al. (2010) observed that differences disappear on a biomass basis, meaning that an increased shoot density can counteract the re-

duced wave attenuating capacity of flexible plants. While previous studies suggest that stiffness can play a role in wave attenuation by vegetation, most studies have been carried out on vegetation types other than seagrass (i.e. salt marsh or macroalgae). Stiffness determines how much, and moreover in what way, a plant moves under the influence of waves. Depending on their stiffness, seagrasses move in a cantilever or a whip like motion (Figure4.1). A transition from the former to the latter takes place with increasing wave amplitude (Manca, 2010) and the rate of this transition varies with stiffness. It is not yet clear what role this type of motion plays in wave attenuation by seagrass.

The effect of shoot density on wave attenuation has been recognised in a number of studies (i.e. Bouma et al., 2005; Chen et al., 2007; Augustin et al., 2009; Prinos et al., 2010), but the number of densities used was generally low (2-3) and not sufficient to qualify its influence on wave attenuation. Augustin et al. (2009) observed that the influence of shoot density on wave attenuation increased with decreasing submergence ratio (defined as the ratio of water depth to vegetation height) for artificial salt marsh; this was recently confirmed for *Posidonia oceanica* mimics (Prinos et al., 2010). The effect of submergence ratio on wave attenuation has been previously addressed by changing the water depth over vegetation of constant height. This approach showed that wave attenuation is directly related to submergence ratio (Fonseca and Cahalan, 1992; Bouma et al., 2005; Augustin et al., 2009; Prinos et al., 2010). However, a change in water depth resulted in a change in wave parameters such as wave height and/or period, making it unclear whether the change in hydrodynamic conditions influenced the results. Hence there is a need to study this aspect by maintaining a constant water depth while varying the vegetation height.

In the past, laboratory studies have neglected the possible effects of a current. While this approach helps to understand the general processes of wave attenuation by vegetation, it is a simplification of the natural environment where most seagrass meadows are exposed to waves superimposed on a tidal flow. The effect of an underlying

current on wave attenuation over unvegetated beds has been recognised (Madsen, 1994) and a field study on kelp (Gaylord et al., 2003) investigated the effect of an alongshore current on wave forces. Gaylord et al. (2003) observed that the current perpendicular to wave propagation reduced wave energy dissipation compared to rigid structures and the reduction increased with increasing flow velocity. So far Gaylord et al. (2003) are the only ones who considered the effect of vegetation on combined waves and currents, and the effect of a current on wave attenuation by seagrass has not yet been addressed.

Previous studies have identified submergence ratio, shoot stiffness and density as important factors in wave attenuation, but a more systematic analysis of their influence on wave attenuation is needed to understand the effect of submerged vegetation on wave height (Bouma et al., 2010) and to incorporate it in coastal design (Fonseca and Cahalan, 1992). This study aims to investigate the impact of those three seagrass traits on wave attenuation. To disentangle the influence that the specific vegetation traits have on waves, simple but mechanically realistic seagrass mimics were developed and used for experiments in a laboratory flume. The effect of submergence ratio is addressed by changing the mimics' leaf length and conducting tests under identical wave conditions in constant water depth. Mimics with three different stiffnesses and bending behaviours were produced and a total of five densities were tested. Another objective for this study was to investigate how a current affects wave attenuation by seagrass. The mimics were therefore exposed to waves with and without an underlying steady current.

4.3. Materials and Methods

4.3.1. Seagrass mimics

This study focused on the seagrass species *Zostera noltii* which is native to the European Atlantic coast (Den Hartog, 1970). In order to disentangle the impact

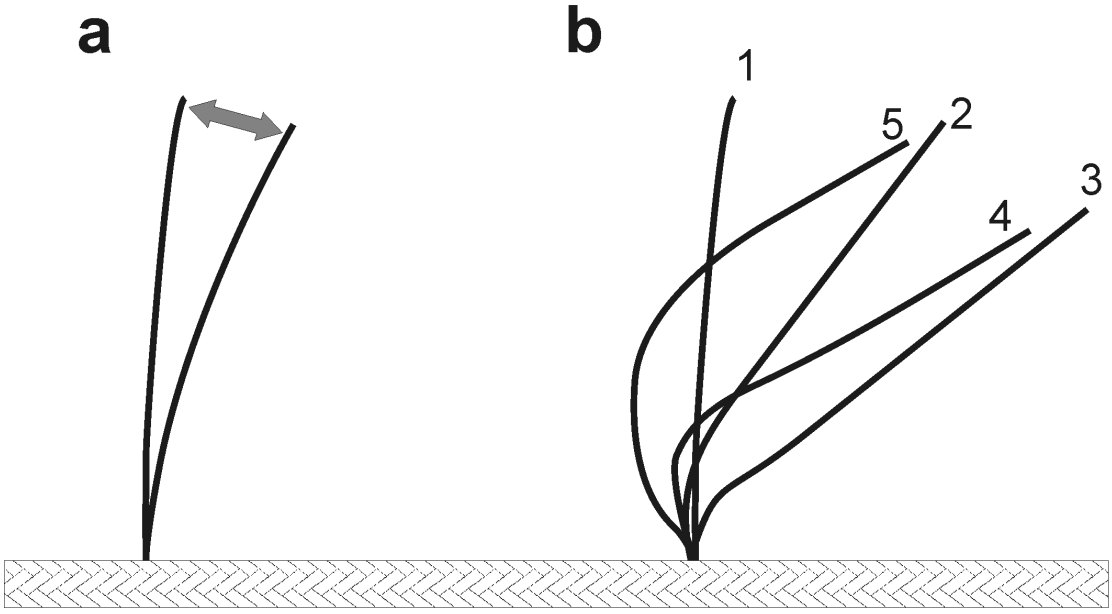

Figure 4.1.: Schematic representation of mimic movement. a. the stiff material moves back and forth like a cantilever and b. both the flexible and very flexible material move in a whip like motion.

of seagrass traits (1) vegetation density, (2) shoot flexibility and (3) leaf length on wave attenuation, while excluding effects of other morphological parameters, plant mimics based on *Z. noltii* were used, as this species has a simple and well described morphology (Den Hartog, 1970). Individual shoots grow from a rhizome which is secured in the ground by roots emerging from its nodes. Shoots consist of a stem or sheath and several ribbon-shaped leaves which can be easily reproduced in realistic mimics. Single traits of the mimics can be changed while maintaining all other characteristics and therefore yielding information on the impact of single vegetation traits on hydrodynamics. Seagrass mimics have been successfully used in the laboratory (Bouma et al., 2005; Fonseca and Koehl, 2006; Ghisalberti and Nepf, 2006), and in field studies (Lee et al., 2001) and are generally accepted. Fonseca and Koehl (2006) used mimics to investigate hydrodynamics within and above seagrass meadows while Lee et al. (2001) investigated the importance of seagrass to associated fauna using mimics. Additionally, mimics have also been widely applied in engineering studies (Stein et al., 1989).

The dimensions of the mimics were based on the natural size and density ranges of

Z. noltii. Leaf width of all mimics was 2 mm ±10% which represents the upper limit of natural width of *Z. noltii* (Phillips and Meñez, 1988). Mimics with three different flexibilities were developed and materials were chosen so as to show different bending behaviour. The stiff mimic (cable ties) was similar to mimics that have been used to represent salt marsh vegetation (Bouma et al., 2005) and moved like a cantilever under wave motion (Figure 4.1a). The flexible material (poly ribbon) bent similar to *Z. noltii* plants in a whip like motion under waves (Figure 4.1b). Finally, a very flexible material (poly pocket strips) was used that bent even more than *Z. noltii* and also showed a whip like motion (Figure 4.1b). Mimic materials that move and behave similar to real vegetation (salt marsh and *Z. noltii*) were found visually by comparing live plants and various mimic materials in a laboratory flume. The material that best simulated the plant's movement was chosen to produce the mimics for this study. Mimic meadows with a density of 1000 and 4000 shoots/m^2 were produced for all flexibilities. Additional meadows with densities of 500, 2000 and 8000 shoots/m^2 were generated for the flexible mimic. These densities cover a wide range of natural densities of *Z. noltii* (Table 4.1) and yield a detailed investigation of the impact of shoot density on wave attenuation.

Leaf lengths under investigation covered the natural range for *Z. noltii* (Table 4.1). The initial leaf length of the flexible and very flexible meadows was 30 cm and during the course of the study it was reduced to 15 cm and then 10 cm to investigate wave attenuation under different submergence ratios, but with constant water depth. For the stiff meadows the initial leaf length was 15 cm which was reduced to 10 cm during the course of the experiments. The combination of the above flexibilities, densities and leaf lengths led to a total of 25 different meadow types (Table 4.1). Each meadow was 3 m long, 0.6 m wide and covered the width of the flume (see below).

To create the meadow the mimics were tied to a canvas mesh with a mesh size of 0.8 cm. To achieve an evenly distributed and yet arbitrarily organised meadow

Table 4.1.: Shoot density and leaf length for *Zostera noltii* and mimics. All meadows in the present study were exposed to waves with and without an underlying current.

vegetation type	shoot density [per m^2]	leaf length [cm]	source
Zostera noltii	4000-22000	6-20	Auby and Labourg, 1996
Zostera noltii	4021-5400	17.3-45.0	Curiel et al., 1996
Zostera noltii	2030-14617	<47.5	Sfriso and Ghetti, 1998
Zostera noltii	256-6144	5-29	Chapter 3
stiff mimic	1000	10 & 15	present study
	4000	10 & 15	present study
flexible mimic	500	10 & 15 & 30	present study
	1000	10 & 15 & 30	present study
	2000	10 & 15 & 30	present study
	4000	10 & 15 & 30	present study
	8000	10 & 15 & 30	present study
very flexible mimic	1000	10 & 15 & 30	present study
	4000	10 & 15 & 30	present study

that would be comparable to a natural distribution in the field, the canvas was segmented into squares of 3.4 x 3.4 cm. For the density of 1000 shoots/m^2 one strip was placed at a random location within each square. For the other densities, the number of strips per square was reduced or increased accordingly. For each meadow, the canvas was then attached to a wooden board and the board was weighed down on the bottom of the flume for deployments.

4.3.2. Experimental setup

Experiments were carried out under controlled conditions in a racetrack wave flume (Figure 4.2a). The oval flume is 0.6 m wide and has a straight working section of 10.8 m. A water depth up to 0.4 m is possible (Hendriks et al., 2006). The flume is equipped with a conveyor belt system and a wave paddle. Unidirectional flows up to 0.45 m s^{-1} (Bouma et al., 2007), waves of varying heights and periods (Chang et al., 2008) or a combination of both may be generated. This feature provided the opportunity to investigate the influence of vegetation traits on waves only as well as

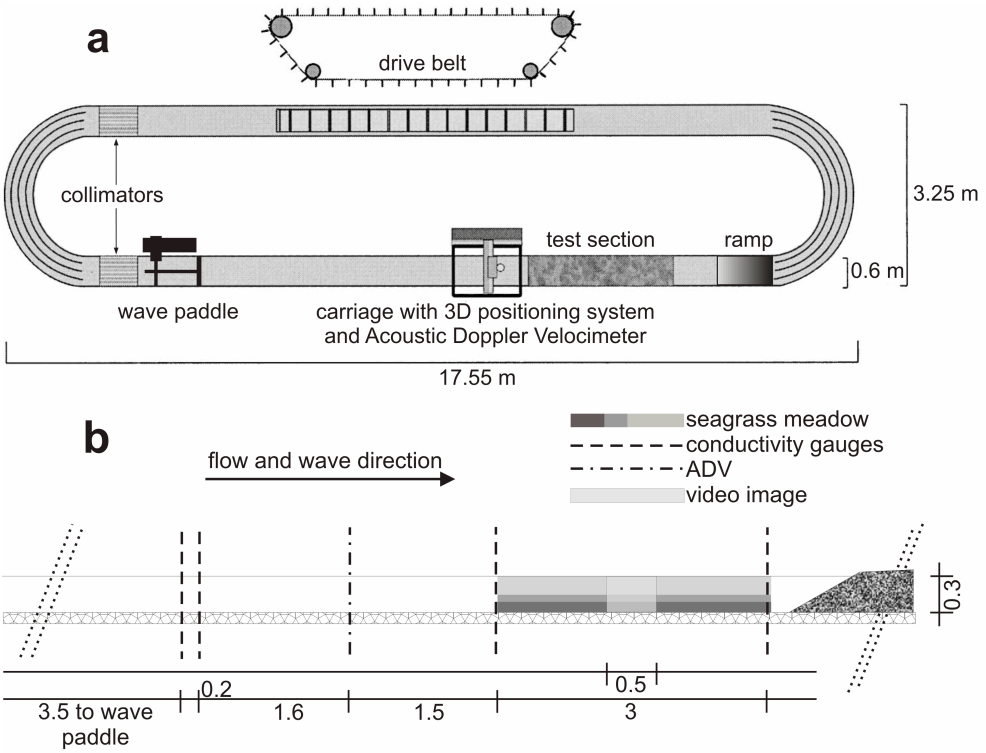

Figure 4.2.: Schematic representation of a. the flume (adapted from Bouma et al., 2005) and b. the setup of instruments (all dimensions in m).

on combinations of waves and steady currents. The latter represent more natural conditions where tidal currents can occur in combination with waves. However, only an incoming tide can be represented during the experiments as flow and waves could only be generated in the same direction. Additionally, the size of the flume allowed running the experiments at full scale and therefore eliminated possible errors that might occur by down-scaling the mimics.

The water depth in the flume was set to 0.3 m which yielded a submergence ratio of 1:1, 2:1 and 3:1 for the respective leaf lengths. All of these ratios have been observed in the field (Koch, 1994; Curiel et al., 1996). Regular waves with a wave height of H = 0.1 m and a wave period of T $\approx$ 1 s were generated by the wave paddle. The waves have been applied to all meadows both with and without an underlying steady current of 0.1 m s^{-1} which corresponds to low tidal currents typical for areas covered with seagrass in the field (Bouma et al., 2005). Additionally, one run was carried out in the absence of seagrass for each hydrodynamic condition as a control.

Wave height was measured with four conductivity gauges (from Danish Hydraulic Institute) at a sampling rate of 25 Hz and recordings were taken for 600 s for each run (Figure 4.2b). Two of the gauges were placed 3.3 m in front of the meadow and spaced 21.5 cm apart to detect occurring reflection. One gauge was placed at the leading edge of the meadow and one at the end of meadow. Additionally, a video camera was used to record seagrass movement through the glass wall of the test section and an Acoustic Doppler Velocimeter (ADV) was used to monitor flow velocities. The filmed section was located 1.5 m into the meadow and film sequences were 300 s long for each run.

4.3.3. Data processing

The data from the two upstream gauges were used to determine the reflection coefficient using the method developed by Baldock and Simmonds (1999). For the two gauges, a phase shift exists between the signals (Figure 4.3a and b) that consists of a positive phase shift for the incident wave trains and a negative phase shift for the reflected wave trains (Frigaard and Brorsen, 1995). To separate the two wave trains within the recorded signal, wave recordings were transformed into the frequency domain using Fast Fourier Transform. The frequency spectra were phase shifted until the incident wave signals at both gauges were in phase and the reflected wave signals were in mutual opposite phase. It was then possible to compute the reflection coefficient and apply a band filter to remove the reflected wave component from the signal (Baldock and Simmonds, 1999). Data were transformed back into the time domain with an Inverse Fast Fourier Transform. Figure 4.3 shows an example of recorded and filtered data for the first wave gauge. The latter is identical to the incident signal (Figure 4.3c) and the difference between the incident and recorded signal is the reflected wave train (Figure 4.3d). Data from the gauges at the beginning and end of the meadow were filtered for the determined reflection if the reflection coefficient exceeded 5% and zero-crossing was used to obtain significant wave height from the

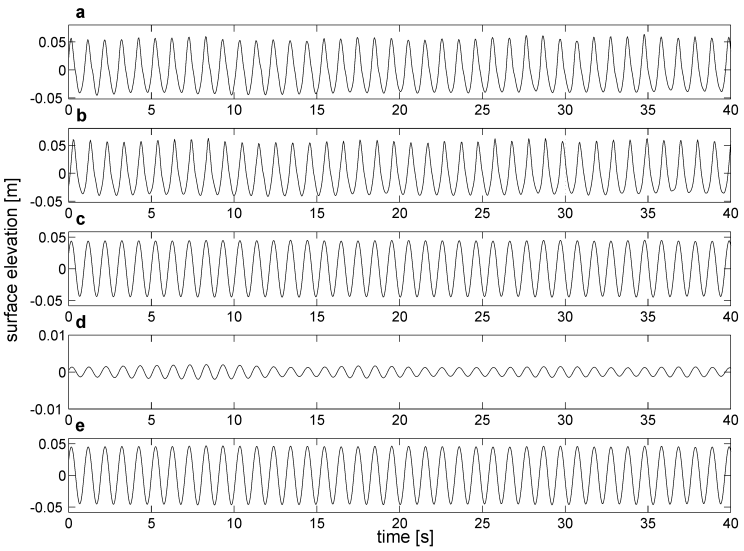

Figure 4.3.: Time series of signals at gauge 1 and 2 for the control run without mimics in the flume under waves only. a. recorded signal at gauge 1; b. recorded signal at gauge 2; c. incident signal at gauge 1; d. reflected signal at gauge 1; e. filtered recorded signal at gauge 1.

filtered time series at the beginning and end of the meadow. From these values the dissipated wave height ΔH per metre of meadow was derived as:

$$\Delta H = \frac{H_{s,b} - H_{s,e}}{x} \tag{4.1}$$

where $H_{s,b}$ and $H_{s,e}$ are the significant wave heights at the beginning and end of the meadow respectively and x is the length of the meadow (3 m). This approach assumes linear wave dissipation along the meadow. Previous studies have shown that the relationship between wave dissipation and distance into a vegetated area is non-linear (Möller et al., 1999; Koch et al., 2009; Bouma et al., 2010). However, linearity is a valid simplification when studying flexible vegetation with relative small wave attenuating capacity over short distances (Fonseca and Cahalan, 1992; Bouma et al., 2005).

As the meadows varied in leaf length as well as density, a parameter that includes both these values was required to compare flume runs. Therefore the leaf area index (LAI = leaf length $*$ leaf width $*$ density) was calculated for each meadow and

consequently used to compare the wave attenuating capacity of each meadow under investigation.

Plant movement was expressed in excursion of the leaf tip which was derived from video recordings. A transparent sheet was placed in front of the computer screen while the video was played back. The maximum tip excursion of 10 leaves per run was marked on the sheet and later measured. Those distances were scaled to full scale using the known height of the window in the flume wall. For the stiff mimic, tip excursion represented the maximum movement of the mimic as the cantilever motion resulted in smaller excursion angles closer to the bed. While the whip like motion of the flexible mimic resulted in higher excursion angles in the middle of the mimic, which in some cases exceeded the excursions of the mimic's tip. An attempt was made to measure the excursion of the central part of the mimics, using black markers half way up the mimics. However, only markers from mimics close to the flume wall could be seen. Since mimics close to the wall were influenced by edge effects, excursion data from those mimics were not representative for all mimics in the meadow and could therefore not be used for analysis. Consequently, the excursion of both mimic types (stiff and flexible) is represented by the tip excursion.

The force required to deflect the stiff mimic from the vertical was measured with a strain gauge (from Gould). A 15 cm long mimic was placed horizontally on a board and the base was fixed in position. The gauge was attached to the tip of the mimic and pulled sideways until the mimic's tip reached a predefined angle. Once the required angle was reached, a reading of the strain gauge was taken. Due to the gauge design, these measurements were carried out in air. Values will therefore differ from forces required in water, however, the values in air show the general relationship between applied force and deflected angle.

4.4. Results

For all seagrass meadows (Appendix B), the reduction of wave height exceeded that during the control runs without mimics in the flume (Figures 4.4 and 4.6). Additionally, an effect of plant stiffness on wave attenuation was obvious when comparing the results from all mimic materials used (Figure 4.4). All three stiffnesses yielded a clear linear relationship of wave dissipation with LAI: $\Delta H = 0.61 * LAI + 0.56$ ($R^2 = 0.94$), $\Delta H = 0.14 * LAI + 0.57$ ($R^2 = 0.84$) and $\Delta H = 0.1 * LAI + 0.56$ ($R^2 = 0.62$) for the stiff, flexible and very flexible mimics respectively. The attenuating effect of the stiff material was much higher for a given LAI compared to the two flexible mimics. This is indicated by the much steeper slope of the regression line for the stiff mimics than the flexible mimics, while the intercept is comparable. While the regression lines indicate that wave attenuation by the very flexible mimic was less than for the flexible one, this difference is driven by a single data point at LAI = 2.4 and the two populations are not significantly different (ANOVA, $F = 0.88$, $p = 0.36$). The very flexible mimics were therefore excluded from further analysis and only data from stiff and flexible mimics will be considered hereafter.

Results also showed that wave dissipation increases with submergence ratio (Figure 4.5). However, the data suggest that the effect of submergence ratio remains almost constant for shoot densities $\leq$2000 shoots per m^2 and increases with increasing density above this value.

Comparing wave attenuation in the absence or presence of an underlying current of 0.1 m s^{-1} revealed that if a current is present, both wave dissipation and the observed canopy height are reduced for any given vegetation length (Figure 4.6). The canopy height reduction by currents is up to 36% for the flexible material with the largest reduction for long flexible leaves compared to shorter ones (Figure 4.6c-g), not surprisingly, it is much smaller for the stiff material (up to 7%, Figure 4.6a-b). Leaf bending due to currents puts leaves lower in the water column where they are exposed to less orbital motion. However, even when comparing meadows with a

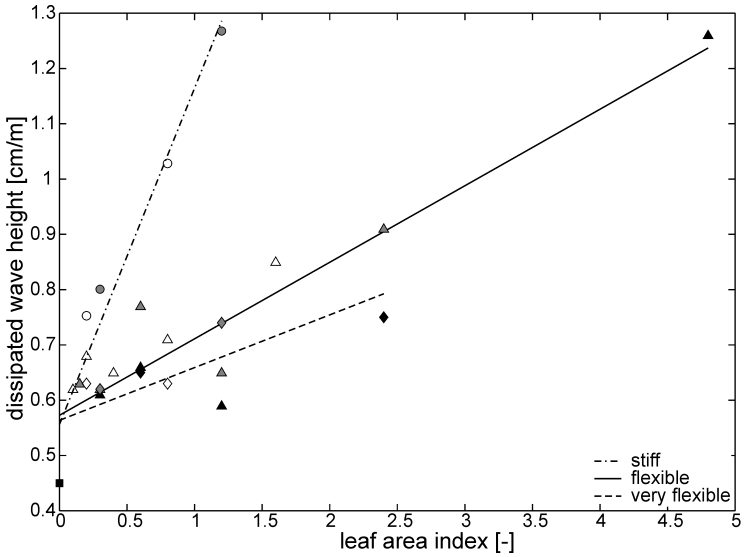

Figure 4.4.: Dissipated wave height in cm/m as a function of leaf area index under waves only. The square indicates the value without any seagrass in the flume. ◯ = stiff mimic; Δ = flexible mimic; ♢ = very flexible mimic. The symbol colours represent leaf lengths: black = 30 cm; grey = 15 cm; white = 10 cm. Linear regression yields for the stiff material $\Delta H = 0.61 * LAI + 0.56$ ($R^2 = 0.94$), for the flexible material $\Delta H = 0.14 * LAI + 0.57$ ($R^2 = 0.84$) and for the very flexible material $\Delta H = 0.1 * LAI + 0.56$ ($R^2 = 0.62$).

similar actual canopy height (Figure 4.6), wave dissipation rates in the presence of a current are lower than in the absence of a current. This indicates that processes other than the position of the leaves in the water column causes the observed reduction in wave attenuation in the presence of a current.

Wave dissipation as a function of canopy height (Figure 4.6) follows a relationship of the form

$$\Delta H = cs^d \tag{4.2}$$

where s is canopy height, c is a scaling factor along the y-axis and d is the scaling exponent that determines the function's rate of growth (Table 4.2). The constant offset between the regression lines with and without a current suggests that the difference between ΔH_w (wave only) and ΔH_{wc} (combined waves and currents) remains constant with canopy height. As flume runs were not available for a single

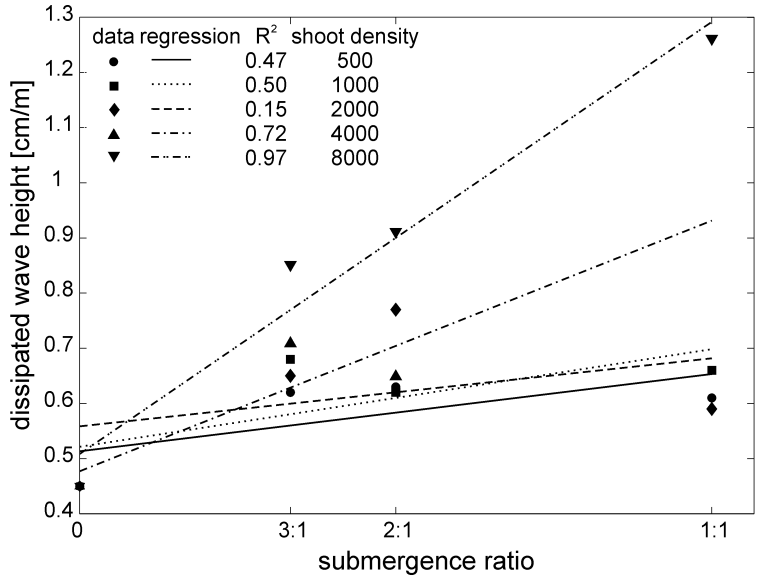

Figure 4.5.: Dependence of wave dissipation on submergence ratio for various shoot densities.

Table 4.2.: Regression parameters for the relationship of wave dissipation and canopy height of the form $\Delta H = cs^d$.

density [shoots/m^2]	current [m s^{-1}]	c	d	R^2
flexible mimics				
500	0	0.55	0.04	0.97
	0.1	0.45	0.05	0.99
1000	0	0.57	0.05	0.94
	0.1	0.48	0.06	0.99
2000	0	0.58	0.05	0.71
	0.1	0.46	0.06	0.83
4000	0	0.59	0.06	0.96
	0.1	0.48	0.06	0.89
8000	0	0.79	0.08	0.90
	0.1	0.57	0.07	0.74
stiff mimics				
1000	0	0.67	0.06	0.99
	0.1	0.54	0.06	0.99
4000	0	0.89	0.1	0.97
	0.1	0.61	0.08	0.96

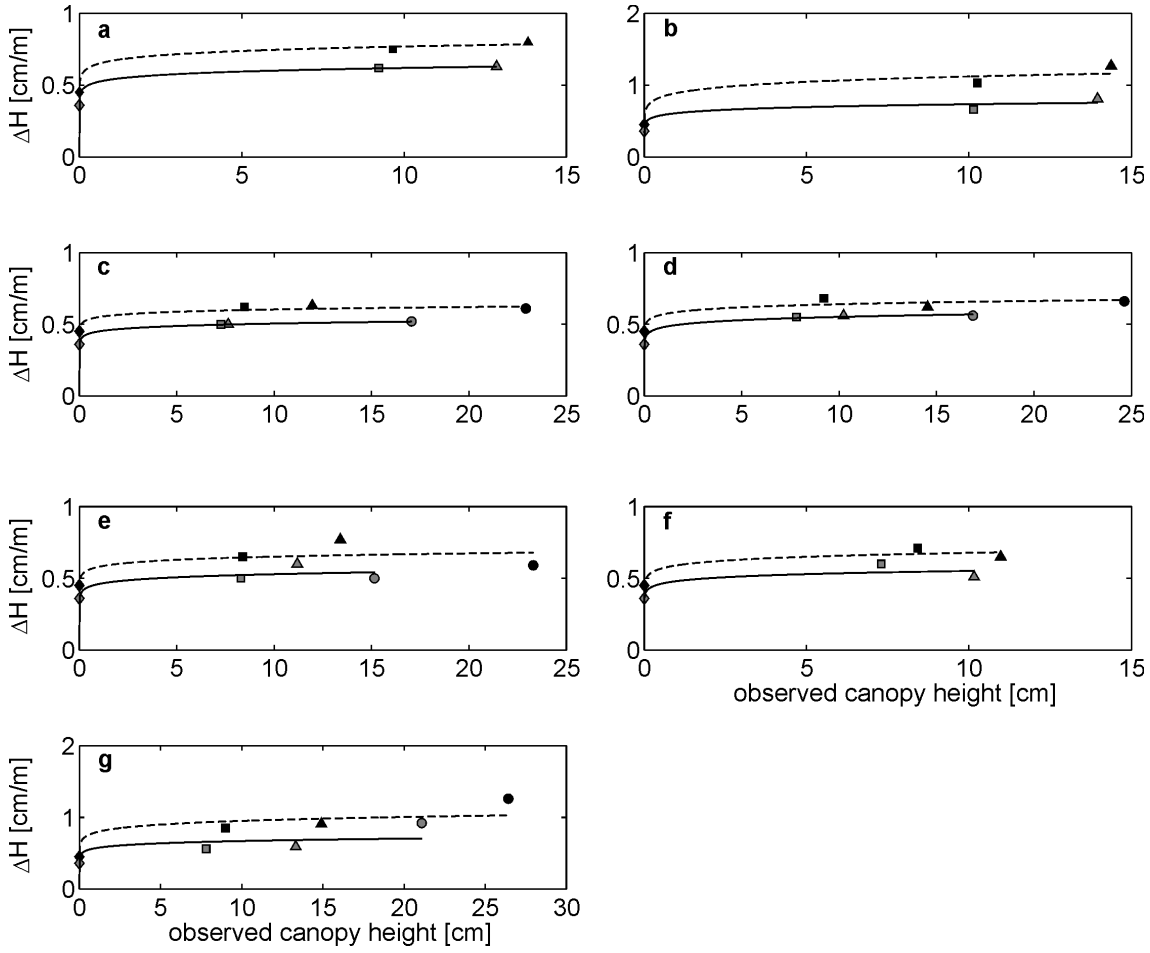

Figure 4.6.: Dissipated wave height ΔH as a function of canopy height for a. stiff mimics, 1000 shoots/m^2; b. stiff mimics, 4000 shoots/m^2; c. flexible mimics, 500 shoots/m^2; d. flexible mimics, 1000 shoots/m^2; e. flexible mimics, 2000 shoots/m^2; f. flexible mimics, 4000 shoots/m^2 and g. flexible mimics, 8000 shoots/m^2. Data for the wave only case are represented by black symbols and their best fit by dotted lines; data for the combined wave and current case are represented by grey symbols and their best fit by solid lines. The shapes of the symbols indicate leaf lengths: $\bigcirc$ = 30 cm; Δ = 15 cm; $\square$ = 10 cm; $\diamondsuit$ = no seagrass.

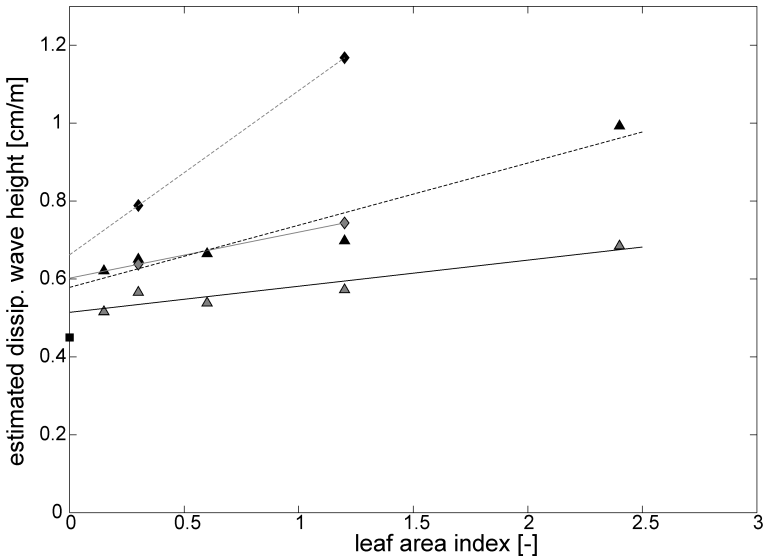

Figure 4.7.: Estimated dissipated wave height for a canopy height of 15 cm based on the regression parameters in Table 4.2. Data for the wave only case are represented by black symbols and their best fit by dashed lines; data for the combined wave and current case are represented by grey symbols and their best fit by solid lines. o represent stiff mimics and Δ represent flexible mimics. The regression lines for the stiff mimics are indicated in grey and not evaluated as they are each based on two data points only. The best fit lines for the flexible mimics are in the absence of a current: $\Delta H = 5 * 10^{-5}s + 0.58$ ($R^2 = 0.92$) and in the presence of a current: $\Delta H = 2 * 10^{-5}s + 0.51$ ($R^2 = 0.87$).

canopy height at all densities, the dependence of ΔH_w and ΔH_{wc} on shoot density was explored using the fitted relationships (Table 4.2) and ΔH_w and ΔH_{wc} were calculated for $s = 15$ cm for all densities. The calculated values showed that the dissipated wave height increased with shoot density both in the presence and absence of an underlying current (Figure 4.7). However, this increase was strongest in the absence of a current.

Another parameter that was reduced in the presence of an underlying current was the excursion of the mimic tips which changed with leaf length, but more importantly with the presence of a current (Figure 4.8). It was noticeable from the videos that the blade movement was not symmetrical and even in the absence of an underlying current, the mimics did not move beyond the vertical against wave advance. This asymmetric movement was caused by the wave field the mimics were exposed to. Although the recorded surface elevation was filtered for reflection for analysis, the

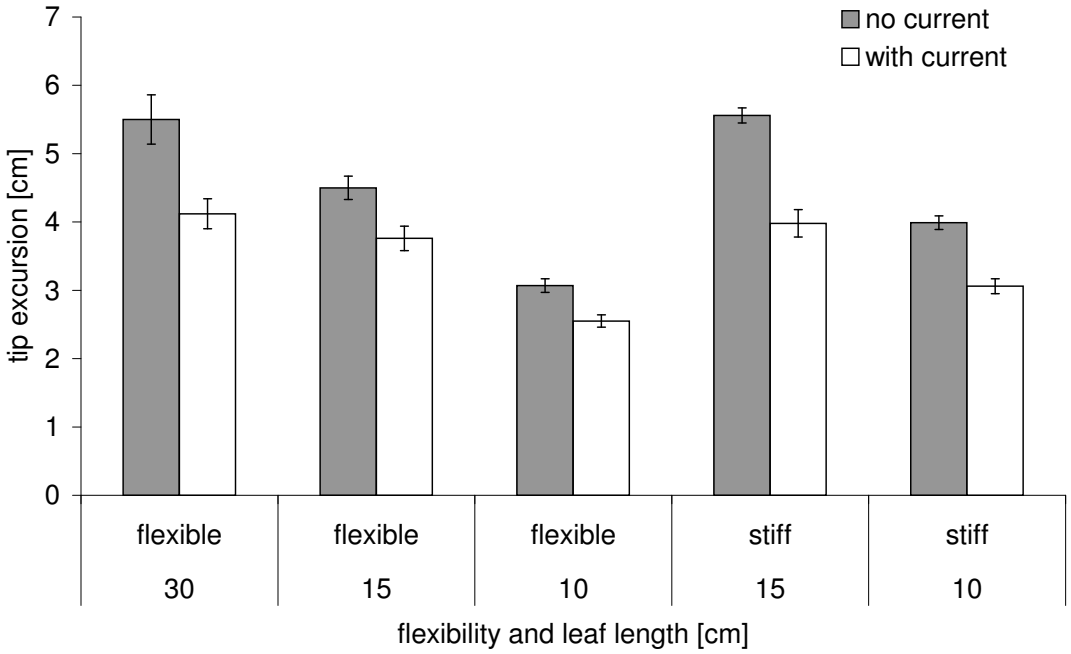

Figure 4.8.: Difference in tip excursion between treatments with waves only and with combined waves and currents. The flexible mimics have a density of 8000 shoots/m^2 and the stiff mimics have a density of 4000 shoots/m^2. Variability is expressed by the standard error.

mimics were exposed to the unfiltered signal (Figure 4.3) and responded accordingly. The recorded waves were asymmetric (Figure 4.3a and b), leading to higher forward motion under the crests and lower backward motion under the troughs. As a result, the leaves were not able to sway back beyond the vertical during the wave cycle.

When considered individually, stiffness, LAI, submergence ratio and current have an effect on wave height dissipation. However, results also indicate that stiffness and LAI can compensate each other (Figure 4.4). Moreover, due to the setup of experiments, a decrease in submergence ratio led to an increase in LAI for a given shoot density (Figure 4.5) which needs to be taken into account when interpreting the effect of submergence ratio on wave attenuation. To explore possible interdependences, stepwise multiple regression was carried out on the whole dataset (Table 4.3). Regression results show that compared to other parameters in this study, submergence ratio has no significant effect on wave height dissipation (β=0.05, t=0.54, p>0.5). From the other parameters, LAI is the dominating factor when estimating

Table 4.3.: Results of stepwise multiple regression for vegetation traits and currents under investigation. The effect of submergence ratio was not significant ($p>0.25$ for all models). * $p<0.001$

	b	standard error b	β*	R^2
Model 1				0.32
constant	0.59	0.04		
LAI	0.10	0.02	0.57	
Model 2				0.57
constant	0.69	0.04		
LAI	0.10	0.20	0.57	
current	-1.87	0.43	-0.50	
Model 3				0.80
constant	0.41	0.05		
LAI	0.11	0.01	0.65	
current	-1.87	0.30	-0.50	
stiffness	0.22	0.04	0.48	

wave height dissipation, followed by the effect of an underlying current (Table 4.3). Stiffness has also been identified as significant, but the values for b and β need to be interpreted with caution. As no quantitative measurements of stiffness were carried out during this study, stiffness was included as an indexed value into the regression analysis.

4.5. Discussion

It has been recognised that submergence ratio, shoot stiffness and density are important factors in wave attenuation by vegetation (Koch et al., 2006b; Bouma et al., 2010). However, previous studies have investigated a combination of several vegetation traits, especially when using real vegetation where traits are species specific and cannot be separated. The work with mimics in this study allowed disentangling the effect of these individual traits and to describe the effect each of them has on wave attenuation individually.

By using mimic meadows with different shoot densities and leaf lengths under constant hydrodynamic conditions, it was possible to show that for a given water

depth, wave attenuation of shallow water waves depends on the leaf area index LAI. This observation applied to all stiffnesses used in this study; however, wave attenuation for a given LAI was much more pronounced for the stiff material. Tests with and without and underlying current revealed that the wave attenuating capacity of seagrass is significantly lower in the presence of a current.

4.5.1. Leaf area index

Previous studies (Ward et al., 1984; Fonseca and Cahalan, 1992; Koch, 1996) showed that seagrass is more effective in attenuating waves the more of the water column it occupies. This led to the general understanding that wave attenuation depends on the submergence ratio. The present results extend these observations by showing that for a given small water depth, LAI as a combination of canopy height and shoot density, can be used as an integrating factor to predict wave attenuation.

In field studies (Ward et al., 1984; Koch, 1996; Koch et al., 2006a) the seagrass canopy remained constant and water depth changed over the tidal cycle. As a result of changing water depth, wave height and period are likely to have changed. The data in Chapter 3 show that waves of different periods are attenuated differently by a *Zostera noltii* canopy and it is possible that this response to differing wave periods is responsible for the difference in wave attenuation capacity with varying water depth. Fonseca and Cahalan (1992) varied water depth during their laboratory study on four different seagrass species. Although they applied waves with constant period, incident wave height varied between runs. Other laboratory studies adopted this approach and also changed the submergence ratio by adjusting water depth over vegetation with constant height (Augustin et al., 2009; Prinos et al., 2010).

During the present study, water depth and wave conditions remained constant and leaf length and shoot density were varied between runs. The results show a linear relationship of wave dissipation with LAI, which suggests that for a given wave in shallow water, a short but dense meadow has the same wave attenuating effect as

a high but scarce meadow of the same leaf area index. This may be explained by the drag each unit leaf area poses on the water movement which in return loses momentum (Kobayashi et al., 1993). The sum of momentum loss generated by the entire leaf area leads to reduced wave energy and can be observed as wave height reduction. As a result it is less relevant where in the water column the biomass is located but the amount of biomass is essential to the rate of wave attenuation. However, this is expected to be valid only for cases where the waves are in shallow water. Under those conditions, the gradient in orbital velocity reaches from the surface to the bottom and interacts with the whole seagrass canopy (Figure 4.9a). In cases where the velocity gradient does not extent through the whole water column, a higher meadow is likely to have a higher attenuating effect, because its upper part would still interact with the wave orbital motion (Figure 4.9b) while a shorter meadow may not reach into the part of the water column that is affected by the wave orbital motion (Figure 4.9c).

In shallow water conditions, the relationship of wave attenuation with LAI suggests that plant species with different growth strategies (scarce but high vs. dense but short) can lead to the same amount of wave attenuation, given they reach the same amount of biomass. If wave attenuation by vegetation could be expressed as a function of biomass, it would be possible to easily compare the wave attenuating capacity of different species. On a biomass level species with differing morphologies could be compared directly and also more complicated morphologies (e.g. branching) could be taken into account.

4.5.2. Stiffness

The materials chosen for the mimics strongly differed in stiffness which led to a different bending behaviour under waves and resulted in different rates of wave attenuation. This agrees with a study carried out on real plants of contrasting stiffness (Bouma et al., 2005). A comparison between rigid and cantilever like structures,

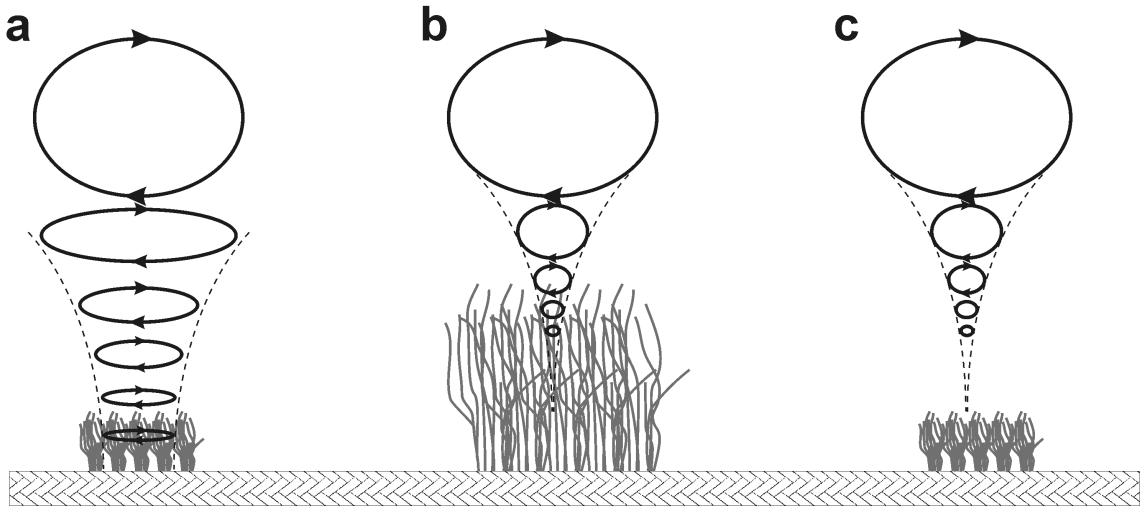

Figure 4.9.: Schematic of the gradient of orbital velocity under waves and its possible interaction with seagrass meadows of varying heights. In shallow water waves interact with the whole seagrass canopy and the bed (a); in deep water waves interact with the upper part of a high seagrass meadow (b), but may not interact with a short seagrass meadow (c).

however, did not yield a significant difference in wave attenuation (Augustin et al., 2009). Hence, it is possible that the type of motion (cantilever vs. whip like motion) is more relevant to wave attenuation than the material stiffness. However, the type of motion is not a constant vegetation parameter, but varies with hydrodynamic forcing. Under low wave forcing, a plant will move like a cantilever while under high wave forcing, it will change to a whip like motion (Manca, 2010). The amount of wave forcing required to change from one type of motion to the other depends on the plant's stiffness. If the plant's wave attenuating capacity depends on the type of motion rather than on the plant's stiffness, this capacity will depend on present wave forcing. It is suggested that this dependence will have a transition from one relationship to another at the point where the type of motion changes from cantilever to whip like.

Nevertheless, a study on *Spartina anglica* and *Puccinellia maritima* (Bouma et al., 2010) found that the effect of stiffness can be compensated by shoot density: The flexible plant (*P. maritima*) dissipated wave height at higher densities as effectively as the stiff one (*S. anglica*) at low densities. This observation was confirmed in the

present study where the flexible materials require approx. four times the leaf area index of the stiff material to yield the same dissipated wave height.

4.5.3. Effect of current

In the presence of a current, wave attenuation showed the same systematic behaviour to that of the wave only case, but the dissipation in wave height was lower for a given canopy height when a current was present (Figure 4.6). The influence of a current on wave attenuation has been recognised for unvegetated beds (Madsen, 1994) and kelp (Gaylord et al., 2003). The presented results confirm that a current also affects wave attenuation by seagrass beds and suggest that previous studies which neglected the effect of underlying currents overestimated the effect of seagrass on wave attenuation in tidal regions.

Wave attenuation by vegetation has three components. Plants (1) provide skin friction due to their surface structure, (2) pose form drag on the flow that depends on their shape and (3) they absorb wave energy by converting it into plant movement. Skin friction depends on the size of the wetted plant area and is therefore independent of flow velocities (Koehl, 1996). The form drag of the plant's frontal area generates turbulence behind the plant which leads to energy dissipation (Nepf, 1999). In the presence of a current, flexible plants change their shape by bending which reduces the frontal area that poses drag on the flow (Vogel, 1994; Boller and Carrington, 2006). This streamlining allows flexible plants to reduce form drag under increased flows compared to rigid structures (Vogel, 1984; Koehl, 1996) which in return may contribute to the reduction in wave attenuation in the presence of a current.

Vegetation also reduces wave energy by transforming it into plant movement. This transformation results in less energy contained in the wave and can thus be observed in a reduced wave height H, because the two parameters are related according to linear wave theory:

$$E = \frac{1}{8}\rho g H^2 \tag{4.3}$$

where E is wave energy, ρ is density of the water and g is gravity. In the wave-only case, seagrass can move freely within the limits of its stiffness and extract energy from the waves. In the presence of a current this movement is restricted (Figure 4.8) and the plants are therefore not able to absorb the same amount of wave energy.

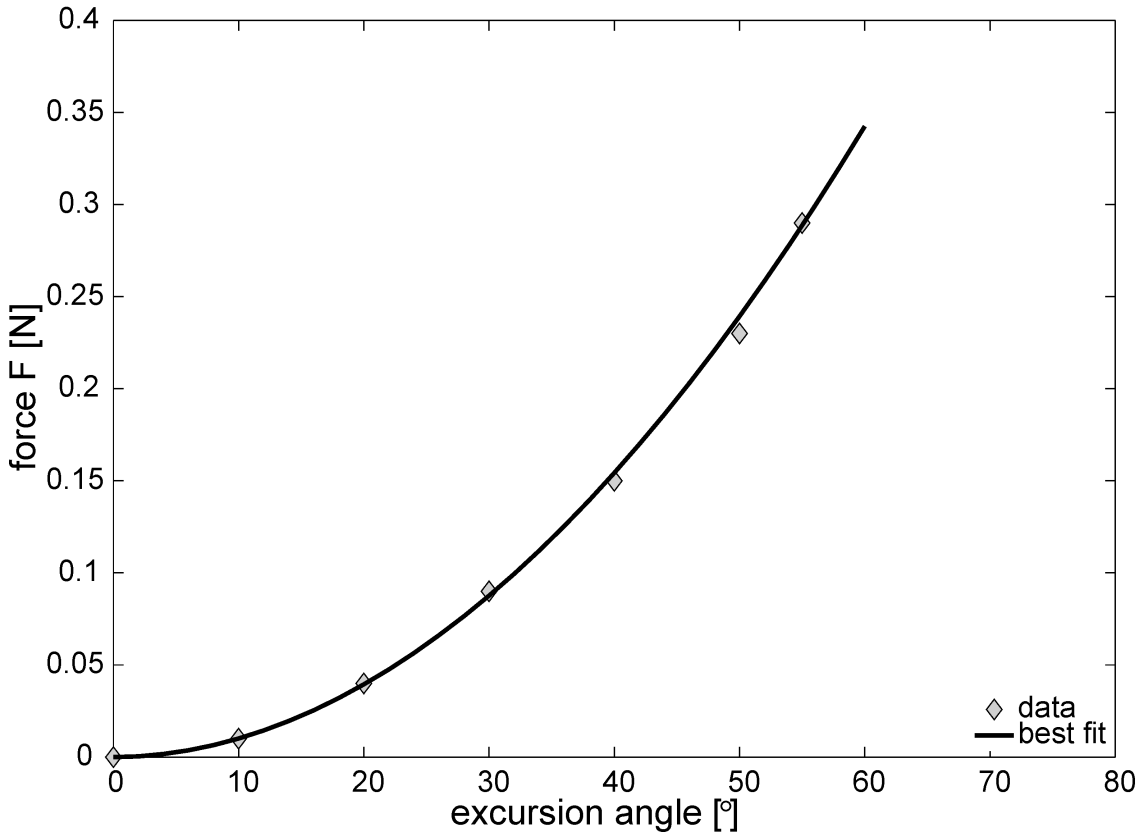

Figure 4.10.: Required force to deflect the stiff mimic from the vertical. The relationship can be described by $F = 10^{-4}\delta^2$ ($R^2 = 0.99$).

An underlying current exerts an initial force on the plants which causes them to bend. This bending leads to a primary tension within the blades and the force required to bend the blade further increases with increasing excursion angle δ (Figure 4.10). The same wave force would therefore generate a smaller plant movement, the higher the initial bend due to a steady current is. A study under unidirectional flow (Boller and Carrington, 2006) showed that initially flexible macroalgae were affected

by flow velocities and behaved like rigid bodies once a critical velocity was exceeded. It could therefore be expected that the motion restrictive nature of the underlying current would increase with increasing flow velocity. Similar to macroalgae (Boller and Carrington, 2006) it may be possible that a critical velocity exists at which the seagrass blades are no longer able to move and wave attenuation would remain constant as flow velocity increased above a threshold value. It is hypothesised that the wave attenuation of plants that are exposed to currents above this threshold would still be higher than wave attenuation in the complete absence of plants due to skin friction and streamlined form drag.

The stiff material in this experiment did not bend significantly and its motion can be described as the back and forth movement of a cantilever (Figure 4.1a). The flexible material, however, did bend under waves as well as under combined waves and currents and showed a whip like motion when it moved against the direction of wave propagation (Figure 4.1b). This whip like motion was equally present with or without a steady current, but had a smaller excursion when a steady current was present. The above explanation would therefore be valid for material that has a cantilever motion as well as for material with a whip like motion and may be applicable for a wide range of vegetation types.

4.5.4. Effect of density and current

For a constant canopy height both ΔH_w and ΔH_{wc} increase with shoot density (Figure 4.7). But the rate of increase differs, which means the underlying current reduces the wave attenuating capacity of seagrass more at higher densities. As it is expected that the wave attenuating capacity decreases with increasing flow velocity, it is surprising to see such a decrease with shoot density in the presence of the same underlying current. This could be explained by wave induced velocities as observed by Luhar et al. (2010). During a laboratory study with artificial *Zostera marina* shoots, they found that a unidirectional flow in the direction of wave propagation

was generated within the meadow which increased with increasing shoot density. Provided the same process took place during the experiments presented here, the wave induced flow would add to the applied current and therefore lead to an increased total current at higher shoot densities. If a higher total current was acting on the seagrass, it could have reduced the wave attenuating capacity more which would explain the increased difference between ΔH_w and ΔH_{wc} with increasing shoot density. However, no data are available on the current velocities within the canopy and more work needs to be done to prove this hypothesis.

4.6. Conclusions

Laboratory experiments with artificial seagrass were used to investigate the effect of leaf length, shoot density and stiffness on wave attenuation in the absence and presence of a tidal current. Results showed that stiffness and leaf area index determine wave attenuation. The leaf area index combines the effect of leaf length and shoot density and therefore indicates that density can compensate for lack of canopy height and vice versa with respect to wave attenuation. The presence of an underlying current led to a reduction in wave attenuation for all meadows under investigation. While this phenomenon could not be fully explained with the data collected during this study, it clearly shows that experiments which are carried out under waves only, overestimate the wave attenuating capacity of seagrass compared to most natural environments where underlying currents are present in the form of tidal flow.

5. General Discussion and Conclusions

5.1. Summary of findings

This thesis aims at quantifying the effect of *Zostera noltii* on wave attenuation and to measure how this effect changes on short (hourly) and medium (monthly) time scales. Particular attention is given to plant and wave parameters that drive such a change. The newly developed mapping technique (Chapter 2) was used to quantify seagrass canopy height and coverage; two parameters that are important for seagrass monitoring and health assessment (Dennison et al., 1993; Duarte et al., 2006). To date surveying techniques that allow mapping of both parameters together required time intensive *in situ* surveys or expensive equipment such as multi-beam sonars. The presented method provides a cost effective and fast remote sensing technique that provides unbiased data and is therefore a valuable contribution to seagrass monitoring and conservation. Moreover, the mapping technique enables detailed seagrass mapping on a much larger scale than would be possible using conventional diving techniques. It can therefore help to define areas of wave attenuation by seagrass. The field study described in Chapter 3 shows that *Zostera noltii* is capable of attenuating waves and highlights that hydrodynamic conditions (e.g. wave height and period) as well as plant characteristics (e.g. shoot density) influence its effectiveness. However, it also highlights the difficulties of assessing bed roughness for

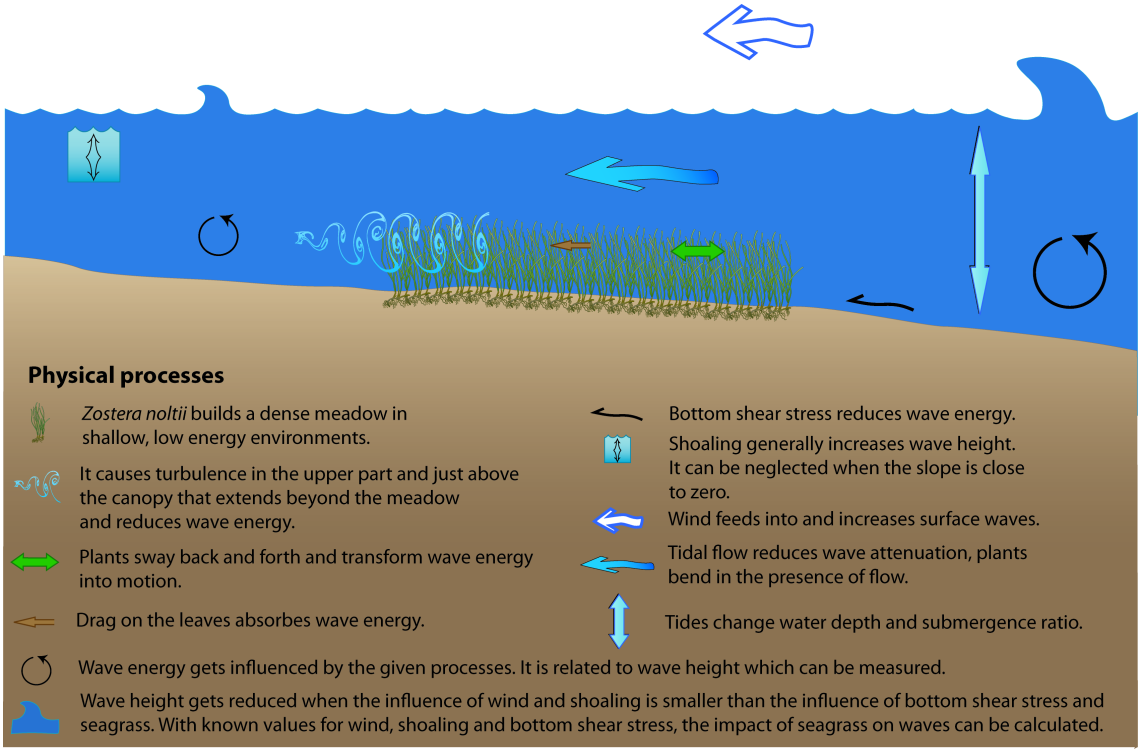

Figure 5.1.: Conceptual diagram of physical processes in and around a *Zostera noltii* meadow.

vegetated beds with methods currently available. Present models were developed for unvegetated beds under the assumption that bed roughness is independent of hydrodynamic forcing (Madsen, 1994) which is not the case for flexible seagrass. In particular for relatively small seagrass species such as *Zostera noltii*, the effect of above ground biomass on bed roughness appears to be too small to be detected with current models in the field (see Section 5.6). The effect of plant morphology was investigated in detail in a laboratory study (Chapter 4) where mimics were used to determine the effect of leaf length, shoot density and stiffness on wave attenuation individually. Additionally, experiments were carried out with and without an underlying current to explore how wave attenuation by vegetation differs between tidal and non-tidal environments. Overall, the presented work improves our knowledge of how wave attenuation gets affected by seagrass in general and by *Zostera noltii* in particular (Figure 5.1) and contributes to the understanding of which plant and wave parameters affect wave attenuation by vegetation.

5.2. The effect of plant morphology on wave attenuation

Plant form and structure is species specific; it can therefore be used to identify taxa (Raven et al., 2005) and help to interpret their structure, origin and development (Bold et al., 1987). In seagrasses, morphological parameters such as leaf shape or plant architecture may show variation between populations, but are generally not affected by seasonal changes (Kuo and Den Hartog, 2006). Leaf length and shoot density, on the other hand, show seasonal variation in many species (Den Hartog, 1970). It is thus important to understand how these seasonal changes affect wave attenuance by seagrass over the annual cycle in order to predict wave attenuation correctly.

5.2.1. Leaf length and shoot density

Zostera noltii shows large variation in above ground biomass throughout the year which can be observed in changing shoot densities as well as leaf lengths. Previous studies (Fonseca and Cahalan, 1992; Bouma et al., 2005; Chen et al., 2007; Augustin et al., 2009; Prinos et al., 2010) showed that changes in shoot density and leaf length can affect wave attenuation by vegetation. It is therefore important to understand what role plant morphology plays in wave attenuation in order to predict the impact of *Z. noltii* on waves over the annual cycle.

The field results of this study show that there is a minimum shoot density for measurable wave attenuation in *Z. noltii*. This agrees with earlier observations for a *Ruppia maritima* meadow (Newell and Koch, 2004). No such threshold was observed during the laboratory measurements of this study, although mimic densities covered the whole range of shoot densities observed during the field study. This discrepancy may be caused by the experimental setup in the laboratory. Tests were carried out in very shallow water (h = 30 cm) and with much smaller submergence ratios (1:1

Figure 5.2.: Large ripples formed in the locations of *Z. noltii* growth in Ryde and most likely stabilised by its root system.

to 3:1) than in the field (average >10:1) and results may therefore not be directly comparable.

In the field, the threshold for *Z. noltii* was between 2,000 and 4,000 shoots/m^2 and therefore at least 3 times larger than the shoot densities observed in winter (625±225 shoots/m^2 in February '09). It can therefore be expected that the effect of *Z. noltii*'s above ground biomass has little impact on wave attenuation during the winter months when storminess is high. It may, however, increase wave attenuation in winter compared to unvegetated areas due to its below ground biomass. The presence of large ripples was observed in locations where seagrass is present (Figure 5.2). It is likely that the root system is binding the sediment and hence stabilises these bed forms throughout the year (Den Hartog, 1970). The larger bed forms would lead to an increased bed roughness k_N (Li and Amos, 1998) compared to unvegetated areas even in winter when shoot densities are at a minimum. However, below ground biomass and bed forms were beyond the scope of this study and the collected data are therefore not sufficient to support this hypothesis.

In Ryde, an increase in energy dissipation with distance from the shore was observed for boat wakes in July when shoot density exceeded a threshold value (Figure 3.11).

Such behaviour has been found for the seagrass *Thalassia testudinum* (Bradley and Houser, 2009) and salt marsh vegetation (Möller et al., 1999). Laboratory studies on two salt marsh species confirmed the observations (Bouma et al., 2010) and Bouma et al. (2005) suggest a division of labour within the meadow where plants on the leading edge absorb more wave energy and consequently create more suitable conditions for other plants closer to shore.

Despite the absence of a threshold value during the laboratory experiments, an increase in wave attenuation with increasing shoot density supported the relevance of shoot density for wave attenuation found in the field. However, the experiments revealed that the combination of shoot density and leaf length as given by the leaf area index (LAI = leaf length $*$ leaf width $*$ shoot density) is a more accurate determining factor for wave attenuation of a given wave in shallow water. Leaf length did not change substantially during the field study and LAI for the field data therefore directly corresponds to shoot density (Appendix A). However, previous studies observed values between 5 and 45 cm for *Z. noltii* (Auby and Labourg, 1996; Curiel et al., 1996) depending on location and time of year. Leaf length could therefore influence LAI significantly.

The lab results show that shoot density and leaf length can compensate each other with respect to wave attenuation. Moreover, flexible plants with high LAI can have the same wave attenuating capacity as stiff plants with low LAI. Similar observations were made for natural salt marsh vegetation in a laboratory flume. Data for the relatively stiff *Spartina anglica* and the relatively flexible *Puccinellia maritima* yielded the same relationship wherein wave attenuation was described as a function of biomass (Bouma et al., 2010).

The results herein show that a single morphological parameter cannot account for all wave attenuation by seagrass and its changes over the year. It is possible to estimate wave attenuation based on a single morphological parameter, provided that other characteristics within a particular habitat change little over time, i.e.

if leaf length remains constant throughout the year, shoot density can be used to estimate changes in wave attenuation and vice versa. However, for a full account of the effect of vegetation on wave dissipation, a combination of morphological plant characteristics needs to be taken into account.

5.2.2. Plant stiffness

Shoot stiffness (defined as its modulus of elasticity E_s) does not change within species and is therefore not directly relevant to investigations of the effect of a single species on wave attenuation. However, it was included in this study to put the results of *Zostera noltii* in the wider context of submerged aquatic vegetation. The effect of stiffness on wave attenuation has been investigated for large macroalgae (Koehl, 1996; Denny and Gaylord, 2002) and for salt marsh (Bouma et al., 2010). Results indicate that stiff vegetation is more effective at attenuating waves. The present experiments on three different stiffnesses with the same LAI generally support this observation (Chapter 4) although no significant difference in wave attenuation between the two flexible materials was found. It is possible that it is not the stiffness, but its bending behaviour that determines the plant's wave attenuating capacity. The stiff mimic moved back and forth as a cantilever under wave motion while the flexible and very flexible mimics showed a whip like movement. The two flexible materials led to similar values for dissipated wave height at a given LAI, but the slope of the regression line for the stiff material was approx. five times higher (Figure 4.4). These results suggest that the type of plant movement (cantilever or whip like) may be more important in defining wave attenuation by vegetation than the plant's modulus of elasticity.

The wave conditions in the present laboratory study remained constant for all tests and it was therefore not possible to observe cantilever as well as whip like motion in a single mimic. However, previous studies on *Posidonia oceanica* mimics found that leaves act as a cantilever under low hydrodynamic forcing and change to whip like

motion with increasing wave amplitude and/or period (Manca, 2010). This suggests that a given material can show both types of motion, provided it is exposed to the appropriate hydrodynamic forcing (Stewart, 2006). As seagrass meadows are exposed to a range of hydrodynamic conditions, it is possible that a single meadow can show cantilever or whip like motion, depending on the hydrodynamic forcing it encounters. If this is the case and the type of plant movement plays a significant role in wave attenuation, the definition of shoot stiffness may need to be extended to include not only the plant's modulus of elasticity, but also its momentary type of motion. Such an extended understanding of stiffness would not be species specific anymore, but would strongly depend on the hydrodynamic conditions which will vary on both spatial and temporal scale in the field.

Although the mimics were generic and no direct models of specific plant species, their stiffnesses covered a range occurring in nature: the flexible model resembled the motion of *Zostera noltii* while the stiff mimic's bending behaviour was similar to that of the salt marsh species *Spartina anglica*. Both species colonise the upper intertidal and can compete for the same location (Bouma et al., 2010), a comparison of the two species under coastal engineering aspects is therefore of high relevance to coastal management. The results from the laboratory study show that the stiff *S. anglica* is more effective at attenuating waves at a given shoot density than *Z. noltii* which agrees well with observations made during a previous field and laboratory study (Bouma et al., 2005). Moreover, the sediment binding capacity of the salt marsh plant is higher, leading to built up of tussocks which have not been observed for *Z. noltii* so far (Bouma et al., 2010). Although higher densities of *Z. noltii* can compensate for the increased wave attenuating capacity of the stiff *S. anglica* (Chapter 4), it is suggested that salt marsh is overall more effective in attenuating waves and therefore directly contributing to coastal protection. Nevertheless, *Z. noltii* is suggested to play an indirect role by stabilising sediments with its root system and therefore preparing the ground for colonisation by salt marsh vegetation. Large scale experiments with salt marsh patches confirmed field observations that

increased turbulence can lead to erosion along the leading edge of salt marsh tussocks (Bouma et al., 2007). Presence of *Z. noltii* meadows in front of those tussocks may stabilise the present sediment and hence reduce erosion. This in return would facilitate the lateral expansion of salt marsh vegetation and therefore indirectly contribute to coastal protection by vegetation.

5.3. The effect of wave parameters on wave attenuation

Natural sea state is composed of a range of wave heights and periods which will vary over time (Kamphuis, 2000). Previous studies suggest that wave parameters can affect wave attenuation by coral reefs (Lowe et al., 2005), salt marsh (Möller, 2006) and seagrass (Lowe et al., 2007; Bradley and Houser, 2009) and it is therefore necessary to consider incident wave forcing when estimating wave attenuation by submerged vegetation.

5.3.1. Wave period

To assess how wave period affects wave attenuation by *Zostera noltii*, natural wind waves and boat wakes were analysed separately during the field study. Wind waves were generated by north-westerly winds and were characterised by 2-4 s periods. Boat wakes had a wave period of 10 s and were generated by ferries leaving from the pier head adjacent to the study site. The effect of each wave type on wave attenuation was investigated in two ways: by calculating the wave drag coefficient C_D which is independent of seasonality, and by comparing the representative energy dissipation factor $f_{e,r}$ which depends on vegetation density and coverage.

C_D remained constant for wave frequencies $<$0.4 Hz and did not change over the year. These results are in contrast to findings in a natural *Thalassia testudinum*

(Bradley and Houser, 2009) and an artificial *Posidonia oceanica* (Manca, 2010) bed. Both studies found that peak frequencies were dissipated more than other wave frequencies in the spectrum. Bradley and Houser (2009) also found reduced values for C_D at frequencies that correspond to the swaying frequency of the seagrass. They suggest that the reduced relative motion between water and vegetation leads to less drag and therefore less energy dissipation at these frequencies. Theoretical approaches have identified the relative velocity between water and vegetation as the determining velocity for drag (Kobayashi et al., 1993; Méndez et al., 1999; Méndez and Losada, 2004) which is supported by studies in macroalgae. Flexible kelp moves synchronous with water motion which reduces drag to values too small to observe significant wave energy dissipation (Elwany et al., 1995). Nevertheless, the relative motion of vegetation is still poorly understood, which is mainly due to the difficulties of measuring plant movement in a field setting.

A difference in wave attenuation between boat wakes and wind waves was observed for the energy dissipation factor $f_{e,r}$. For the short period wind waves, $f_{e,r}$ remained constant along the instrumented transect for all deployments. The same was observed for boat wakes in autumn, winter and spring. In summer, however, $f_{e,r}$ for boat wakes showed a decrease towards the shore similar to the exponential decay found in other submerged vegetation (Möller et al., 1999; Bouma et al., 2005; Bradley and Houser, 2009). This suggests that the shoot density threshold above which wave dissipation can be observed varies with wave period. For the longer period boat wakes the threshold lies between approx. 2,000 and 4,000 shoots/m^2, while for short period wind waves the threshold is expected to be $\geq$4,500 shoots/m^2 as it was not exceeded during this study.

5.3.2. Wave height

Laboratory studies showed that percentage wave attenuation increases with increasing wave height (Fonseca and Cahalan, 1992; Augustin et al., 2009; Prinos et al.,

2010). Higher waves lead to higher wave orbital velocities which in return exert a higher shear stress on the seabed and over vegetation (Chen et al., 2007). For rough turbulent flow, the rate of wave energy dissipation is positively correlated with the product of shear stress and wave orbital velocity (Dean and Dalrymple, 1991) which leads to the observed relationship between wave height and attenuation.

Wave height was held constant during the laboratory experiments of this study and the wave spectra recorded in the field were composed of a variety of wave heights. It was therefore not possible to directly assess the impact of wave height on attenuation. It was possible to indirectly assess the effect of orbital velocity on wave attenuance by relating the drag coefficient C_D to the vegetation Reynolds number ($Re_v = bu_b/\nu$). However, the results only allow limited conclusions for the effect of wave height as the maximum horizontal orbital velocity u_b also depends on water depth, which varied over time during field measurements.

C_D was found to increase with decreasing Re_v, while with increasing vegetation Reynolds number C_D approaches a constant value. This indicates that the drag coefficient becomes independent of orbital velocity in rough turbulent conditions (Kobayashi et al., 1993; Méndez et al., 1999; Méndez and Losada, 2004). A relationship of the form $C_D = a + (b/Re_v)^c$ was confirmed recently in the field (Bradley and Houser, 2009). The data presented in Chapter 3 fit a relationship of the same form and show that it is independent of wave period: the relationship of C_D and Re_v for low period wind waves as well as higher period boat wakes are described by the same equation:

$$C_D = 0.06 + \left(\frac{153}{Re_v}\right)^{1.45} \tag{5.1}$$

The scatter around this fit increased when significant wave heights less than 0.1 m were considered which suggests that the accuracy of the relationship decreased with decreasing significant wave height. However, significant wave heights in this study did not exceed 0.16 m and more data, especially on higher waves are required to

investigate the effect of wave height on eq. 5.1 and how this is affected by water depth.

5.4. The impact of submergence ratio on wave attenuation

In tidal environments, seagrasses are exposed to changing water depths over the tidal cycle. The effect of these depth changes is most pronounced in the intertidal where a depth change on the decimetre scale can lead to a multiple increase in submergence ratio, i.e. the ratio between water depth and vegetation height. *Zostera noltii* is an intertidal species and it is therefore important to consider the effects of submergence ratio on wave attenuation in order to assess wave attenuation by *Z. noltii* correctly.

In the field, water depth varied between 0 and 3 m over an almost constant leaf length (13±3 cm) throughout the year, yielding submergence ratios up to 23:1. The present understanding is that seagrass attenuates waves best when it occupies >50% of the water column (Ward et al., 1984; Fonseca and Cahalan, 1992; Koch et al., 2006a). In this study (Chapter 3), wave height reduction along the transect was observed in submergence ratios up to 8:1; four times larger than the one suggested previously (Fonseca and Cahalan, 1992). Nevertheless, the observation that seagrass reduces wave height more effectively at lower water depths matches previous observations (Koch et al., 2006a). Koch (2001) compared results from several field and laboratory studies and found a positive correlation of wave attenuation with submergence ratio. A field study on *Ruppia maritima* supports this correlation, as it observed a linear relationship between wave attenuation and water depth for two different leaf lengths (Newell and Koch, 2004). Newell and Koch (2004) also found that wave attenuance over *R. maritima* was highest when the canopy occupied the whole water column which confirms observations by Fonseca and Cahalan (1992) who found a significant effect of submergence ratio on wave attenuation in three out of four seagrass species

during a laboratory study. A more recent numerical and physical modelling study supports the effect of submergence ratio on wave attenuation, but also shows that the upper depth limit for wave attenuation by vegetation depends on the incident hydrodynamic forcing (Chen et al., 2007). The model suggests that wave period and orbital velocity determine how effectively seagrass attenuates waves in water depths too deep for the waves to 'feel the bottom', but shallow enough for the waves to interact with the seagrass canopy. This possible dependence on other hydrodynamic parameters may explain field observations of wave attenuation in a 5 m deep *Amphibolis antarctica* meadow (Verduin and Backhaus, 2000) and a *Posidonia oceanica* bed at 15 m depth (Granata et al., 2001).

The effect of combined submergence ratio and wave forcing has been indirectly addressed in several laboratory studies (Fonseca and Cahalan, 1992; Bouma et al., 2005; Augustin et al., 2009; Prinos et al., 2010). During these experiments submergence ratio was varied by changing water depth over a constant vegetation height. While such an approach reproduces field conditions where water depth changes over a tidal cycle, it also leads to changes in wave height and/or period. It is therefore difficult to distinguish between the effects of submergence ratio and wave forcing and thus to interpret the results with respect to submergence ratio only. The current study (Chapter 4) allowed assessment of the effect of submergence ratio without possible effects introduced by changes in wave parameters such as wave height and period, as mimics with different leaf lengths were exposed to identical monochromatic waves in a constant water depth. In agreement with field observations in *R. maritima* (Newell and Koch, 2004) results show a linear relationship of wave dissipation with submergence ratio for a range of shoot densities (Figure 4.5). The data suggest that the effect of submergence ratio remains almost constant for shoot densities $\leq$2000 shoots/m^2 and increases with increasing density above this value. This observation is very similar to the result that a minimum density was required to observe wave attenuation in the field. However, it may be an artefact of the dataset as data for 2000 shoots/m^2 did not show good correlation ($R^2 = 0.15$) and

the density of 4000 shoots/m^2 lack data for a submergence ratio of 1:1. Despite the reduced dataset for densities of 4000 shoots/m^2, the experiments confirm previous findings that wave attenuation increases with increasing submergence ratio under field conditions where change in submergence ratio is caused by changes in water depth over the tidal cycle.

Submergence ratio also varied along the instrumented transect due to bottom slope. Even though the slope was too small ($\sim$ 1:550) to cause significant wave reflection (Chapter 3), it resulted in a height difference of $\sim$0.7 m between the inner and outermost station. This has led to significant differences in submergence ratio along the transect, especially at low water depths. While submergence ratio has not been directly taken into account during analysis of the field data, it was included indirectly by analysing each section of the transect individually. As a result plots like Figure 3.10 are based on data from different intervals in time for each section of the transect.

The results also revealed that attenuation of shallow water waves is driven by leaf area index and not submergence ratio alone. While LAI will not change on the same time scales as water depth in nature, the laboratory experiments allowed investigation of its impact on attenuation of a given wave type. Comparison of test results revealed that for a constant water depth a meadow with low leaf length (high submergence ratio) but high shoot density can lead to the same amount of wave attenuation than a meadow with high leaf length (low submergence ratio) and low shoot density (Figure 4.5). It is concluded that the amount of biomass determines the rate of wave attenuation rather than where in the water column it is located. However, this conclusion is based on meadows where biomass is evenly distributed throughout the height of the canopy (e.g. *Zostera noltii*) and it is not yet known whether the same applies to species that have more biomass in the upper (*Amphibolis antarctica*) or lower (*Posidonia oceanica*) part of the canopy.

5.5. The effect of an underlying current on wave attenuation

In the natural environment, seagrass is often exposed to a combination of waves and currents generated by tidal flows. It is recognised that an underlying current can affect a given wave energy flux and consequently the associated wave friction factor f_w (Madsen, 1994). However, for unvegetated beds this effect is negligible if the current acts perpendicular to the approaching waves (Mathisen and Madsen, 1996a, 1999). This was the case during the field study in Ryde and the current's effect on incident waves was therefore considered small. The current may, however, have an impact on the posture of the seagrass meadow as the leaves are likely to bend and align themselves with the flow (Fonseca and Koehl, 2006; Backhaus and Verduin, 2008). Studies on the kelp *Nereocystis luetkeana* showed that a current perpendicular to wave advance can reduce wave attenuation by changing the relative velocity between the water and the vegetation (Gaylord et al., 2003). *Nereocystis luetkeana* is a large canopy forming species that usually occupies most of the water column and the findings by Gaylord et al. (2003) suggest that currents perpendicular to wave propagation need to be considered when investigating wave attenuation by kelp vegetation. However, it is not clear whether the same applies to small meadow-forming seagrass species such as *Zostera noltii*.

No data were available on leaf posture during this field study and it was therefore not possible to investigate whether the principles observed in kelp also apply to the seagrass in Ryde. Instead, the effect of a current was included in the laboratory experiments where the effect of a steady current in the direction of wave propagation was explored. In the presence of a current wave attenuation was reduced by 13-36% compared to the no-current scenario, depending on mimic stiffness and LAI. The steady current led to leaf bending and reduced leaf motion, however, it did not affect the type of movement (cantilever or whip like). During the experiments, only

a current velocity of 0.1 m s^{-1} was tested, but it is hypothesised that leaf motion will be restricted further with increasing flow velocity. Such behaviour was observed in macroalgae that eventually behaved like rigid bodies once the velocity exceeded a critical value (Boller and Carrington, 2006). The results from the present study did not indicate that reduction of wave attenuation by the current depends on canopy height, but a relationship with shoot density was observed. The available data are not sufficient to explain this observation. Nevertheless, the results indicate that data collected under waves only may overestimate wave attenuation by seagrass in areas where currents are present in the form of tidal flow.

5.6. Hydrodynamic roughness of *Zostera noltii*

The physical roughness of seagrass includes canopy height, shoot density and coverage and is a measure of a meadow's health and growth state (Duarte et al., 2006). Summer values for canopy height and coverage of *Zostera noltii* in Ryde were measured with a profiling sonar (Chapter 2) and monthly local measurements of leaf length and shoot density were taken during on-foot visits during low tide when the site was exposed. The latter changed throughout the year which suggests that the physical roughness of the seagrass meadow will have varied.

It has been shown for unvegetated beds that roughness affects the energy dissipation factor $f_{e,r}$ by imposing a hydraulic roughness k_N on the flow (Kamphuis, 1975; Nielsen, 1992; Madsen, 1994). Attempts have been made to apply the relationship between k_N and $f_{e,r}$ to vegetated beds (Bradley and Houser, 2009; Manca, 2010). In the laboratory, Manca (2010) found an increase of k_N with increasing shoot density, while Bradley and Houser (2009) were not able to find a relationship between roughness length and seagrass morphology based upon field results. In the present study, k_N did not vary significantly over the year. These observations suggest that while shoot density affects hydraulic roughness, it is not possible to identify it under

field conditions, because other parameters may play a role. Simplified laboratory conditions, however, eliminated some of the other complicating factors and therefore enhanced the signal of shoot density on k_N. The results from both previous studies found that hydraulic roughness is a fraction of the canopy height which agreed with observations under currents (Neumeier, 2007). In the present study, hydraulic roughness values exceeded leaf length for all deployments and therefore do not support previous findings. However, they agree with roughnesses found for artificial triangular bars (Mathisen and Madsen, 1996a,b, 1999), rippled sands (Iwagaki and Kakinuma, 1967) and coral reefs (Lowe et al., 2005). It is possible that the effect of large ripples observed inside the *Z. noltii* bed (Figure 5.2) on k_N dominate the hydraulic roughness and compared to this, the effect of *Z. noltii*'s above ground biomass was too small to be detected under field conditions. Previous studies showed that the energy dissipation factor $f_{e,r}$ reduces non-linearly towards the shore over submerged vegetation (Méndez et al., 1999; Newell and Koch, 2004; Bradley and Houser, 2009; Bouma et al., 2010). The lack of such a non-linear trend in $f_{e,r}$ across the sandflat supports the hypothesis that k_N in Ryde is dominated by the present bed forms and not by the presence of *Z. noltii*. The constant spatial distribution of $f_{e,r}$ for natural waves indicates that the beach profile has adjusted to the constant presence of waves and aligned itself in a way that friction and therefore applied shear stress is minimum along the profile. The constant temporal distribution of $f_{e,r}$ suggests that the profile remains stable throughout the year and no summer and winter states exist at the study site. This is supported by profiles monitored by the Channel Coastal Observatory (Figure 5.3) which do not show a significant change (ANOVA, F = 1.82, p = 0.15, n = 52) for the duration of the field study (CCO, 2011).

If the influence of *Z. noltii* on wave attenuation of average wave conditions (2-4 s period wind waves) is small compared to the effect of the seabed, the profile would be stable even in the absence of seagrass. This overall stability of the profile could be the reason why the *Z. noltii* meadow established itself at this location. A stable

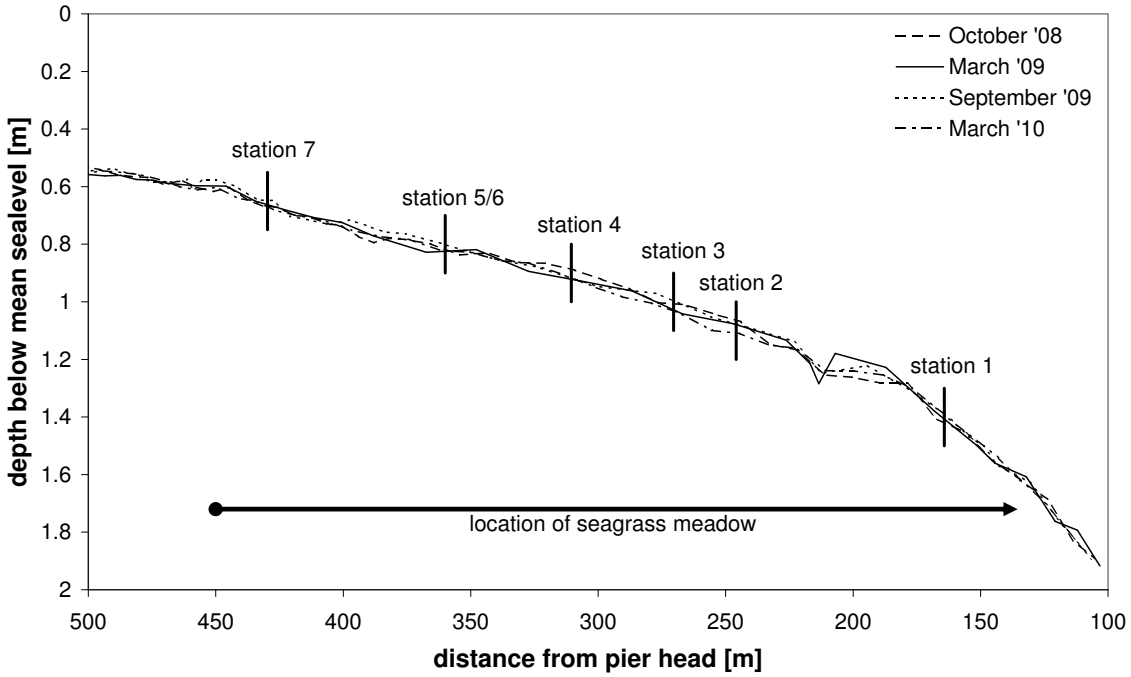

Figure 5.3.: Beach profiles taken along the instrumented transect, running approx. south-north (CCO, 2011). Distances are given with respect to the pier head north of the transect. The extent of seagrass growth towards the pier head is not known.

profile promotes seedlings to take root, and vegetative shoots may develop from rhizomes without being eroded or covered with sediment before they manage to establish. Once the meadow is established, its stabilising function (Amos et al., 2004; Widdows et al., 2008) will help keeping the profile stable, making it more robust against storm effects.

Moreover, the data suggest that *Zostera noltii*'s above ground biomass does not contribute significantly to energy dissipation and bed roughness and therefore coastal protection during winter when storminess is high. However, its root system may stabilise the sediment throughout the year and therefore contribute indirectly to coastal protection by reducing erosion. It is important to note that the data only allows these conclusions for *Zostera noltii*. Other seagrass species that show a higher above ground biomass, especially during winter, may provie a significant and direct contribution to coastal protection by dissipating wave energy reaching the shore.

5.7. Critical analysis of methods used

5.7.1. Choice of species under investigation

The seagrass species *Zostera noltii* was chosen, because it is native to Britain and highly abundant across Europe which enabled easy access to study sites. Additionally, it showed a high seasonality which enabled the investigation of varying above ground biomass in the field without the necessity of changing study sites and the coupled problems of changing boundary conditions such as differences in bathymetry or wave conditions.

However, the size of *Z. noltii* led to difficulties during data analysis. The effect of such a small species on wave attenuation is small and therefore difficult to detect in naturally variable field data. It is hypothesised that results would have been more pronounced and consequently more robust if a larger species such as *Zostera marina* would have been used. Nevertheless, it was possible to show that *Z. noltii* reduces wave energy under certain conditions (e.g. a minimum shoot density is required) and these results are promising in the context of the general effect of submerged flexible vegetation on wave attenuation as it can be expected that the effect of larger species is more pronounced and detectable throughout the whole year.

Another possible source of inaccuracy in the data was caused by the study sites vicinity to the pier in Ryde. This proximity to a solid structure may have caused refraction effects in the recorded wave field which makes robust interpretation of the field results difficult. However, the site provided the best compromise between accessibility, safety and data quality. As the site needed to monitored over a whole year, it was decided to choose a site close to Southampton that could be easily accessed on a regular basis. The general location in Ryde fulfilled this condition and, moreover, provided a large continuous *Z. noltii* meadow (approximately 40 ha) which ensured a sufficiently long transect for wave measurements with seagrass cover. As some instruments required connection to a power source and logging

station, it was consequently necessary to operate close to a dry, stable platform that could hold a generator and electrical equipment. And since it was envisaged to also collect data in winter when weather conditions may be rough, it was considered unsafe to construct a temporary platform elsewhere on Ryde Sand. Overall, Ryde pier provided a very suitable base for data collection and it is suggested that possible effects on the wave field by the pier's structure would not have been up for discussion, if the seagrass growing in its vicinity would have been bigger (i.e. *Z. marina*) and hence its effect on wave attenuation more pronounced.

5.7.2. Use of hydrodynamic equations

During the field study (Chapter 3), wave parameters were calculated based on linear wave theory. However, this may not be an accurate simplification of the local wave field in Ryde. Time series, especially of boat wakes (Figure 3.8a), suggest that present waves may not be linear and better represented by other wave models (e.g. cnoidal waves). It was nevertheless decided to use a linear approach, because the subsequent models for computing energy dissipation and drag coefficients were based on the assumption that linear wave theory applies. If a different wave model would have been used during the initial steps of analysis, the validity of those models would have been questionable. Previous studies have successfully applied linear wave theory to wind waves (Lowe et al., 2007; Bradley and Houser, 2009; Mullarney and Henderson, 2010) and boat wakes (Koch, 2002; Ciavola, 2005; Garel et al., 2008) under similar conditions and it was therefore considered a reasonable approximation of the wave conditions encountered in Ryde.

5.7.3. Use of seagrass mimics

The mimics used to represent seagrass during the laboratory experiments were found by visual comparison of live plants and various mimic materials in a laboratory flume.

The material that best simulated the plant's movement was chosen to produce the mimics for this study. This approach varied from other studies with plant mimics where mimic material was chosen as to match plant properties such as modulus of elasticity and material density as closely as possible (Folkard, 2005; Manca, 2010). However, the present study did not intend to model any plant species perfectly, but to explore the general effect of the plant properties stiffness, leaf length and density on wave attenuation. Nevertheless, it should be noted that the visual comparison was done under unidirectional flow while the experiments for this study were carried out under orbital wave motion. It is therefore assumed that a behavioural similarity under unidirectional flow corresponds to a similarity under oscillatory movement. This, however, may not be the case as differences in flexural stiffness may lead to a different response time to changes in flow direction (i.e. under waves) while those differences may not become apparent under constant unidirectional flow (Dijkstra and Uittenbogaard, 2010).

5.8. Future work

The work presented here shows that plant morphology as well as wave and tidal parameters have an effect on wave attenuation by *Zostera noltii*. Moreover, this study revealed that those parameters can influence each other's impact on wave attenuation. Hydrodynamics can influence morphological threshold values (e.g. minimum shoot density) that need to be exceeded before wave attenuation can be observed and morphological parameters can in return change the impact hydrodynamics have on wave attenuation; the effect of an underlying current, for example, depends on plant stiffness. Studies that consider these interactions are still rare and future work should focus more on these interactions to evaluate their importance in wave attenuation by vegetation. From the present study four research topics were identified that would help assessing the effect of hydro-morphodynamic interactions.

1. It was shown in Chapter 2 that leaf length is a good approximation for canopy height in the field, however the laboratory study (Chapter 4) confirmed previous findings that canopy height reduces under the presence of a current (Fonseca et al., 1982). Many seagrass monitoring programmes include leaf length measurements as part of the meadow's health assessment, but usually do not record canopy height (Buia et al., 2004). It would save time and money for additional surveys, if the collected data could be used to predict wave attenuation. However, this would require an understanding of the difference between leaf length and canopy height from a hydrodynamic perspective. Detailed field and laboratory studies should be carried out to investigate the relationship between these two parameters for different seagrass species and under varying hydrodynamic conditions.

2. Tests on three different seagrass mimics (Chapter 4) confirmed earlier results (Bouma et al., 2005, 2010) that wave attenuation increases with increasing plant stiffness. Nevertheless, no significant difference was observed between the two materials that moved in a whip like motion and an artificial salt marsh material that moved in a cantilever motion yielded the same wave attenuation as stiff material (Augustin et al., 2009). Laboratory studies (Manca, 2010) showed that vegetation of a certain stiffness can exhibit both motion types (cantilever or whip like) depending on hydrodynamic forcing. While it is likely that very flexible species like *Z. noltii* show whip like motion under all field conditions and very stiff species (e.g. *Spartina alterniflora*) always move as a cantilever, species of a medium stiffness (e.g. *Posidonia sp.*) may vary between the two types of motion under changing hydrodynamic conditions. It should therefore be explored how the type of motion affects wave attenuation and under what conditions individual species change their behaviour from one motion type to the other.

3. During the laboratory study (Chapter 4) is was found that leaf area index determines wave attenuation and a study on salt marsh suggested that wave attenuation can be described as a function of biomass which is independent of species (Bouma

et al., 2010). A possible dependence on biomass rather than individual morphological parameters could explain observations made in *Z. noltii* (Chapter 3) and *Ruppia maritima* (Newell and Koch, 2004) where a minimum shoot density was required before an effect on wave attenuation could be observed. Both species have relatively narrow, short vegetative shoots which lead to low biomass values per shoot. If a minimum biomass per m^2 was required before wave attenuation could be detected, both species would need to exceed a certain density to achieve such threshold biomass. No critical density values have been observed for larger seagrass species where a critical biomass may have been reached at much lower densities. More research is needed on the effect of species independent biomass on wave attenuation and the existence of a possible minimum threshold value. A relationship of wave attenuation by vegetation to biomass instead of species specific parameters would allow direct comparison of the wave attenuating capacity between species and ecosystems.

4. Including an underlying current in the laboratory experiments (Chapter 4) revealed that studies under waves only overestimate wave attenuation by seagrass in tidal environments. However, the experimental setup of this study investigated currents only in the direction of wave propagation. A study on kelp (Gaylord et al., 2003) showed that even currents perpendicular to wave advance can affect wave attenuation by vegetation even though it has no significant effect on the waves (Mathisen and Madsen, 1996a, 1999). In order to predict wave attenuation by vegetation under natural conditions it is necessary to define the effect of an underlying current on wave attenuation by vegetation and to include the angle between flow direction and wave propagation.

APPENDIX

A. Field data

Table A.1.: Measured leaf length (±standard deviation, n = 10) and shoot density for all deployments in Ryde. Coordinates are given in WGS 84. LAI is based on a constant leaf width of 2 mm.

date	latitude [North]	longitude [West]	leaf length [cm]	shoot density [per m^2]	LAI [m^2 m^{-2}]
October '08	50 44 09.1	1 09 39.1	21, 22, 18, 18, 20, 20, 18, 21	1689	0.67
November '08	50 44 05.9	1 09 38.7	10, 10, 8, 7, 11, 6, 10, 10, 5, 8	1144	0.19
	50 44 09.1	1 09 39.3	14, 20, 16, 13, 18, 13, 14, 12, 10, 12	744	0.21
	50 44 08.2	1 09 38.3	14, 13, 15, 15, 17, 16, 9, 15, 12, 14	1011	0.28
	50 44 09.4	1 09 39.3	14, 13, 12, 14, 12, 12, 19, 15, 13, 12	1344	0.37
December '08	50 44 09.0	1 09 39.3	20, 20, 22, 10, 13, 15, 23, 22, 24, 21	1533	0.58
	50 44 09.2	1 09 39.2	8, 12, 12, 8, 12, 8, 7, 13, 11, 10	1000	0.20

A. Field data

date	latitude [North]	longitude [West]	leaf length [cm]	shoot density [per m^2]	LAI [m^2 m^{-2}]
	50 44 09.9	1 09 39.3	16, 14, 14, 20, 18, 18, 11, 15, 10, 14	311	0.09
December '08	50 44 09.5	1 09 39.1	15, 13, 21, 21, 22, 12, 17, 19, 20, 12	1356	0.47
	50 44 10.2	1 09 39.5	21, 15, 17, 16, 18, 21, 18, 15, 21, 16	677	0.24
January '09	50 44 08.8	1 09 39.6	20, 19, 19, 14, 25, 20, 18, 18, 22, 21	856	0.34
	50 44 09.4	1 09 39.6	9, 12, 12, 11, 11, 9, 7, 13, 13, 10	1011	0.22
	50 44 09.8	1 09 40.1	8, 5, 7, 5, 8, 9, 9, 9, 7, 6	1967	0.29
	50 44 09.8	1 09 40.0	11, 14, 21, 4, 13, 9, 9, 11, 16, 12	667	0.16
February '09	50 44 08.6	1 09 40.6	5, 11, 14, 10, 4, 8, 9, 3, 7, 5	956	0.15
	50 44 09.1	1 09 40.2	13, 7, 20, 5, 19, 7, 18, 9, 6, 18	522	0.13
	50 44 09.9	1 09 39.6	11, 9, 7, 6, 5, 10, 16, 3, 6, 10	567	0.09
	50 44 10.3	1 09 41.1	8, 15, 9, 10, 8, 18, 10, 6, 12, 5	456	0.09
March '09	50 44 08.9	1 09 39.9	8, 5, 5, 8, 9, 7, 7, 10, 8, 10	856	0.13

date	latitude [North]	longitude [West]	leaf length [cm]	shoot density [per m^2]	LAI [m^2 m^{-2}]
	50 44 09.4	1 09 39.9	7, 8, 12, 11, 9, 7, 6, 8, 8, 8	911	0.15
March '09	50 44 09.8	1 09 40.6	10, 12, 16, 9, 9, 7, 8, 8, 6, 7	578	0.11
	50 44 08.7	1 09 39.5	11, 10, 3, 11, 6, 5, 7, 9, 8, 10	744	0.12
April '09	50 44 10.0	1 09 40.4	10, 9, 11, 13, 12, 11, 10, 11, 5, 10	789	0.16
	50 44 09.9	1 09 40.6	18, 17, 18, 9, 13, 11, 10, 12, 10, 12	689	0.18
	50 44 09.7	1 09 41.6	10, 11, 15, 10, 12, 12, 14, 5, 7, 6	1089	0.22
	50 44 08.8	1 09 41.6	10, 13, 14, 15, 12, 11, 12, 6, 7, 9	844	0.18
May '09	50 44 09.5	1 09 39.8	15, 12, 10, 11, 17, 6, 9, 8, 10, 11	2278	0.50
	50 44 09.2	1 09 39.7	15, 11, 13, 8, 18, 13, 14, 14, 13, 15	1311	0.35
	50 44 09.1	1 09 39.6	14, 12, 14, 15, 16, 14, 16, 13, 14, 15	1500	0.43
	50 44 08.1	1 09 39.7	12, 13, 11, 11, 12, 12, 14, 13, 11, 12	1322	0.32
June '09	50 44 09.2	1 09 40.0	12, 11, 5, 13, 14, 16, 13, 15, 14, 17	3867	1.01

A. Field data

date	latitude [North]	longitude [West]	leaf length [cm]	shoot density [per m^2]	LAI [m^2 m^{-2}]
	50 44 09.2	1 09 40.1	15, 15, 14, 14, 13, 15, 15, 13, 16, 15	6244	1.81
June '09	50 44 10.6	1 09 39.7	13, 13, 9, 10, 12, 11, 9, 12, 10, 11	2856	0.63
	50 44 09.7	1 09 40.8	20, 17, 19, 18, 19, 17, 19, 21, 17, 18	3156	1.17
July '09	50 44 09.3	1 09 39.3	12, 15, 20, 12, 14, 13, 16, 13, 18, 16	4022	1.20
	50 44 10.0	1 09 39.8	12, 11, 12, 9, 10, 11, 12, 11, 8, 16	3811	0.85
	50 44 09.5	1 09 40.2	15, 14, 13, 17, 17, 17, 16, 15, 15, 15	3911	1.20
	50 44 08.5	1 09 39.9	12, 12, 21, 13, 18, 17, 11, 12, 12, 12	4911	1.38
August '09	50 44 08.8	1 09 39.4	14, 13, 18, 16, 13, 19, 16, 14, 13, 10	4522	1.32
	50 44 09.1	1 09 40.4	14, 10, 13, 13, 12, 11, 11, 10, 13, 14	3978	0.96
	50 44 09.5	1 09 39.9	11, 10, 10, 9, 9, 11, 10, 9, 9, 8	4167	0.80
	50 44 09.3	1 09 40.3	13, 13, 12, 13, 12, 16, 13, 15, 14, 14	5878	1.59
September '09	50 44 08.8	1 09 39.6	14, 12, 15, 14, 20, 21, 13, 12, 13, 12	3611	1.05

date	latitude [North]	longitude [West]	leaf length [cm]	shoot density [per m^2]	LAI [m^2 m^{-2}]
	50 44 09.4	1 09 40.2	12, 14, 13, 12, 13, 11, 13, 11, 10, 14	2144	0.53
September '09	50 44 09.6	1 09 39.7	9, 9, 12, 13, 8, 14, 12, 12, 9, 8	2267	0.48
	50 44 09.7	1 09 40.3	15, 14, 14, 11, 17, 14, 15, 13, 14, 13	2289	0.64
October '09	50 44 09.4	1 09 39.6	12, 12, 10, 13, 15, 17, 10, 12, 14, 11	1867	0.47
	50 44 09.4	1 09 39.7	13, 11, 12, 10, 12, 16, 12, 15, 9, 10	2044	0.49
	50 44 09.1	1 09 39.9	11, 12, 12, 14, 12, 18, 16, 18, 15, 15	1367	0.39
	50 44 08.6	1 09 39.3	9, 12, 13, 13, 10, 10, 15, 15, 12, 13	2122	0.52

A. Field data

Plots of all wave spectra can be found on the enclosed CD-ROM. File names consist of three parts that allow unique identification of the interval used to generate the plot:

1. The letter code indicates the month during which the data was collected.

month	October '08	February '09	May '09	July '09	October '09
code	Oct08	Feb	May	Jul	Oct09

1. The first number indicates the station at which the data was collected.
2. The second number indicates the time interval during the relevant deployment at which the data was collected; identical numbers indicate the same time interval.

For example, the data for files Feb_1_58.fig and Feb_5_58.fig were collected simultaneously during the February '09 deployment. The former was collected at station 1 while the latter was collected at station 5.

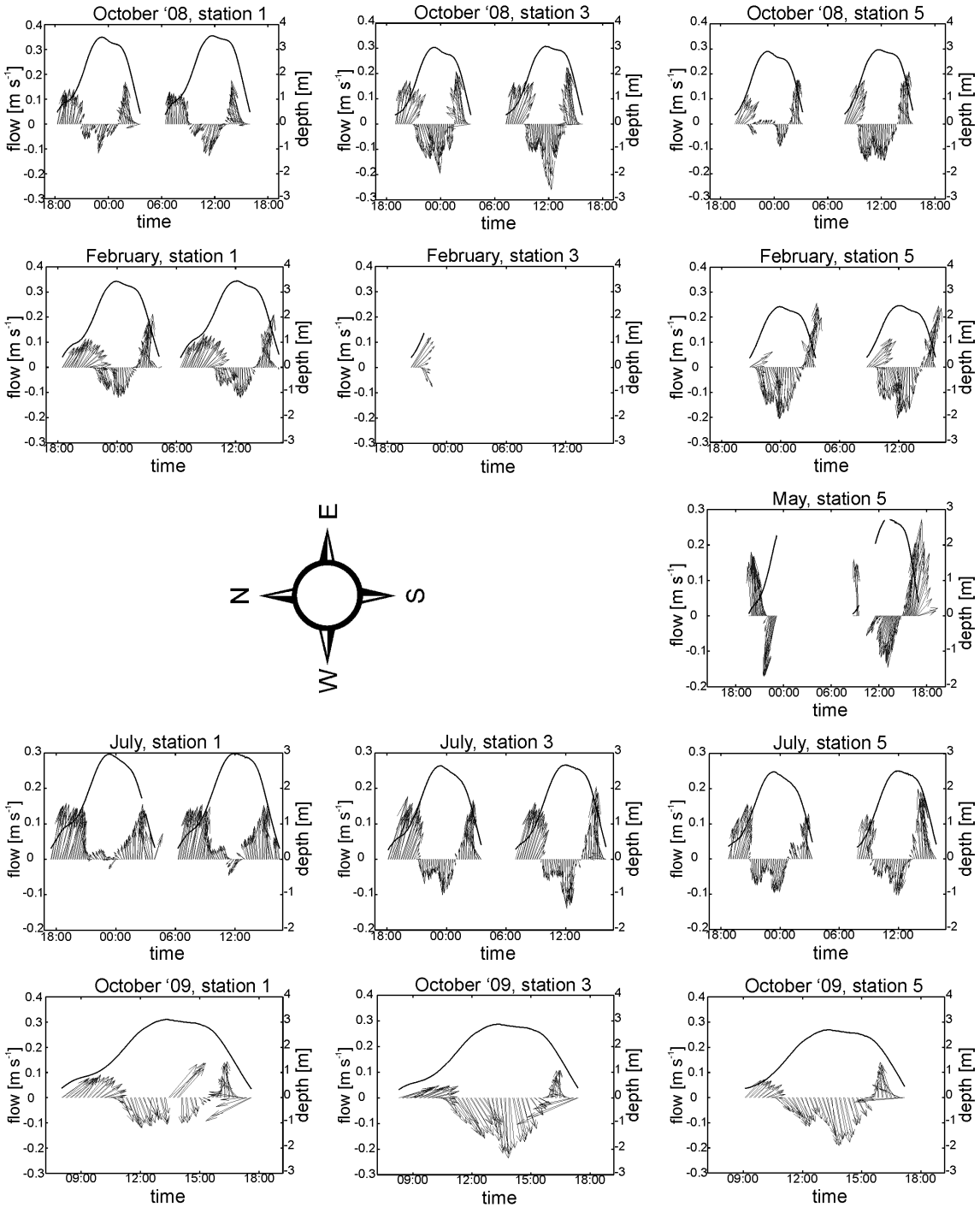

Figure A.1.: Tidal flow conditions for stations 1, 3 and 5 for all deployments. Note that for the May deployment flow data is only available at station 5/6. At station 3 in February only limited data is available due to instrument failure. The solid line represents the tidal elevation.

B. Laboratory data

Table B.1.: Meadow and flow conditions, and measured significant wave heights for laboratory tests.

mimic material	density [m^{-2}]	leaf length [cm]	current [m s^{-1}]	H_s at beginning of meadow [cm]	H_s at end of meadow [cm]	ΔH [cm/m]
control	-	-	0	9.55	8.19	0.45
	-	-	0.1	7.51	6.43	0.36
very	1000	30	0	9.71	7.74	0.65
flexible	1000	30	0.1	7.73	5.97	0.58
	1000	15	0	9.82	7.94	0.62
	1000	15	0.1	7.74	6.05	0.56
	1000	10	0	9.87	7.87	0.63
	1000	10	0.1	7.64	6.50	0.53
	4000	30	0	9.72	7.47	0.75
	4000	30	0.1	7.82	6.00	0.61
	4000	15	0	10.06	7.85	0.74
	4000	15	0.1	7.87	6.12	0.59
	4000	10	0	9.72	7.82	0.63
	4000	10	0.1	7.60	6.04	0.52
flexible	500	30	0	9.76	7.94	0.61

mimic material	density [m^{-2}]	leaf length [cm]	current [m s^{-1}]	H_s at beginning of meadow [cm]	H_s at end of meadow [cm]	ΔH [cm/m]
flexible	500	30	0.1	7.69	6.12	0.52
	500	15	0	10.00	8.12	0.63
	500	15	0.1	7.68	6.17	0.50
	500	10	0	9.83	7.96	0.62
	500	10	0.1	7.63	6.13	0.50
	1000	30	0	9.74	7.75	0.66
	1000	30	0.1	7.77	6.10	0.56
	1000	15	0	9.70	7.85	0.62
	1000	15	0.1	7.72	6.04	0.56
	1000	10	0	9.79	7.75	0.68
	1000	10	0.1	7.73	6.08	0.55
	2000	30	0	9.34	7.57	0.59
	2000	30	0.1	7.44	5.94	0.50
	2000	15	0	9.92	7.62	0.77
	2000	15	0.1	7.90	6.12	0.60
	2000	10	0	9.80	7.86	0.65
	2000	10	0.1	7.59	6.08	0.50
	4000	15	0	9.78	7.82	0.65
	4000	15	0.1	7.78	6.12	0.55
	4000	10	0	9.97	7.83	0.71
	4000	10	0.1	7.79	5.99	0.60
	8000	30	0	9.50	5.72	1.26
	8000	30	0.1	7.63	4.88	0.92
	8000	15	0	9.63	6.90	0.91
	8000	15	0.1	7.57	5.79	0.59

mimic material	density [m^{-2}]	leaf length [cm]	current [m s^{-1}]	H_s at beginning of meadow [cm]	H_s at end of meadow [cm]	ΔH [cm/m]
flexible	8000	10	0	9.68	7.14	0.85
	8000	10	0.1	7.30	5.61	0.56
stiff	1000	15	0	9.74	7.34	0.80
	1000	15	0.1	7.66	5.78	0.63
	1000	10	0	9.81	7.55	0.75
	1000	10	0.1	7.73	5.86	0.62
	4000	15	0	9.53	5.73	7.27
	4000	15	0.1	7.48	5.06	0.81
	4000	10	0	9.75	6.66	1.03
	4000	10	0.1	7.48	5.50	0.66

Determination of reflection

Reflected waves were removed from the recorded signal using the method by Baldock and Simmonds (1999). The method was implemented through a MatLab script that was provided by Dr. T. Baldock. The script is based on equations developed by Frigaard and Brorsen (1995) and was expanded to also apply to sloping beds. The slope for this analysis was set to zero, as the present experiments were carried out over a flat bed.

The first two gauges were used to determine reflection; they were spaced 21.5 cm apart. This spacing fulfilled the condition that the distance between the gauges is $<\frac{1}{4}$ of the incident wave length (Frigaard and Brorsen, 1995) since the wave length in this study was 1.4 m.

The method assumes linear wave theory and Baldock and Simmonds (1999) recommend to remove sub and super harmonics. The spectra were therefore filtered for a range of 0.1 Hz above and below the peak frequency of 0.98 Hz with a low and high pass cut-off filter respectively.

From the first two gauges, the incident and reflected wave amplitudes and the resulting reflection coefficient (reflected wave amplitude / incident wave amplitude) was computed. For seven tests during the course of the experiments the reflection coefficient exceeded 5% and in those cases the reflected wave train was removed from the signals recorded by all other gauges during the run (i.e. directly in front of and behind the mimic meadow). This filtering was carried out in the frequency domain as well.

C. Abstract of conference paper on laboratory data

The effect of organism traits and tidal currents on wave attenuation by submerged vegetation

Maike Paul[1], Tjeerd Bouma[2] and Carl L. Amos[1]

1 Introduction

It is widely recognized that submerged seagrass vegetation can have a significant impact on wave attenuation. To correctly account for the effect of seagrass on wave attenuation in coastal protection and management, it is important to understand which vegetation traits and hydrodynamic parameters drive wave attenuation by vegetation (Teeter et al., 2001, Patil and Singh, 2009).

This study investigates the impact of submergence ratio, shoot stiffness and density on wave attenuation. Additionally, and to our knowledge for the first time, this study investigates how a tidal current affects wave attenuation by seagrass. In the natural environment most seagrass meadows are exposed to waves superimposed on a tidal flow and the effect of this underlying current on wave attenuation by vegetation is not yet known.

2 Materials and Methods

Two mechanically realistic seagrass mimics with different bending behavior (cantilever vs. whip-like) were developed and several meadows were produced to cover a wide range of natural densities (500-8000 shoots/m^2) and leaf lengths (10-30 cm). Experiments were carried out under controlled conditions in a racetrack wave flume with a straight working section of 10.8 m and 0.6 m width with a constant water depth of 0.3 m. The flume is equipped with a conveyor belt system and a wave paddle, which allows generating unidirectional flow, regular waves or a combination of both. Wave heights were measured at the leading edge and at the end of the meadow for at least 600 s per run. Additionally, a video camera was used to record seagrass movement through the glass wall of the test section.

From the wave recordings, dissipated wave height ΔH per meter meadow was derived as:

$$\Delta H = (H_1 - H_2)/x \quad (1)$$

with ΔH dissipated wave height [-]

H_1 wave height at leading edge of meadow [m]

H_2 wave height at end of meadow [m]

x length of meadow [m]

The leaf area index (LAI = leaf length * leaf width * density, $m^2\ m^{-2}$) was calculated for each meadow and used to compare the wave attenuating capacity, as the meadows varied in leaf length as well as density. Plant movement was expressed in excursion of the leaf tip which was derived from video recordings.

3 Results

An effect of plant stiffness on wave attenuation was apparent when comparing the results from both materials. The attenuating effect of the stiff material was much higher for any given LAI compared to the flexible mimics, unless LAI was negligibly low. However, the flexible mimic was

[1] University of Southampton, Waterfront Campus, European Way, Southampton SO14 3ZH, United Kingdom, maike.paul@soton.ac.uk; cla8@noc.soton.ac.uk

[2] Netherlands Institute of Ecology, Centre for Estuarine and Marine Ecology, P.O. Box 140, 4400 AC Yerseke, The Netherlands, T.Bouma@nioo.knaw.nl

able to reach the same dissipated wave height at approx. four times the LAI of the stiff mimic (Figure 1a).

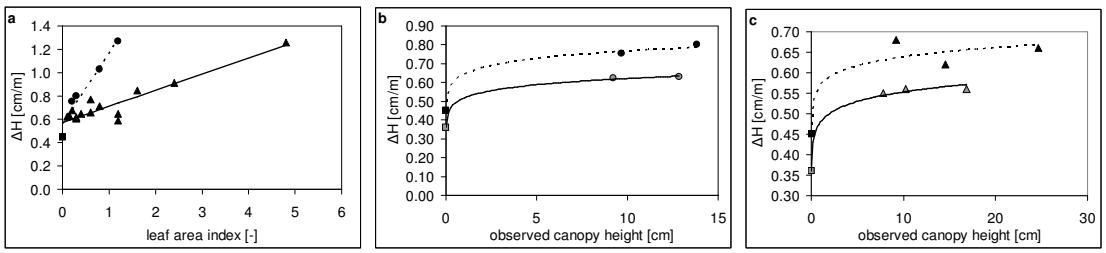

Figure 1: Dissipated wave height as a function of a) leaf area index under waves only and of canopy height for b) stiff mimics and c) flexible mimics at 1000 shoots per m^2. ● = stiff, ▲ = flexible, ■ = no seagrass, black symbols represent the wave only case and grey symbols represent the combined wave and current case.

The presence of an underlying current reduced wave dissipation as well as the observed canopy height at any given vegetation length. The canopy height reduction caused by bending is, however, not the only process affecting wave attenuation, as wave dissipation rates are still lower in the presence of a current when comparing meadows with a similar actual canopy height (see examples in Figure 1b-c). Comparison of data from all runs shows that ΔH increases linearly with shoot density for a given canopy height and this increase is more pronounced in the absence of an underlying current.

4 Discussion and Conclusions

Results showed that stiffness and leaf area index determine wave attenuation. The leaf area index combines the effect of leaf length and shoot density and therefore indicates that density can compensate for lack of canopy height and vice versa with respect to wave attenuation. Additionally, a higher LAI can lead to the same dissipation rate for a flexible plant than a stiff plant at lower LAI, which suggests that different growth strategies can lead to the same effect on wave attenuation.

The presence of an underlying current led to a reduction in wave attenuation for all meadows. The current bent the leaves, leading to a primary tension within the blades which restricted plant movement and hence wave dissipation. Reduced plant movement and wave dissipation were present for both materials, suggesting that the current affects wave dissipation independent of the vegetation's bending behavior. Reduction of wave dissipation increased with increasing shoot density which could not be fully explained with the data collected during this study. However, the results clearly show that experiments which are carried out under waves only overestimate the wave attenuating capacity of seagrass compared to most natural environments where underlying currents are present in the form of tidal flow.

5 Acknowledgements

The authors kindly acknowledge the use of MatLab code for zero-crossing and wave reflection provided by Dr U. Neumeier and Dr T. Baldock, respectively. The lab experiments were possible thanks to a Peter Killworth Memorial Scholarship and the first author would like to thank Christel and Dieter from the Stiftung zur Förderung Paulscher Promotionen for uncounted hours of invaluable help during preparation and execution of the experiments.

6 References

Patil, S.; Singh, V. P. (2009): Hydrodynamics of Wave and Current Vegetation Interaction. In: Journal of Hydrologic Engineering, Vol. 14, pp. 1320-1333; ISSN 1084-0699.

Teeter, A. M.; Johnson, B. H.; Berger, C.; Stelling, G.; Scheffner, N. W.; Garcia, M. H.; Parchure, T. M. (2001): Hydrodynamic and sediment transport modelling with emphasis on shallow-water, vegetated areas (lakes, reservoirs, estuaries and lagoons). In: Hydobiologia, Vol. 444, pp. 1-23; ISSN 0018-8158.

Bibliography

Ainslie, M. A. and McColm, J. G. (1998). A simplified formula for viscous and chemical absorption in sea water. *The Journal of the Acoustical Society of America*, 103(3):1671–1672.

Alexandre, A., Cabaço, S., Santos, R., and Serrão, E. A. (2006). Timing and success of reproductive stages in the seagrass *Zostera noltii*. *Aquatic Botany*, 85:219–223.

Amos, C. L., Bergamasco, A., Umgiesser, G., Cappucci, S., Cloutier, D., DeNat, L., Flindt, M., Bonardi, M., and Cristante, S. (2004). The stability of tidal flats in Venice Lagoon - the results of *in-situ* measurements using two benthic, annular flumes. *Journal of Marine Systems*, 51:211–241.

Amos, C. L., Daborn, G. R., and Christian, H. A. (1992). *In situ* erosion measurements of fine-grained sediments from the Bay of Fundy. *Marine Geology*, 108:175–196.

Asano, T., Tsutsui, S., and Sakai, T. (1988). Wave damping characteristics due to seaweed. In *35th Coastal Engineering Conference in Japan*, pages 138–142. Japan Society of Civil Engineers (JSCE). (in Japanese).

Asmus, H. and Asmus, R. (2000a). ECSA - Workshop on intertidal seagrass beds and algal mats: organisms and fluxes at the ecosystem level (Editorial). *Helgoland Marine Research*, 54:53–54.

Asmus, H. and Asmus, R. (2000b). Material exchange and food web of seagrass beds

in the Sylt-Rømø Bight: how significant are community changes at the ecosystem level? *Helgoland Marine Research*, 54:137–150.

Auby, I. and Labourg, P. J. (1996). Seasonal dynamics of *Zostera noltii* Hornem. in the bay of Arcachon (France). *Journal of Sea Research*, 35(4):269–277.

Augustin, L. N., Irish, J. L., and Lynett, P. (2009). Laboratory and numerical studies of wave damping by emergent and near-emergent wetland vegetation. *Coastal Engineering*, 56:332–340.

Backhaus, J. O. and Verduin, J. J. (2008). Simulating the interaction of seagrasses with their ambient flow. *Estuarine, Coastal and Shelf Science*, 80:563–572.

Baldock, T. E. and Simmonds, D. J. (1999). Separation of incident and reflected waves over sloping bathymetry. *Coastal Engineering*, 38(3):167–176.

Ballesta, L., Pergent, G., Pasqualini, V., and Pergent-Martini, C. (2000). Distribution and dynamics of *Posidonia oceanica* beds along the Alberes coastline. *Comptes Rendus de l'AcadÃ©mie des Sciences, Sciences de la Vie/Life Sciences*, 323:407–414.

Barbier, E. B., Koch, E. W., Silliman, B. R., Hacker, S. D., Wolanski, E., Primavera, J. H., Granek, E. F., Polansky, S., Aswani, S., Cramer, L. A., Stoms, D. M., Kennedy, C. J., Bael, D., Kappel, C. V., Perillo, G. M. E., and Reed, D. J. (2008). Coastal Ecosystem - Based Management with Nonlinear Ecologial Functions and Values. *Science*, 319.

Battjes, J. (1974). Surf similarity. In *Proceedings of the 14th Coastal Engineering Conference*, pages 466–480. American Society of Civil Engineers, Restion, Va.

Bold, H. C., Alexopoulos, C. J., and Delevoryas, T. (1987). *Morhology of Plants and Fungi*. Harper-Collins, New York, 5th edition.

Boller, M. L. and Carrington, E. (2006). The hydrodynamic effects of shape and size change during reconfiguration of a flexible macroalga. *Journal of Experimental Biology*, 209(10):1894–1903.

Borg, J. A., Attrill, M. J., Rowden, A. A., Schembri, P. J., and Jones, M. B. (2005). Architectural characteristics of two bed types of the seagrass *Posidonia oceanica* over different spatial scales. *Estuarine, Coastal and Shelf Science*, 62(4):667–678.

Borum, J., Duarte, C. M., Krause-Jensen, D., and Greve, T. M. (2004). European seagrasses: an introduction to monitoring and management. Technical report, EU project Monitoring and Managing of European Seagrasses.

Bouma, T. J., De Vries, M. B., and Herman, P. M. J. (2010). Comparing ecosystem engineering efficiency of 2 plant species with contrasting growth strategies. *Ecology*, 91(9):2696–2704.

Bouma, T. J., De Vries, M. B., Low, E., Peralta, G., Tánczos, I. C., van de Koppel, J., and Herman, P. M. J. (2005). Trade-offs related to ecosystem engineering: A case study on stiffness of emerging macrophytes. *Ecology*, 86(8):2187–2199.

Bouma, T. J., van Duren, L. A., Temmerman, S., Claverie, T., Blanco-Garcia, A., Ysebaert, T., and Herman, P. M. J. (2007). Spatial flow and sedimentation patterns within patches of epibenthic structures: Combining field, flume and modelling experiments. *Continental Shelf Research*, 27:1020–1045.

Bradley, K. and Houser, C. (2009). Relative velocity of seagrass blades: Implications for wave attenuation in low-energy environments. *Journal of Geophysical Research*, 114(F01004):1–13.

Brun, F. G., Pérez-Pastor, A., Hernández, I., Vergara, J. J., and Pérez-Lloréns, J. L. (2006). Shoot organization in the seagrass *Zostera noltii*: implications for space occupation and plant architecture. *Helgoland Marine Research*, 60:59–69.

Brun, F. G., Vergara, J. J., Hernández, I., and Pérez-Lloréns, J. L. (2005). Evidence for vertical growth in *Zostera noltii Hornem. Botanica Marina*, 48(5-6):446–450.

Buia, M. C., Gambi, M. C., and Dappiano, M. (2004). Seagrass systems. In Gambi, M. C. and Dappiano, M., (editors), *Mediterranean Marine Benthos: a Manual*

of Methods for its Sampling and Study, volume 11 (Suppl. 1) of *Biologia Marina Mediterranea*, pages 133–183. SIBM Publ., Genova.

Burke, L., Kura, Y., Kassem, K., Revenga, C., Spalding, M., and McAllister, D. (2001). Pilot Analysis of Global Ecosystems: Coastal Ecosystems. Technical report, World Resources Institute, Washington D.C.

Cancemi, G., Baroli, M., De Falco, G., Agostini, S., Piergallini, G., and Guala, I. (2000). Cartografia integrata delle praterie superficiali come indicatore dell'impatto antropico sulla fascia costiera. *Biologia Marina Mediterranea*, 7(2):509–516. (in Italian).

CCO (2009). Aerial image of the Solent (2005). [accessed 16/06/2009]. Available from: www.channelcoast.org.

CCO (2011). Survey data for profile RYD23 [accessed 24/02/2011]. Available from www.channelcoast.org.

Chang, E. R., Veeneklaas, R. M., Buitenwerf, R., Bakker, J. P., and Bouma, T. J. (2008). To move or not to move: determinants of seed retention in a tidal marsh. *Functional Ecology*, 22:720–727.

Charpentier, A., Grillas, P., Lescuyer, F., Coulet, E., and Auby, I. (2005). Spatio-temporal dynamics of a *Zostera noltii* dominated community over a period of fluctuating salinity in a shallow lagoon, Southern France. *Estuarine, Coastal and Shelf Science*, 64:307–315.

Chen, S. N., Sanford, L. P., Koch, E. W., Shi, F., and North, E. W. (2007). A nearshore model to investigate the effects of seagrass bed geometry on wave attenuation and suspended sediment transport. *Estuaries and Coasts*, 30(2):296–310.

Ciavola, P. (2005). Sediment Resuspension in the Lagoon of Venice: Short-term Observations of Natural and Anthropogenic Processes. *Zeitschrift fÃŒr Geomorphologie supplement series*, 141:1–15.

Collins, M. J. and Ansell, K., (editors) (2000). *Solent Science - A Review*. Proceedings in Marine Science. Elsevier, Amsterdam.

Connolly, R. M. (1994). A comparison of fish assemblages from seagrass and unvegetated areas of a southern Australian estuary. *Marine and Freshwater Research*, 45:1033–1044.

Cooper, N. J. (2005). Wave dissipation across intertidal surfaces in the Wash tidal inlet, Eastern England. *Journal of Coastal Research*, 21(1):28–40.

Crawford, C. M., Mitchell, I. M., and Macleod, C. K. A. (2001). Video assessment of environmental impacts of salmon farms. *ICES Journal of Marine Science*, 58:445–452.

Curiel, D., Bellato, A., Rismondo, A., and Marzocchi, M. (1996). Sexual reproduction of *Zostera noltii Hornemann* in the lagoon of Venice (Italy, north Adriatic). *Aquatic Botany*, 52:313–318.

Dalrymple, R. A., Kirby, J. T., and Hwang, P. A. (1984). Wave diffraction due to areas of energy dissipation. *Journal of Waterway, Port, Coastal and Ocean Engineering*, 110(1):67–79.

De Falco, G., Baroli, M., Murru, E., Piergallini, G., and Cancemi, G. (2006). Sediment analysis evidences two different depositional phenomena influencing seagrass distribution in the Gulf of Oristano (Sardinia, Western Mediterranean). *Journal of Coastal Research*, 22(5):1043–1050.

De Falco, G., Ferrari, S., Cancemi, G., and Baroli, M. (2000). Relation between sediment distribution and *Posidonia oceanica* seagrass. *Geo-Marine Letters*, 20:50–57.

de la Vega-Leinert, A. C. and Nicholls, R. J. (2008). Potential implications of sea-level rise for Great Britain. *Journal of Coastal Research*, 24(2):342–357.

de los Santos, C. B., Brun, F. G., Bouma, T. J., Vergara, J. J., and Pérez-Lloréns, J. L. (2010). Acclimation of seagrass *Zostera noltii* to co-occurring hydrodynamic and light stresses. *Marine Ecology Progress Series*, 398:127–135.

Dean, R. G. and Dalrymple, R. A. (1991). *Water wave mechanics for engineers and scientists*. Englewood Cliffs, NJ.

Den Hartog, C. (1970). *The sea-grasses of the world*. North Holland Publishing Company, Amsterdam.

Den Hartog, C. (1994). Suffocation of a littoral *Zostera* bed by *Enteromorpha radiata*. *Aquatic Botany*, 47(1):21–28.

Dennison, W. C., Orth, R. J., Moore, K. A., Stevenson, J. C., Carter, V., Kollar, S., Bergstrom, P. W., and Batiuk, R. A. (1993). Assessing water quality with submersed aquatic vegetation. *Bioscience*, 43:86–94.

Denny, M. W. (1988). *Biology and the mechanics of the wave swept environment*. Princeton University Press, Princeton, New Jersey.

Denny, M. W. and Gaylord, B. (2002). The mechanics of wave-swept algae. *Journal of Experimental Biology*, 205(10):1355–1362.

Dijkstra, J. T. and Uittenbogaard, R. E. (2010). Modeling the interaction between flow and highly flexible aquatic vegetation. *WATER RESOURCES RESEARCH*, 46.

Duarte, C. M. (1987). Use of echo sounder tracing to estimate the aboveground biomass of submersed plants in lakes. *Canadian Journal of Fisheries and Aquatic Sciences*, 44:732–735.

Duarte, C. M., Fourqurean, J. W., Krause-Jensen, D., and Olesen, B. (2006). Dynamics of Seagrass Stability and Change. In Larkum, A. W. D., Orth, R. J., and Duarte, C. M., (editors), *Seagrasses: Biology, Ecology and Conservation*, pages 271–294. Springer, Berlin.

Duarte, C. M. and Kirkman, H. (2001). Methods for the measurement of seagrass abundance and depth distribution. In Short, F. T. and Coles, R. G., (editors), *Global seagrass research methods*, pages 141–153. Elsevier Science bv, Amsterdam.

Duarte, C. M., Merino, M., Agawin, N. S. R., Uri, J. S., Fortes, M. D., Gallegos, M. E., Marbà, N., and Hemminga, M. A. (1998). Root production and belowground seagrass biomass. *Marine Ecology Progress Series*, 171:97–108.

Dubi, A. and Tørum, A. (1997). Wave energy dissipation by kelp vegetation. In Edge, B., (editor), *25th International Conference on Coastal Engineering*, pages 2626–2639, Orlando, Florida, USA. American Society of Civil Engineers.

Elwany, M. H. S., O'Reilly, W. C., Guza, R. T., and Flick, R. E. (1995). Effect of Southern California kelp beds on waves. *Journal of Waterway Port Coastal and Ocean Engineering-Asce*, 121:143–150.

Folkard, A. M. (2005). Hydrodynamics of model *Posidonia oceanica* patches in shallow water. *Limnology and Oceanography*, 50(5):1592–1600.

Fonseca, M. S. (1996). The role of seagrasses in nearshore sedimentary processes: a review. In Nordstrom, K. F. and Roman, C. T., (editors), *Estuarine Shores: Evolution, Environments and Human Alterations*, pages 261–286. Wiley, Chichester.

Fonseca, M. S. and Cahalan, J. A. (1992). A preliminary evaluation of wave attenuation by four species of seagrass. *Estuarine, Coastal and Shelf Science*, 35:565–576.

Fonseca, M. S. and Fisher, J. S. (1986). A comparison of canopy friction and seagrass movement between four species of seagrass with reference to their ecological restoration. *Marine Ecology*, 29:15–22.

Fonseca, M. S., Fisher, J. S., Ziemann, J. C., and Thayler, G. W. (1982). Influence of the seagrass, *Zostera marina L.*, on current flow. *Estuarine, Coastal and Shelf Science*, 15:351–364.

Fonseca, M. S. and Koehl, M. A. R. (2006). Flow in seagrass canopies: The influence of patch width. *Estuarine, Coastal and Shelf Science*, 67:1–9.

Frigaard, P. and Brorsen, M. (1995). A time-domain method for separating incident and reflected irregular waves. *Coastal Engineering*, 24:205–215.

Gacia, E. and Duarte, C. M. (2001). Sediment retention by a Mediterranean *Posidonia oceanica* meadow: The balance between deposition and resuspension. *Estuarine, Coastal and Shelf Science*, 52:505–514.

Gambi, M. C., Nowell, A. R. M., and Jumars, P. A. (1990). Flume observations on flow dynamics in *Zostera marina* (eelgrass) beds. *Marine Ecology Progress Series*, 61:159–169.

Garel, E., Fernandez, L. L., and Collins, M. (2008). Sediment resuspension events induced by the wake wash of deep-draft vessels. *Geo-Marine Letters*, 28:205–211.

Gaylord, B., Denny, M. W., and Koehl, M. A. R. (2003). Modulation of wave forces on kelp canopies by alongshore currents. *Limnology and Oceanography*, 48(2):860–871.

Ghisalberti, M. and Nepf, H. M. (2006). The structure of the shear layer over rigid and flexible canopies. *Environmental Fluid Mechanics*, 6(3):277–301.

Gobert, S., Cambridge, M. L., Velimirov, B., Pergent, G., Lepoint, G., Bouquegneau, J. M., Dauby, P., Pergent-Martini, C., and Walker, D. I. (2006). Biology of *Posidonia*. In Larkum, A. W. D., Orth, R. J., and Duarte, C. M., (editors), *Seagrasses:Biology, Ecology and Conservation*, pages 387–408. Springer, Berlin.

Gordon, L. and Lohrmann, A. (2001). Near-shore Doppler current meter wave spectra. Technical report, Nortek.

Granata, T. C., Serra, T., Colomer, J., Casamitjana, X., Duarte, C. M., and Gacia, E. (2001). Flow and particle distributions in a nearshore meadow before and after a storm. *Marine Ecology Progress Series*, 218:95–106.

Grillas, P., Charpentier, A., Auby, I., Lescuyer, F., and Coulet, E. (2000). Spatial dynamics of *Zostera noltii* over a 5-year period of fluctuating salinity in the Vaccares Lagoon, France. In Pergent, G., Pergent-Martini, C., Buia, M. C., and Gambi, M. C., (editors), *Proceedings 4th International Seegrass Biology Workshop*, volume 7 (2), pages 377–380, Korsika, France.

Heck, J. K. L. and Valentine, J. F. (2006). Plant-herbivore interactions in seagrass meadows. *Journal of Experimental Marine Biology and Ecology*, 330:420–436.

Hemprich, F. G. and Ehrenberg, C. G. (1900). *Symbolae physicae seu Icones Adhuc Inditeae: coroprum naturalium novorum aut minus cognitorum.* Botanica. Berolini. (in Latin).

Hendriks, I. E., van Duren, L. A., and Herman, P. M. J. (2006). Turbulence levels in a flume compared to the field: Implications for larval settlement studies. *Journal of Sea Research*, 55(1):15–29.

IUCN (2010). IUCN Red List of Threatened Species. Version 2010.4. [accessed 04/04/2011]. Available from: www.iucnredlist.org.

Iwagaki, Y. and Kakinuma, T. (1967). On the bottom friction factors off five Japanese coasts. *Coastal Engineering in Japan*, 10:13–22.

James, W. F. and Barko, J. W. (2000). Sediment resuspension dynamics in canopy- and meadow-forming submersed macrophyte communities. *Aquatic Plant Control Research Program, U.S. Army corps of Engineers.*

Jonsson, I. G. (1966). Wave boundary layers and friction factors. In *10th Conference on Coastal Engineering*, volume 1, Reston. American Society of Civil Engineers.

Kamphuis, J. W. (1975). Friction factor under oscillatory waves. *Journal of Waterway Port Coastal and Ocean Engineering-Asce*, 101(WW2):135–144.

Kamphuis, J. W. (2000). *Introduction to coastal engineering and management*, volume 16 of *Advanced Series on Ocean Engineering.* World Scientific, Singapore, New Jersey, London, Hong Kong.

Kenny, A. J., Cato, I., Desprez, M., Fader, G., Schuttenheim, R. T. E., and Side, J. (2003). An overview of seabed-mapping technologies in the context of marine habitat classification. *ICES Journal of Marine Science*, 60:411–418.

Knutson, P. L., Seeling, W. N., and Inskeep, M. R. (1982). Wave dampening in *Spartina alterniflora* marshes. *Wetlands*, 2:87–104.

Kobayashi, N., Raichle, A. W., and Asano, T. (1993). Wave attenuation by vegetation. *Journal of Waterway, Port, Coastal and Ocean Engineering*, 119:30–48.

Koch, E. W. (1994). Hydrodynamics, Diffusion-Boundary Layers and Photosynthesis of the Seagrasses *Thalassia testudinum* and *Cymodocea nodosa*. *Marine Biology*, 118(4):767–776.

Koch, E. W. (1996). Hydrodynamics of a shallow *Thalassia testudinum* bed in Florida, U.S.A. In Kuo, J., Phillips, R. C., Walker, D. I., and Kirkman, H., (editors), *Seagrass Biology: Proceedings of an International Workshop*, pages 105–109.

Koch, E. W. (2001). Beyond light: physical, geological, and geochemical parameters as possible submerded aquatic vegetation habitat requirements. *Estuaries*, 24:1–17.

Koch, E. W. (2002). Impact of boat-generated waves on seagrass habitat. *Journal of Coastal Research*, 37:66–74.

Koch, E. W., Ackerman, J. D., Verduin, J. J., and van Keulen, M. (2006a). Fluid dynamics in seagrass ecology: from molecules to ecosystems. In Larkum, A. W. D., Orth, R. J., and Duarte, C. M., (editors), *Seagrasses: Biology, Ecology and Conservation*, pages 193–225. Springer, Berlin.

Koch, E. W., Barbier, E. B., Silliman, B. R., Reed, D. J., Perillo, G. M. E., Hacker, S. D., Granek, E. F., Primavera, J. H., Muthiga, N., Polansky, S., Halpern, B. S., Kennedy, C. J., Kappel, C. V., and Wolanski, E. (2009). Non-linearity in ecosystem services: temporal and spatial variability in coastal protection. *Frontiers in Ecology and the Environment*, 7(1):29–37.

Koch, E. W. and Gust, G. (1999). Water flow in tide- and wave-dominated beds of the seagrass *Thalassia testudinum*. *Marine Ecology Progress Series*, 184:63–72.

Koch, E. W., Sanford, L. P., Chen, S. N., Shafer, D. J., and McKee Smith, J. (2006b). Waves in seagrass systems: review and technical resommendations.

Technical report, US Army Corps of Engineers U.S. Army Engineer Research and Development Center.

Koehl, M. A. R. (1996). When does morphology matter? *Annual Review of Ecology and Systematics*, 27:501–542.

Komatsu, T., Igarashi, C., Tatsukawa, K., Sultana, S., Matsuoka, Y., and Harada, S. (2003). Use of multi-beam sonar to map seagrass beds in Otsuchi Bay on the Sanriku Coast of Japan. *Aquatic Living Resources*, 16:223–230.

Krogstad, H. E., Barstow, S. F., Haug, O., and Peters, D. J. H. (1998). Directional distributions in wave spectra. In ASCE, (editor), *WAVES'97*, pages 883–895.

Kuo, J. and Den Hartog, C. (2006). Seagrass morphology, anatomy, and ultrastructure. In Larkum, A. W. D., Orth, R. J., and Duarte, C. M., (editors), *Seagrasses: Biology, Ecology and Conservation*, pages 51–87. Springer.

Lasagna, R., Montefalcone, B., Alberelli, C., Bianchi, N., Corradi, N., and Morri, C. (2006). Distribuzione dei sedimenti in una prateria di *Posidonia oceanica*. In *Ecologia. Atti del XV Congresso Nazionale della SocietÃ Italiana di Ecologia*, Torino. (in Italian).

Lavery, A. C., Schmitt, R. W., and Stanton, T. K. (2003). High-frequency acoustic scattering from turbulent oceanic microstructure: the importance of density fluctuations. *Journal of the Acoustical Society of America*, 114:2685–2697.

Lee, S. Y., Fong, C. W., and Wu, R. S. S. (2001). The effects of seagrass (*Zostera japonica*) canopy structure on associated fauna: a study using artificial seagrass units and sampling of natural beds. *Journal of Experimental Marine Biology and Ecology*, 259(1):23–50.

Lefebvre, A., Thompson, C. E. L., and Amos, C. L. (2010). Influence of *Zostera marina* canopies on unidirectional flow, hydraulic roughness and sediment movement. *Continental Shelf Research*, 30(16):1783–1794.

Lefebvre, A., Thompson, C. E. L., Collins, K. J., and Amos, C. L. (2009). Use of a

high-resolution profiling sonar and a towed video camera to map a *Zostera marina* bed, Solent, UK. *Estuarine, Coastal and Shelf Science*, 82:323–334.

Lentz, S. and Raubenheimer, B. (1999). Field observations of wave setup. *Journal of Geophysical Research-Oceans*, 104(C11):25867–25875.

Leonard, L. A. and Croft, A. L. (2006). The effect of standing biomass on flow velocity and turbulence in *Spartina alterniflora* canopies. *Estuarine, Coastal and Shelf Science*, 69:325–336.

Li, M. Z. and Amos, C. L. (1998). Predicting ripple geometry and bed roughness under combined waves and currents in a continental shelf environment. *Continental Shelf Research*, 18:941–970.

Lobeck, R. T. G. (1995). *A study into coastal change between the Beaulieu River and Calshot Spit over the past 125 years.* PhD thesis, University of Southampton.

Løvås, S. M. and Tørum, A. (2001). Effect of the kelp *Laminaria hyperborea* upon sand dune erosion and water particle velocities. *Coastal Engineering*, 44:37–63.

Lowe, R. J., Falter, J. L., Bandet, M. D., Pawlak, G., Atkinson, M. J., Monismith, S. G., and Koseff, J. R. (2005). Spectral wave dissipation over a barrier reef. *Journal of Geophysical Research - Oceans*, 110(C04001).

Lowe, R. J., Falter, J. L., Koseff, J. R., Monismith, S. G., and Atkinson, M. J. (2007). Spectral wave flow attenuation within submerged canopies: Implications for wave energy dissipation. *Journal of Geophysical Research - Oceans*, 112(C05018).

Luhar, M., Coutu, S., Infantes, E., Fox, S., and Nepf, H. M. (2010). Wave-induced velocities inside a model seagrass bed. *Journal of Geophysical Research - Oceans*, 115(C12005).

Madsen, J. D., Chambers, P. A., James, W. F., Koch, E. W., and Westlake, D. K. (2001). The interaction between water movement, sediment dynamics and submersed macrophytes. *Hydrobiologia*, 444:71–84.

Madsen, O. S. (1976). Wave climate on the continental margin: Elements of its mathematical description. In Stanley, D. J. and Swift, D. J. P., (editors), *Marine Sediment Transport and Enrivonmental Management*, pages 65–87. John Wiley and Sons, New York.

Madsen, O. S. (1994). Spectral wave-current bottom boundary layer flows. In Edge, B. L., (editor), *24. Conference of Coastal Engineering*, pages 384–398, Kobe, Japan. Am. Soc. of Civil Eng.

Magne, R., Ardhuin, F., Rey, V., and Herbers, T. H. C. (2005). Topographical scattering of waves: Spectral approach. *Journal of Waterway Port Coastal and Ocean Engineering-Asce*, 131(6):311–320.

Manca, E. (2010). *Effects of* Posidonia oceanica *seagrass on nearshore waves and wave-induced flows*. PhD thesis, University of Southampton.

Mateo, M. A., Sanchez-Lizaso, J. L., and Romero, J. (2003). *Posidonia oceanica* "banquettes": a preliminary assesment of the relevance for meadow carbon and nutrients budget. *Estuarine, Coastal and Shelf Science*, 56:85–90.

Mathisen, P. P. and Madsen, O. S. (1996a). Waves and currents over a fixed rippled bed. 1. Bottom roughness experienced by waves in the presence and absence of currents. *Journal of Geophysical Research - Oceans*, 101(C7):16533–16542.

Mathisen, P. P. and Madsen, O. S. (1996b). Waves and currents over a fixed rippled bed. 2. Bottom and apparent roughness experienced by currents in the presence of waves. *Journal of Geophysical Research - Oceans*, 101(C7):16543–16550.

Mathisen, P. P. and Madsen, O. S. (1999). Waves and currents over a fixed rippled bed. 3. Bottom and apparent roughness for spectral waves and currents. *Journal of Geophysical Research*, 104(C8):18447–18461.

McDonald, C. B., Koseff, J. R., and Monismith, S. G. (2006). Effects of the depth on coral height ratio on drag coefficients for unidirectional flow over coral. *Limnology and Oceanography*, 51(3):1294–1301.

Méndez, F. J. and Losada, I. J. (2004). An empirical model to estimate the propagation of random breaking and nonbreaking waves over vegetation fields. *Coastal Engineering*, 51(2):103–118.

Méndez, F. J., Losada, I. J., and Losada, M. A. (1999). Hydrodynamics induced by wind waves in a vegetation field. *Journal of Geophysical Research*, 104(C8):18383–18396.

MetOffice (2010). Southern England: climate, download from www.metoffice.gov.uk/climate/uk/so on 11.10.2010.

Möller, I. (2006). Quantifying saltmarsh vegetation and its effect on wave height dissipation: Results from a UK East coast saltmarsh. *Estuarine, Coastal and Shelf Science*, 69:337–351.

Möller, I., Spencer, T., French, J. R., Leggett, D. J., and Dixon, M. (1999). Wave transformation over salt marshes: a field and numerical modelling study from North Norfolk, England. *Estuarine, Coastal and Shelf Science*, 49:411–426.

Mork, M. (1996). The effect of kelp in wave damping. *Sarsia*, 80:323–327.

Mullarney, J. C. and Henderson, S. M. (2010). Wave-forced motion of submerged single-stem vegetation. *Journal of Geophysical Research - Oceans*, 115(C12061):1–14.

Nepf, H. M. (1999). Drag, turbulence, and diffusion in flow through emergent vegetation. *Water Resources Research*, 35:479–489.

Nepf, H. M., Sullivan, J. A., and Zavistoski, R. A. (1997). A model for diffusion within emergent vegetation. *Limnology and Oceanography*, 42(8):1735–1745.

Neumeier, U. (2007). Velocity and turbulence variations at the edge of saltmarshes. *Continental Shelf Research*, 27(8):1017–1205.

Neumeier, U. and Amos, C. L. (2006). The influence of vegetation on turbulence and flow velocities in European salt-marshes. *Sedimentology*, 53:259–277.

Neumeier, U. and Ciavola, P. (2004). Flow resistance and associated sedimentary processes in a *Spartina maritima* saltmarsh. *Journal of Coastal Research*, 20:435–447.

Newell, R. I. E. and Koch, E. W. (2004). Modeling seagrass density and distribution in response to changes in turbidity stemming from bivalve filtration and seagrass sediment stabilization. *Estuaries*, 27:793–806.

Nielsen, P. (1992). *Coastal Bottom Boundary Layers and Sediment Transport*. Advanced Series on Ocean Engineering. World Scientific Publishing, Singapore.

Norris, J. G., Wyllie-Echeverria, S., Mumford, T., Bailey, A., and Turner, T. (1997). Estimating basal area coverage of subtidal seagrass beds using underwater videography. *Aquatic Botany*, 58:269–287.

OSPAR (2004). 2004 Initial OSPAR List of Threatened and/or Declining Species and Habitats.

Pasche, E. and Deußfeld, N. (2003). Hydro- und Morphodynamik in Seegraswiesen. *Hansa International Maritime Journal*, pages 67–73. (in German).

Pasqualini, V., Pergent-Martini, C., Clabaut, P., and Pergent, G. (1998). Mapping of *Posidonia oceanica* using aerial photographs and side scan sonar: application off the island of Corsica (France). *Estuarine, Coastal and Shelf Science*, 47:359–367.

Patil, S. and Singh, V. P. (2009). Hydrodynamics of wave and current vegetation interaction. *Journal of Hydrologic Engineering*, 14(12):1320–1333.

Paul, M. and Amos, C. L. (2011). Spatial and seasonal variation in wave attenuation over *Zostera noltii*. *Journal of Geophysical Research*, 116(C08019).

Paul, M., Bouma, T. J., and Amos, C. L. (2011a). The effect of organism traits and tidal currents on wave attenuation by submerged vegetation. In *5th International Short Conference on Applied Coastal Research (SCACR)*, Aachen.

Paul, M., Bouma, T. J., and Amos, C. L. (in review). Wave attenuation by submer-

ged vegetation: combining the effect of organism traits and tidal current. *Marine Ecology Progress Series*.

Paul, M., Lefebvre, A., Manca, E., and Amos, C. L. (2011b). An acoustic method for the remote measurement of seagrass metrics. *Estuarine, Coastal and Shelf Science*, 93:68–79.

Pergent-Martini, C., Pasqualini, V., Ferratt, L., Pergent, G., and Fernandez, C. (2005). Seasonal dynamics of *Zostera noltii Hornem.* in two Mediterranean lagoons. *Hydrobiologia*, 543:233–243.

Peterson, C. H., Luettich, R. A., Micheli, F., and Skilleter, G. A. (2004). Attenuation of water flow inside seagrass canopies of differing structure. *Marine Ecology Progress Series*, 268:81–92.

Phillips, R. C. and Meñez, E. G. (1988). Seagrasses. *Smithsonian Contributions to the Marine Sciences*, 34.

Pihl, L., Baden, S., Kautsky, N., Ronnback, P., Soderqvist, T., Troell, M., and Wennhage, H. (2006). Shift in fish assemblage structure due to loss of seagrass *Zostera marina* habitats in Sweden. *Estuarine, Coastal and Shelf Science*, 67:123–132.

Prager, E. J. and Halley, R. B. (1999). The influence of seagrass on Shell Layers and Florida bay mudbanks. *Journal of Coastal Research*, 15(4):1151–1162.

Prinos, P., Stratigaki, V., Manca, E., Losada, I. J., Lara, J. L., Sclavo, M., Caceres, I., and Sanchez-Arcilla, A. (2010). Wave propagation over *Posidonia oceanica*: Large scale experiments. In Grüne, J. and Klein Breteler, M., (editors), *Hydralab III Joint Transnational Access User Meeting*, pages 57–60, Hannover.

Raubenheimer, B., Guza, R. T., and Elgar, S. (1996). Wave transformation across the inner surf zone. *Journal of Geophysical Research-Oceans*, 101(C11):25589–25597.

Raubenheimer, B., Guza, R. T., and Elgar, S. (2001). Field observations

of wave-driven setdown and setup. *Journal of Geophysical Research-Oceans*, 106(C3):4629–4638.

Raven, P. H., Eichhorn, S. E., and Evert, R. F. (2005). *Biology of Plants*. W.H. Freeman, New York, 7th edition.

Roe, H. S. J., Griffiths, G., Hartman, M., and Crisp, N. (1996). Variability in biological distributions and hydrography from concurrent acoustic Doppler current profiler and SeaSoar surveys. *ICES Journal of Marine Science*, 53(2):131–138.

Sabol, B. M., Kannenberg, J., and Skogerboe, J. G. (2009). Integrating Acoustic Mapping into Operational Aquatic Plant Management: a case study in Wisconsin. *Journal of Aquatic Plant Management*, 47:44–52.

Sabol, B. M., Melton, R. E., Chamberlain, R., Doering, P., and Haunert, K. (2002). Evaluation of a digital echo sounder system for detection of submersed aquatic vegetation. *Estuaries*, 25(1):133–141.

Samiaji, J. (2001). *The ecology of* Zostera noltii *bed ecosystem in the Solent*. PhD thesis, University of Southampton.

Schanz, A. and Asmus, H. (2003). Impact of hydrodynamics on development and morphology of intertidal seagrasses in the Wadden Sea. *Marine Ecology Progress Series*, 261:123–134.

Sfriso, A. and Ghetti, P. F. (1998). Seasonal variation in biomass, morphometric parameters and production of seagrasses in the lagoon of Venice. *Aquatic Botany*, 61(3):207–223.

Short, F. T., Carruthers, T. J. B., Dennison, W. C., and Waycott, M. (2007). Global seagrass distribution and diversity: A bioregional model. *Journal of Experimental Marine Biology and Ecology*, 350(1-2):3–20.

Soulsby, R. L. (1997). *Dynamics of Marine Sands: a Manual for Practical Applications*. Thomas Telford, London.

Stein, D., Arns, L., Eichweber, G., Faubel, A., and Regier, M. (1989). Erosionsschutz im Seewasserbau - Untersuchung der Wirkung von künstlichen Seegrasmatten auf Sedimentationsvorgänge. Technical report, Ruhr-Universtität Bochum, Fakultät Bauingenieurwesen. (in German).

Stewart, H. L. (2006). Hydrodynamic consequences of flexural stiffness and buoyancy for seaweeds: a study using physical models. *Journal of Experimental Biology*, 209:2170–2181.

Teeter, A. M., Johnson, B. H., Berger, C., Stelling, G., Scheffner, N. W., Garcia, M. H., and Parchure, T. M. (2001). Hydrodynamic and sediment transport modelling with emphasis on shallow-water, vegetated areas (lakes, reservoirs, estuaries and lagoons). *Hydrobiologia*, 444:1–23.

Thompson, C. E. L., Amos, C. L., and Umgiesser, G. (2004). A comparison between fluid shear stress reduction by halophytic plants in Venice Lagoon, Italy and Rustico Bay, Canada - analyses of *in situ* measurements. *Journal of Marine Systems*, 51(1-4):293–308.

Thornton, E. B. and Guza, R. T. (1982). Energy saturation and phase speeds measured on a natural beach. *Journal of Geophysical Research-Oceans and Atmospheres*, 87(NC12):9499–9508.

Tonks, V. L. (2008). *An Investigation into the Sediment Processes on Ryde Sandflat using Grain Trend Analysis*. Msc, University of Southampton.

Tubbs, C. R. and Tubbs, J. M. (1983). The distribution of *Zostera* and its exploitation by wildfowl in the Solent, Southern England. *Aquatic Botany*, 15:223–239.

Tyler-Walters, H. (2008). *Zostera noltii*. Dwarf eelgrass. In *Marine Life Information Network: Biology and Sensitivity Key Information Sub-programme [on-line]*. Plymouth: Marine Biological Association of the United Kingdom. [accessed 15/07/2009]. Available from: http://www.marlin.ac.uk/speciesfullreview.php?speciesID=4601.

Van Lent, F., Nienhuis, P. H., and Verschuure, J. M. (1991). Production and biomass of the seagrasses *Zostera noltii Hornem.* and *Cymodocea nodosa (Ucria) Aschers.* at the Banc d'Arguin (Mauritania, NW Africa): a preliminary approach. *Aquatic Botany*, 41(4):353–368.

Verduin, J. J. and Backhaus, J. O. (2000). Dynamics of Plant-Flow Interactions for the Seagrass *Amphibolis antarctica*: Field Observations and Model Simulations. *Estuarine, Coastal and Shelf Science*, 50:185–204.

Verduin, J. J., Backhaus, J. O., and Walker, D. I. (2002). Estimates of pollen dispersal and capture within *Amphibolis antarctica (Labill.) sonder* and *aschers. ex aschers.* meadows. *Bulletin of Marine Science*, 71(3):1269–1277.

Vis, C., Hudon, C., and Carignan, R. (2003). An evaluation of approaches used to determine the distribution and biomass of emergent and submerged aquatic macrophytes over large spatial scales. *Aquatic Botany*, 77:187–201.

Vogel, S. (1984). Drag and Flexibility in Sessile Organisms. *American Zoologist*, 24(1):37–44.

Vogel, S. (1994). *Life in moving fluids: the physical biology of flow.* Princeton University Press, Princeton, N.J., 2nd edition.

Ward, L. G., Kemp, W. M., and Boynton, W. E. (1984). The influence of waves and seagrass communities on suspended particulates in an estuarine embayment. *Marine Geology*, 59:85–103.

Warren, J. D. and Peterson, B. J. (2007). Use of a 600-kHz Acoustic Doppler Current Profiler to measure estuarine bottom type, relative abundance of submerged aquatic vegetation, and eelgrass canopy height. *Estuarine, Coastal and Shelf Science*, 72:53–62.

Warren, J. D., Stanton, T. K., Wiebe, P. H., and Seim, H. E. (2003). Inference of biological and physical parameters in an internal wave using multiple-frequency, acoustic-scattering data. *ICES Journal of Marine Science*, 60:1033–1046.

Wayne, C. J. (1976). The effect of sea and marsh grass on wave energy. *Coastal Research Notes*, 14:6–8.

Widdows, J., Pope, N. D., Brinsley, M. D., Asmus, H., and Asmus, R. (2008). Effect of seagrass beds (*Zostera noltii* and *Z. marina*) on near-bed hydrodynamics and sediment resuspension. *Marine Ecology Progress Series*, 358:125–136.